

hep-ph/9912459

CERN-TH/99-311; McGill-99/33
TPI-MINN-99/53, UMN-TH-1828-99

A Higgs or Not a Higgs?

What to Do if You Discover a New Scalar Particle

C.P. Burgess,^a J. Matias^b and M. Pospelov ^c^a *Physics Department, McGill University**3600 University St., Montréal, Québec, Canada, H3A 2T8.*^b *Theory Division, CERN, CH-1211 Genève 23, Switzerland.*^c *Theoretical Physics Institute, University of Minnesota**431 Tate Laboratory of Physics, Minneapolis, MN, USA 55455.*

Abstract

We show how to systematically analyze what may be inferred should a new scalar particle be discovered in collider experiments. Our approach is systematic in the sense that we perform the analysis in a manner which minimizes *a priori* theoretical assumptions as to the nature of the scalar particle. For instance, we do *not* immediately make the common assumption that a new scalar particle is a Higgs boson, and so must interact with a strength proportional to the mass of the particles with which it couples. We show how to compare different observables, and so to develop a decision tree from which the nature of the new particle may be discerned. We define several categories of models, which summarize the kinds of distinctions which the first experiments can make.

1. Introduction

Suppose that you have just learned that a new scalar particle has been discovered. After your immediate euphoria there are a number of things which you should do (*e.g.*: call friends, pay off bets, feverishly write papers, book flights to Stockholm, *etc.*). After this, your next wish will probably be to know what the new discovery means. Is it the Standard Model (SM) Higgs? Is this the first sign of supersymmetry? If so, if the scalar is neutral is it a Higgs or is it a sneutrino? Is it a technipion?

We hope that once these reactions have passed — or even before — you will remember and reread this paper, since our goal here is to show how to answer these, and other, issues. We intend here to show how to combine current experimental results with the new information about the new particle, and infer what its properties are in as unprejudiced a manner as is now possible. We have no particular axe to grind, and so wish to make this inference in a manner which does not build in from the beginning lots of theoretical prejudices as to what the new scalar means. We use the language of effective theories to efficiently organize the extant experimental information in a way which allows a relatively objective comparison of the evidence in favour of the various theoretical possibilities. We mean to complement in this way the very many detailed studies of the implications for Higgs searches of various specific models [1] – [3], and to provide a general language within which such models may be efficiently compared.

Our main assumption in our analysis is that, at least for a short time, only one (or a few) scalar particles are initially discovered, and that any others of the zoo of undiscovered particles are reasonably heavy compared to the scales presently being scoured for Higgses. Here ‘reasonably heavy’ might mean as heavy as, say, several hundred GeV, which puts such particles out of reach of experiments at LEP, HERA and the current generation of hadron colliders. This assumption has two key advantages: (*i*) it is broad enough to include most of the models which are of current interest, and (*ii*) it is quite predictive since it permits a systematic parameterization of the scalar particle couplings in terms of the effective theory which is obtained when all of the heavier particles are integrated out. Any ‘non-decoupling’ and slowly decoupling effects of these heavier particles will be

automatically encoded amongst the effective couplings of this lagrangian.

The other main assumption we make is that the Yukawa couplings of the newly observed scalar are dominantly flavour-diagonal. Although we make this assumption mainly on the grounds of simplicity, we do not believe it to be a major limitation on the applicability of our analysis because of the impressive limits which exist on many types of flavour-changing processes. These typically require the couplings to light fermions of the lightest scalar state in most models to be approximately flavour diagonal. We nevertheless regard a model-independent study of the bounds on flavour-changing scalar couplings to be worthwhile to pursue, but defer such an analysis to future work.

Our presentation proceeds in the following way. First, the next section (§2) presents the most general low-dimension interactions which are possible between new scalars and the other well-known elementary particles. So long as experiments cannot reach energies high enough to probe the next threshold for new physics the effective couplings which appear in this effective action encode all of the information that can be learnt, even in principle, about the new scalars. Then, §3 and §4 relate these effective interactions to observables in order to see in a general way which kinds of experiments are sensitive to which kinds of scalar-particle properties. §3 concentrates on scalar production and decays, while §4 specializes to the contribution of virtual scalar exchange for processes having no scalars in the initial or final state. Contact with specific models is made in §5, where the effective couplings of §2 are computed as functions of the underlying couplings for various choices for the models which might describe this underlying, higher-energy physics.

The many studies of scalar-particle phenomenology in particular models shows that tree-level perturbation theory can be insufficiently accurate in some situations, due to the importance of next-to-leading-order (NLO) corrections or to genuine nonperturbative effects. It is therefore important to be clear how these contributions arise within the effective-lagrangian approach used here. If the important nonleading contributions involve high-energy particles, then they must be included in §5, where these degrees of freedom are integrated out to generate the effective couplings. If, on the other hand, the important nonleading terms involve only light particles – typically QCD effects, in practice – they

must be included in §3 and §4 where the low-energy theory is used to compute expressions for observables. We emphasize that the use of tree level, say, in §3 and §4 is *not* inconsistent with obtaining the higher-order (or nonperturbative) contributions to observables, so long as these arise at high energies and have been included when computing the effective couplings in §5.

All of our results are finally pulled together in §6, in which we show which observables best differentiate amongst the various kinds of possible models for scalar-particle physics. We discuss in this section a ‘decision tree’ which may be used to decide whether the new particle is an element of an ‘elementary’ electroweak multiplet or is a composite boson; or whether it is an electroweak doublet or a member of another multiplet; if it is a supersymmetric scalar or the familiar Higgs from the SM, *etc.*. In particular, we use the possible low-energy couplings to divide models into 16 categories. We present these categories as being the proper expression of the information which experimenters are likely to be able to obtain shortly after the discovery of any new scalar, in that they can fairly quickly differentiate from which category of model a new scalar originates. It is also possible to differentiate amongst models within any particular category, but this is likely to take longer as it requires more detailed information.

2. General Effective Interactions for New Spinless Particles

As stated in the introduction, the central assumption which organizes our analysis is that only one (or a few) new scalar particles are initially found, with all other new particles being sufficiently heavy to continue evading detection, at least initially. It is important to emphasize that, given the current state of the experimental art, these undiscovered heavy particles need not actually be excessively heavy.

For example, it might happen that new scalars are discovered with masses near 100 GeV, but that all other undiscovered new particles in the underlying theory have masses which are at least 200 GeV. This kind of mass heirarchy is already sufficient to ensure the validity of the considerations presented here. Of course, the heavier any other undiscovered particles may be, the better approximation it is to use only the lowest-dimension

interactions of the effective theory.

Under these assumptions the interactions of the observed particles are described in terms of the lowest-dimension interactions within the effective theory obtained by integrating out all of the heavier undiscovered particles. These effective interactions must be constructed from local operators involving only fields which correspond to the observed particle spectrum. They must also respect all of the symmetries which are believed to hold exactly, and which act only among the particles which appear in the low-energy theory. That is, they must be invariant with respect to Lorentz and electromagnetic and $SU_c(3)$ (colour) gauge invariance.

Notice that (linearly-realized) invariance with respect to the SM electroweak gauge group, $SU_L(2) \times U_Y(1)$, should *not* be imposed *a priori*, unless it becomes established that the observed degrees of freedom actually do fill out electroweak multiplets. Indeed, determining the evidence in favour or against this possibility is part of the main motivation for the analysis we here present. (It is important to realise in this regard that there is no physical difference between completely ignoring $SU_L(2) \times U_Y(1)$ gauge invariance and nonlinearly realizing it by introducing a collection of would-be Goldstone bosons [4]. This choice is purely a matter of convenience, and is similar to the choice between using a unitary or renormalizable gauge in a renormalizable gauge theory: the nonlinear realization brings ease of loop calculations and power-counting; while ignoring the gauge symmetries makes the physical particle content and interactions easier to see [5].)

Of course, in the event that the effective theory does not couple in a gauge-invariant way to the known massive spin-one particles, Z^0 and W^\pm the effective theory must violate unitarity at sufficiently high energies [6], [5]. Far from invalidating the use of such effective lagrangians at low energies, high-energy pathologies such as this are invaluable because they indicate the energies at which the effective description fails. As such they provide an upper bound on the masses of other degrees of freedom, whose interactions cure the high-energy unitarity problems of the low-energy effective theory.

2.1) Effective Interactions Having Dimension ≤ 4

We now turn to the enumeration of the possible interactions which can arise in the effective theory. We take its particle content to consist of the usual garden-variety fermions and gauge bosons, plus a recently-discovered collection of N neutral scalar bosons: h_i , $i = 1, \dots, N$. Only interactions which explicitly involve the hypothetical newly-discovered scalar are listed here, although a list of corresponding effective interactions amongst the presently-known particles are presented and analyzed in a similar spirit in ref. [7].

With these particles, and assuming electromagnetic and colour gauge invariance (and Lorentz invariance), the most general possible lowest-dimension interactions are:

$$\mathcal{L}_{\text{eff}} = \mathcal{L}^{(2)} + \mathcal{L}^{(3)} + \mathcal{L}^{(4)} + \mathcal{L}^{(5)} + \dots \quad (1)$$

with the dimension-two and -three operators given by

$$\begin{aligned} \mathcal{L}^{(2)} &= -\frac{1}{2}m_i^2 h_i^2 \\ \mathcal{L}^{(3)} &= -\frac{\nu_{ijk}}{3!} h_i h_j h_k - \frac{a_Z^i}{2} Z_\mu Z^\mu h_i - a_W^i W_\mu^* W^\mu h_i, \end{aligned} \quad (2)$$

where the Einstein summation convention applies to all repeated indices, and the reality of \mathcal{L}_{eff} implies the reality of all of the coupling constants.

More interactions arise at dimension four.:

$$\mathcal{L}^{(4)} = \mathcal{L}_{\text{kin}} + \mathcal{L}_{\text{scalar}}^{(4)} + \mathcal{L}_{\text{fermion}}^{(4)} + \mathcal{L}_{\text{vector}}^{(4)}, \quad (3)$$

with $\mathcal{L}_{\text{kin}} = -\frac{1}{2}\partial^\mu h_i \partial_\mu h_i$ denoting the usual kinetic terms for canonically-normalized scalar fields,

$$\begin{aligned} \mathcal{L}_{\text{scalar}}^{(4)} &= -\frac{\lambda_{ijkl}}{4!} h_i h_j h_k h_l \\ \mathcal{L}_{\text{fermion}}^{(4)} &= -\sum_{Q(f)=Q(f')} \bar{f} \left(y_{ff'}^i + i\gamma_5 z_{ff'}^i \right) f' h_i, \end{aligned} \quad (4)$$

and

$$\mathcal{L}_{\text{vector}}^{(4)} = - \left(\frac{b_z^{ij}}{4} Z_\mu Z^\mu + \frac{b_w^{ij}}{2} W_\mu^* W^\mu \right) h_i h_j - \frac{g_z^{ij}}{2} h_i \overleftrightarrow{\partial}_\mu h_j Z^\mu. \quad (5)$$

The various coefficients in this last expression satisfy numerous reality and symmetry conditions. For example, all of the bosonic effective couplings are real, and are symmetric under the interchange of their subscripts i and j — *e.g.* $b_z^{ij} = b_z^{ji}$ — except for g_z^{ij} , which is antisymmetric. Notice that this antisymmetry of g_z^{ij} implies that the corresponding interaction does not arise if there is only one neutral scalar.

- *Unphysical Scalars:*

When computing loops using this effective lagrangian it is usually convenient to work in a manifestly renormalizable gauge.¹ In these gauges there are two unphysical scalars, z and w , which become the longitudinal spin states of the Z and W in unitary gauge. In these gauges the neutral scalar z must be included as one of the scalars participating in the effective interactions just described, as well as including the related couplings involving the charged scalar w .

2.2) Some Dimension-5 Operators

With very few exceptions, interactions having dimension five or higher are not required for our purposes, since their effects are negligible compared with those just listed. This is guaranteed so long as all particles which are integrated out in producing this effective lagrangian are sufficiently heavy. This is fortunate because higher-dimensional interactions can be as numerous as the proverbial grains of sand on the beach. An analysis of some higher dimensional operators can be found in [8].

Among the exceptions mentioned in the previous paragraph are interactions which couple the scalars to photons and gluons, since these interactions have no lower-dimension counterparts with which to compete. There are four interactions of this type which arise

¹ It is always possible to choose such a gauge, even when \mathcal{L}_{eff} is not explicitly $SU_L(2) \times U_Y(1)$ gauge invariant, by rewriting the lagrangian using a nonlinear realization of the gauge group [5].

at lowest dimension:

$$\mathcal{L}_{g,\gamma}^{(5)} = -c_g^i G_{\mu\nu}^\alpha G_\alpha^{\mu\nu} h_i - \tilde{c}_g^i G_{\mu\nu}^\alpha \tilde{G}_\alpha^{\mu\nu} h_i - c_\gamma^i F_{\mu\nu} F^{\mu\nu} h_i - \tilde{c}_\gamma^i F_{\mu\nu} \tilde{F}^{\mu\nu} h_i, \quad (6)$$

where $F_{\mu\nu}$ and $G_{\mu\nu}^\alpha$ are, respectively, the electromagnetic and gluon field strengths, and a tilde over a field strength denotes the usual Hodge dual: $\tilde{F}_{\mu\nu} = \frac{1}{2} \epsilon_{\mu\nu\lambda\rho} F^{\lambda\rho}$. Some dimension-five interactions involving the photon and the Z boson are also useful to include for the same reasons:

$$\mathcal{L}_{Z\gamma}^{(5)} = -c_{Z\gamma}^i Z_{\mu\nu} F^{\mu\nu} h_i - \tilde{c}_{Z\gamma}^i Z_{\mu\nu} \tilde{F}^{\mu\nu} h_i, \quad (7)$$

where $Z_{\mu\nu} = \partial_\mu Z_\nu - \partial_\nu Z_\mu$.

2.3) Special Case 1: Only One New Neutral Scalar

An important special case is the (second-most) pessimistic scenario in which only a single neutral scalar is found — *i.e.* $N = 1$. (This is the case considered in detail in many of the later sections.) Denoting the sole new scalar field in this case by h , the above effective interactions simplify considerably, to become:

$$\mathcal{L}^{(2)} + \mathcal{L}^{(3)} = -\frac{m_h^2}{2} h^2 - \frac{\nu}{3!} h^3 - \frac{a_Z}{2} Z_\mu Z^\mu h - a_W W_\mu^* W^\mu h, \quad (8)$$

and

$$\mathcal{L}_{\text{int}}^{(4)} = - \sum_{Q(f)=Q(f')} \bar{f} \left(y_{ff'} + i\gamma_5 z_{ff'} \right) f' h - \frac{\lambda}{4!} h^4 - \left(\frac{b_Z}{4} Z_\mu Z^\mu + \frac{b_W}{2} W_\mu^* W^\mu \right) h^2. \quad (9)$$

The dimension-five interactions of eqs. (6) and (7) are also possible in this case:

$$\begin{aligned} \mathcal{L}_{g,\gamma}^{(5)} = & -c_g G_{\mu\nu}^\alpha G_\alpha^{\mu\nu} h - \tilde{c}_g G_{\mu\nu}^\alpha \tilde{G}_\alpha^{\mu\nu} h - c_\gamma F_{\mu\nu} F^{\mu\nu} h - \tilde{c}_\gamma F_{\mu\nu} \tilde{F}^{\mu\nu} h \\ & - c_{Z\gamma} Z_{\mu\nu} F^{\mu\nu} h - \tilde{c}_{Z\gamma} Z_{\mu\nu} \tilde{F}^{\mu\nu} h. \end{aligned} \quad (10)$$

2.4) Special Case 2: Two Scalars Subject to a Conservation Law

Another important special case arises when there is more than one scalar but conservation laws exist which forbid many of the terms in \mathcal{L}_{eff} . This would happen, for example, if the new scalar carried a conserved quantum number such as lepton number. (The sneutrino would be this kind of scalar, for example, in supersymmetric models if lepton number should not be broken.) In this section we identify the lowest-dimension couplings which can survive in this case, assuming there to be only one new (complex) scalar, $\mathcal{H} = (h_1 + ih_2)/\sqrt{2}$.

Assuming the W and Z do not also carry this quantum number, this kind of scalar can have only the following low-dimension interactions with bosons:

$$\begin{aligned} \mathcal{L}_{\text{bose}}^{(2)} + \mathcal{L}_{\text{bose}}^{(3)} + \mathcal{L}_{\text{bose}}^{(4)} = & -m_h^2 \mathcal{H}^* \mathcal{H} - \frac{\lambda}{4} (\mathcal{H}^* \mathcal{H})^2 \\ & - \left(\frac{b_z}{2} Z_\mu Z^\mu + b_w W_\mu^* W^\mu \right) \mathcal{H}^* \mathcal{H} - ig_z \mathcal{H}^* \overleftrightarrow{\partial}_\mu \mathcal{H} Z^\mu. \end{aligned} \quad (11)$$

Most of the dimension-four fermion-scalar couplings considered above must also vanish for this kind of scalar. This is because there are not many potentially conserved global quantum numbers which it is possible for the fermions to carry, given only the known particles and low-dimension interactions. The only candidates are the accidental symmetries of the Standard Model itself: baryon number, B , and the flavour of each generation of lepton, L_e , L_μ and L_τ . For instance, if $B(\mathcal{H}) \neq 0$, then there are no dimension-four B -conserving fermion interactions possible at all because the requirement of colour neutrality automatically implies the B neutrality of all Lorentz-scalar fermion bilinears. The same is also true if total lepton number, $L = L_e + L_\mu + L_\tau$, is conserved and is carried by \mathcal{H} .

At dimension four the only nontrivial possibilities arise if \mathcal{H} carries only some of L_e , L_μ or L_τ and either total lepton number is not conserved, or it is conserved but is not carried by \mathcal{H} (as might happen if $L_e(\mathcal{H}) = -L_\mu(\mathcal{H})$, say). In this case nontrivial dimension-four couplings are possible between \mathcal{H} and neutrinos, ν , and/or between \mathcal{H} and charged leptons, ℓ :

$$\mathcal{L}_{\text{fermi}}^{(4)} = - \left[\bar{\ell}_a \left(y_{ab}^\ell + i\gamma_5 z_{ab}^\ell \right) \ell_b + \bar{\nu}_a \left(y_{ab}^\nu + i\gamma_5 z_{ab}^\nu \right) \nu_b \right] \mathcal{H} + \text{c.c.} \quad (12)$$

The precluding of so many low-dimension interactions by the assumed conservation law makes some of the higher-dimension operators more important than they would be otherwise. In particular, only the operators of eqs. (12) mediate \mathcal{H} decay, and these operators are also forbidden if either B or L are conserved and carried by \mathcal{H} . Unless \mathcal{H} decays are themselves forbidden by B or L conservation, decays must in this case be mediated by operators of even higher dimension. For example if $B(\mathcal{H}) = -L(\mathcal{H}) = 1$ and both of these symmetries are unbroken, then the decay $\mathcal{H} \rightarrow n \bar{\nu}$ is allowed, but the lowest-dimension effective operators which can mediate scalar decay first arise at dimension seven, such as:

$$\mathcal{L}_{\text{decay}}^{(7)} = \kappa \epsilon^{\alpha\beta\gamma} \mathcal{H} (\bar{q}_\alpha q_\beta^c) (\bar{q}_\gamma \nu). \quad (13)$$

In any case, for the present purposes we must keep in mind the possibility that the new scalar might be very long-lived in this scenario.

2.5) Special Case 3: The Standard Model

The Standard Model itself furnishes what is probably the most important special case to consider. It is a particular instance of the single-scalar scenario described earlier. Because, true to its name, the SM really does provide the standard against which other models are compared, we treat this example in more detail than the special cases just considered. (This more detailed discussion is duplicated for other models of interest in section 5, below.) We consider first the tree level contributions to the effective lagrangian, and then discuss the nature of the radiative corrections to these tree-level results.

2.5.1) Tree-Level Predictions

The dominant SM contributions to the effective interactions of dimension four or less arise at tree level, and are given in terms of ratios of the relevant particle masses to the fundamental expectation value, $v = (\sqrt{2} G_F)^{-1/2} = 246$ GeV.

The explicit expressions at dimension three are:

$$\nu = \frac{6 m_h^2}{v}, \quad a_z = \frac{2 M_z^2}{v} = \frac{e M_z}{s_w c_w}, \quad a_w = \frac{2 M_w^2}{v} = \frac{e M_w}{s_w}, \quad \text{SM(tree)} \quad (14)$$

where e is the electromagnetic coupling, while s_w c_w are the sine and cosine of the weak mixing angle, θ_W . The dimension four interactions are:

$$\lambda = \frac{6 m_h^2}{v^2}, \quad b_z = \frac{2 M_z^2}{v^2} = \frac{e^2}{2 s_w^2 c_w^2}, \quad b_w = \frac{2 M_w^2}{v^2} = \frac{e^2}{2 s_w^2}, \quad \text{SM(tree)} \quad (15)$$

and

$$y_{ff'} = \frac{m_f}{v} \delta_{ff'}, \quad z_{ff'} = 0 \quad \text{SM(tree)}. \quad (16)$$

The purpose of the rest of this paper is to find to what extent predicted relationships, such as these, amongst the effective couplings can be experimentally established using current (and future) data.

2.5.2) SM Radiative Corrections

Of course the SM predictions of eqs. (14), (15) and (16) are modified at one-loop level and beyond. These corrections are not required for most of the present purposes because upcoming experiments will not be sensitive to small corrections to these relations. The same point also holds in most – but not all (see below) – of the models considered in what follows, so for many purposes it suffices to restrict our calculations to tree level.

The only exceptions to this statement arise when the leading-order prediction is zero — or very small because of suppressions by small factors, such as light particle masses — and if the same is not true for the radiative corrections. It is therefore important to examine carefully the predictions for unusually small effective couplings. One might worry that the vanishing of $z_{ff'}$ in eq. (16), and the extremely small predictions there for $y_{ff'}$, might be suspicious on these grounds. Although this worry can be justified for some other models, the small size of these couplings is not changed when higher SM loops are considered. For the $y_{ff'}$ this is because vanishing Yukawa coupling imply the existence of new chiral symmetries, and these symmetries ensure that the higher-loop corrections are themselves also proportional to the tree-level values, $\delta y_{ff'} \propto y_{ff'}$. Similar considerations apply to the $z_{ff'}$ since this coupling breaks the discrete symmetry, CP . Loop corrections to these are therefore also suppressed by the very small size of SM CP -violation. (See refs. [9] – [13] for one and two-loop calculations of effective couplings in the SM.)

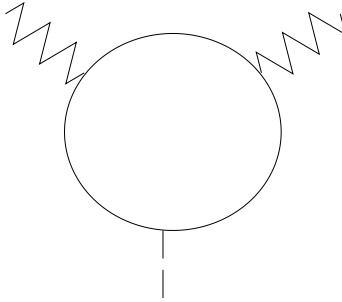


Figure (1):

The Feynman graph which contributes the leading contribution to the effective dimension-five vertices of eqs. (6) and (7) at one loop.

An example of an important SM radiative correction arises if \mathcal{L}_{eff} is applied at scales below the top-quark mass. At these scales the t quark has been integrated out, and this integration induces the dimension-five operators of eq. (6), through the fermion loop of Fig. (1). Using the flavour-diagonal Yukawa couplings, $y = y_{ff}$ and $z = z_{ff}$, of eq. (4), and working to leading order in the inverse fermion mass, $1/m$, the effective couplings which result are:

$$c_k = \frac{y \alpha_k \mathcal{C}_k}{6\pi m}, \quad \tilde{c}_k = \frac{z \alpha_k \mathcal{C}_k}{6\pi m} \quad (\text{heavy-fermion loop}). \quad (17)$$

Here $k = \gamma, g$ denotes either the photon or gluon and $\alpha_\gamma = \alpha$ and $\alpha_g = \alpha_s$ are their respective fine structure constants. \mathcal{C}_k denotes the quadratic Casimir of the corresponding gauge generators, t_a , as represented on the fermions: $\text{Tr}(t_a t_b) = \mathcal{C} \delta_{ab}$. Explicitly, for photons: $\mathcal{C}_\gamma = Q_f^2 N_c(f)$ where Q_f is the fermion charge in units of e , and $N_c(f) = 1(3)$ if f is a lepton (quark); while for gluons: $\mathcal{C}_g = \frac{1}{2}$ for quarks (and $\mathcal{C}_g = 0$ for leptons).

The generalization of eq. (17) to the h - Z - γ effective interaction is straightforward. Starting from c_γ or \tilde{c}_γ one simply replaces one factor of the fermion charge with the vector part of its coupling to the Z : $e Q_f \rightarrow e g_V / (s_w c_w)$, and multiplies by 2 to compensate for the fact that the two spin-one particles are no longer identical. The result is

$$c_{Z\gamma} = \left(\frac{y \alpha}{3\pi m} \right) \frac{N_c Q_f g_V}{s_w c_w}, \quad \tilde{c}_{Z\gamma} = \left(\frac{z \alpha}{3\pi m} \right) \frac{N_c Q_f g_V}{s_w c_w}, \quad (18)$$

where g_V is normalized such that $g_V = \frac{1}{2} T_{3f} - Q_f s_w^2$ for a SM fermion. Here T_{3f} is the third component of the fermion's weak isospin.

Specializing these expressions to the SM tree-level Yukawa couplings, and including the next-to-leading QCD corrections [9] – [12], finally gives the t -quark contributions $\tilde{c}_g = \tilde{c}_\gamma = 0$ and:

$$c_g = \frac{\alpha_s}{12\pi v} \left(1 + \frac{11\alpha_s}{4\pi} \right), \quad c_\gamma = \frac{2\alpha}{9\pi v} \left(1 - \frac{\alpha_s}{\pi} \right) \quad \text{and} \quad c_{Z\gamma} = \frac{\alpha(1 - 8s_w^2/3)}{6\pi v s_w c_w} \left(1 - \frac{\alpha_s}{\pi} \right). \quad (19)$$

We quote subleading α_s corrections to these couplings because these corrections can be numerically significant. We do so for both the photon and gluon couplings even though there are other corrections to the same order in α_s to the gluon coupling which cannot be absorbed into an overall coefficient of the effective coupling, c_g [11]. We postpone our more detailed discussion of these other corrections to our later applications to h production in hadron colliders. As we shall see, although it is important that all such contributions be considered in order to have the complete QCD corrections, these do not depend on the heavy degrees of freedom, permitting the heavy physics to be usefully summarized by the QCD-corrected effective couplings c_g and \tilde{c}_g .

2.5.3) Other SM Contributions to hgg and $h\gamma\gamma$ Interactions

As might be expected given the insensitivity of result (19) to the heavy-particle masses (in this case m_t), the couplings c_i and \tilde{c}_i are potentially useful quantities for experimentally differentiating amongst various theoretical models. In order to identify those contributions which depend on new degrees of freedom, it is useful to summarize here the other SM contributions to the processes $h \rightarrow gg$ and $h \rightarrow \gamma\gamma$,

For general processes, such as the reaction $e^+e^- \rightarrow h\gamma$ considered in a later section, box graph and other contributions make it impossible to summarize all one-loop SM results as corrections to the $h\gamma\gamma$ vertex. Furthermore since many of our potential applications are to energies $\sqrt{s} \gtrsim M_W, M_Z$, the effects of virtual W and Z particles do not lend themselves to an analysis in terms of local effective interactions within some sort of low-energy effective lagrangian.

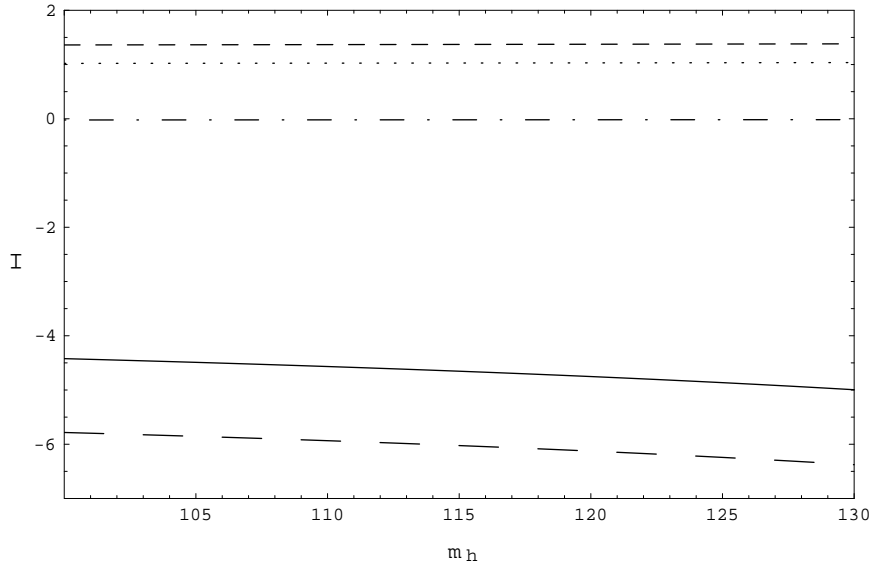


Figure (2):

A comparison of the different contributions to c_γ and c_g as a function of the Higgs mass. Concerning c_γ , the long dashed line stands for the W contribution, $-I_1\left(\frac{M_W^2}{m_h^2}\right)$, the short-dashed line represents the top contribution, $3\left(\frac{2}{3}\right)^2 I_{\frac{1}{2}}\left(\frac{m_t^2}{m_h^2}\right)$, the dashed-dotted lines are the real and imaginary part of the quark contribution (which practically overlap on this scale). The dotted line is the top quark contribution to c_g : $I_{\frac{1}{2}}\left(\frac{m_t^2}{m_h^2}\right)$.

There is an important class of reactions for which SM loop contributions can be expressed quite generally in terms of the effective couplings c_i and \tilde{c}_i , however. These consist of processes for which both gluons (or photons) and the scalar h are on shell, such as the decays $h \rightarrow gg$ or $h \rightarrow \gamma\gamma$, or parton-level processes like gluon fusion or photon-photon collisions. The contribution of light SM particles, like electrons or light quarks, to these interactions can be regarded as contributions to the effective couplings c_i and \tilde{c}_i even though an effective lagrangian treatment of the particles in these processes is not strictly justified. This is possible because the gauge invariance of the hgg (or $h\gamma\gamma$) vertex forces it to have the same tensor structure as have the operators of eq. (6), up to invariant q^2 -dependent functions which become constants when evaluated on shell.

We now record the contributions to c_i and \tilde{c}_i which are obtained in this way for the contributions of SM particles. Evaluating the contribution of spins 0, $\frac{1}{2}$ and 1 to the one-loop graph, Fig. (1), or differentiating the vacuum polarization with respect to the Higgs *v.e.v.* gives $\tilde{c}_k = 0$ and:

$$\begin{aligned} c_g^{SM} &= \frac{\alpha_s}{12\pi v} \sum_q I_{\frac{1}{2}} \left[\frac{m_q^2}{m_h^2} \right], \\ c_\gamma^{SM} &= c_\gamma^{SM}(\text{up-type fermions}) + c_\gamma^{SM}(\text{down-type fermions}) + c_\gamma^{SM}(W) \quad (20) \\ &= \frac{\alpha}{6\pi v} \left[\sum_q 3Q_q^2 I_{\frac{1}{2}} \left(\frac{m_q^2}{m_h^2} \right) + \sum_\ell I_{\frac{1}{2}} \left(\frac{m_\ell^2}{m_h^2} \right) - I_1 \left(\frac{M_W^2}{m_h^2} \right) \right], \end{aligned}$$

where the spin-dependent functions, $I_s(r)$, are given by ref. [9],[11],[14],:

$$\begin{aligned} I_0(r) &= 3r \left[1 + 2r f(r) \right] \rightarrow -\frac{1}{4} + O\left(\frac{1}{r}\right), \\ I_{\frac{1}{2}}(r) &= 3 \left[2r + r(4r-1) f(r) \right] \rightarrow 1 + O\left(\frac{1}{r}\right), \quad (21) \\ I_1(r) &= 3 \left[3r + \frac{1}{2} - 3r(1-2r) f(r) \right] \rightarrow \frac{21}{4} + O\left(\frac{1}{r}\right). \end{aligned}$$

The large-mass limit is displayed explicitly in these expressions, and the function $f(r)$ is given by

$$f(r) = \begin{cases} -2 \left[\arcsin \left(\frac{1}{2\sqrt{r}} \right) \right]^2 & \text{if } r > \frac{1}{4}; \\ \frac{1}{2} \left[\ln \left(\frac{\eta_+}{\eta_-} \right) \right]^2 - \frac{\pi^2}{2} + i\pi \ln \left(\frac{\eta_+}{\eta_-} \right) & \text{if } r < \frac{1}{4}; \end{cases} \quad (22)$$

with $\eta_\pm = \frac{1}{2} \pm \sqrt{\frac{1}{4} - r}$. Similar expressions for the $c_{z\gamma}$ couplings can be found in ref. [2].

Notice that eqs. (20) reduce to expressions (19) when specialized to only the t -quark, in the large- m_t limit. Notice also that, in contrast with the cancellation of the m_t dependence in the ratio $y_t/m_t = 1/v$ in eq. (19), the contribution of light-particle loops to scalar-photon and scalar-gluon couplings are suppressed by a power of the light mass over m_h . As a result, the total scalar-photon coupling tends to be dominated by loops containing heavy particles, for which the effective lagrangian description is quite good.

Some remarks are in order about the numerical size of the various contributions (see Fig. (2)), for a light Higgs between 100 to 130 GeV. The W contribution always dominates,

with $-I_1\left(\frac{M_W^2}{m_h^2}\right)$ ranging between -5.78 and -6.39 between these Higgs masses, while the lowest-order top quark contribution $3\left(\frac{2}{3}\right)^2 I_{\frac{1}{2}}\left(\frac{m_t^2}{m_h^2}\right)$ ranges between 1.36 and 1.38 . QCD corrections and the b quark contribution are also numerically significant in what follows, since even though they are small – less than 10% of the top-quark contribution – new physics contributions are typically of the same order.

3. Connecting to Observables: Production and Decay

Given the assumption that all new particles (apart from the hypothetical newly-discovered scalar) are heavy, *all* underlying models must reduce, in their low-energy implications, to the effective lagrangian of the previous section. It follows that if empirical access is limited to this low-energy regime, then measurements of the effective couplings provide the only possible information available with which to experimentally distinguish the various underlying possibilities.

There are therefore two key questions.

- Q1. How are the effective couplings best measured? That is, which experimental results depend on which of the effective interactions?
- Q2. What do measurements of the effective interactions teach us about the underlying physics? (That is, how do the effective couplings depend on the more fundamental couplings of the various possible underlying models?)

It is the purpose of the next two sections to make the connection between \mathcal{L}_{eff} and observables, and connections to underlying models are made in §5. Since any unambiguous observation of the new scalar particle(s) involves the detection of their production and decay, this section starts with these two kinds of processes. The discussion of the indirect influence of virtual scalars on interactions involving other particles is the topic of the following section, §4. Since these virtual effects provide important constraints on the nature of the scalar particles, the bounds they imply are also included in §4.

3.1) Scalar Decays

The dominant scalar decays are described by those interactions in \mathcal{L}_{eff} which are linear in the new scalar field(s). There are three kinds of such terms, giving couplings to fermions, massive gauge bosons and massless gauge bosons. Which of these gives the dominant scalar decay mode depends on the relative size of the corresponding effective couplings, making an experimental study of the branching ratios for the various kinds of decays a first priority once such a scalar is discovered.

3.1.1) Decays to Fermions

Consider first scalar decay into a fermion antifermion pair. The scalar rest-frame differential decay rate into polarized fermion pairs, $h \rightarrow f(p, s) \bar{f}'(\bar{p}, \bar{s})$, depends on the effective Yukawa couplings in the following way:

$$\frac{d\Gamma_{\text{pol}}}{d^3 p} = \frac{N_c}{32\pi^2 m_h E \bar{E}} \left[(|y|^2 + |z|^2)(-p \cdot \bar{p} - m \bar{m} s \cdot \bar{s}) + (|y|^2 - |z|^2)(p \cdot \bar{s} \bar{p} \cdot s - p \cdot \bar{p} s \cdot \bar{s}) + i(yz^* - y^* z)(m s \cdot \bar{p} + \bar{m} \bar{s} \cdot p) \right]. \quad (23)$$

Here E (\bar{E}) is the energy of the fermion (antifermion) in the rest frame of the decaying scalar, while m and \bar{m} are their masses, and s^μ and \bar{s}^μ are their spin four-vector. N_c is a colour factor, given by $N_c = 3$ if the daughter fermions are quarks, and by $N_c = 1$ otherwise.

$y = y_{ff'}$ and $z = z_{ff'}$ denote the relevant effective Yukawa couplings of $\mathcal{L}_{\text{fermion}}^{(4)}$. Notice that it is in principle possible to measure separately the modulus of both y and z , as well as their relative phase, so long as both the polarizations and decay distributions of the daughter fermion are measured.

Unfortunately, in the most likely scenario it will not be possible to measure the polarizations of the daughter fermions. In this case rotation invariance ensures the decay is isotropic in the decaying scalar's rest frame, leaving only the total unpolarized partial rate as an observable for each decay channel. In this case the rest-frame partial decay rate becomes:

$$\Gamma_{ff'} = \frac{N_c m_h}{8\pi} \left[(|y|^2 + |z|^2)(1 - 2r_+) - \frac{2m\bar{m}}{m_h^2} (|y|^2 - |z|^2)(1 - 4r_+ + 4r_-^2)^{\frac{1}{2}} \right], \quad (24)$$

where $r_{\pm} = (m^2 \pm \overline{m}^2)/(2m_h^2)$. Clearly a measurement of $\Gamma_{ff'}$ only is insufficient in itself to measure *both* $|y|$ and $|z|$ separately.

3.1.2) Decays to W 's and Z 's

If $m_h > 160$ GeV, then decays into pairs of electroweak gauge bosons are possible. In this case the rest-frame rate for decays into polarized bosons, $h \rightarrow W^-(p, s)W^+(\overline{p}, \overline{s})$, is:

$$\frac{d\Gamma_{\text{pol}}}{d^3 p} = \frac{|a_w|^2}{32\pi^2 m_h E^2} (s \cdot \overline{s}). \quad (25)$$

Here s^μ and \overline{s}^μ are the polarization vectors for the daughter gauge bosons.

Since eq. (25) shows that the measurement of the W polarizations in this decay gives no additional information about the values of the effective couplings, we specialize to the unpolarized partial rate for this decay, which is:

$$\Gamma_{WW} = \frac{|a_w|^2}{64\pi} \left(\frac{m_h^3}{M_w^4} \right) \left(1 - 4 \frac{M_w^2}{m_h^2} + 12 \frac{M_w^4}{m_h^4} \right) \left(1 - 4 \frac{M_w^2}{m_h^2} \right)^{\frac{1}{2}}. \quad (26)$$

Similarly, if $m_h > 180$ GeV then the decay $h \rightarrow ZZ$ is allowed. The expression for the partial rate for this decay is given by making the replacements $M_w \rightarrow M_z$ and $|a_w|^2 \rightarrow \frac{1}{2}|a_z|^2$ in expression (26).

h decay into massive gauge bosons with the W 's or Z 's off-shell can also be important, especially for a light Higgs. Under certain circumstances this may be obtained straightforwardly from the SM result [12] – [15]. For example, if only the trilinear scalar/gauge-boson couplings are important, then the decay rates may be obtained simply by multiplying the SM expressions given in [12] by the overall factor $|a_w/a_w^{SM}|^2$ (or $|a_z/a_z^{SM}|^2$ as appropriate), where the SM couplings, a_w^{SM} and a_z^{SM} , are given explicitly by eq. (14). An example of where this procedure could fail would be the final state $W/Z + f\overline{f}'$, say, if the effective Yukawa couplings (y and z) are important, since this requires the inclusion of diagrams directly coupling the scalar to fermions which are usually neglected in the SM.

3.1.3) Decays to Photons

Decays of neutral scalars may be described in terms of the dimension-five operators of eq. (6). The decay rate into polarized photons, $h \rightarrow \gamma(p, \lambda)\gamma(\tilde{p}, \tilde{\lambda})$, is most simply computed in a gauge for which $p \cdot s = \tilde{p} \cdot s = \tilde{p} \cdot \tilde{s} = 0$, where $s^\mu(p, \lambda)$ and $\tilde{s}^\mu(\tilde{p}, \tilde{\lambda})$ are the photon polarization vectors, with λ and $\tilde{\lambda}$ their helicities. The result is isotropic in the scalar rest frame, with rate:

$$\Gamma_{\text{pol}}(h \rightarrow \gamma\gamma) = \frac{m_h^3}{8\pi} \left[|c_\gamma|^2 (1 - |s \cdot \tilde{s}|^2) + |\tilde{c}_\gamma|^2 |s \cdot \tilde{s}|^2 \right]. \quad (27)$$

Measurement of the photon polarization therefore permits, in principle, a disentangling of the two relevant couplings, $|c_\gamma|^2$ and $|\tilde{c}_\gamma|^2$.

The unpolarized decay rate may be computed straightforwardly, giving:

$$\Gamma(h \rightarrow \gamma\gamma) = \frac{m_h^3}{4\pi} \left(|c_\gamma|^2 + |\tilde{c}_\gamma|^2 \right). \quad (28)$$

3.1.4) $Z\gamma$ decays

The decay of the neutral scalar into a photon and Z -boson may occur if $m_h > m_Z$. The unpolarized decay rate, calculated with the use of the effective interaction (7), is given by

$$\Gamma(h \rightarrow Z\gamma) = \frac{m_h^3}{8\pi} \left(1 - \frac{M_Z^2}{m_h^2} \right)^3 \left(|c_{Z\gamma}|^2 + |\tilde{c}_{Z\gamma}|^2 \right). \quad (29)$$

3.1.5) Inclusive Decays into Hadrons

The dimension-five operators of eq. (6) also include h -gluon interactions. These are more difficult to relate to exclusive decay rates because of the extra complication of performing the hadronic matrix element of the gluon operators. Such matrix-element complications do not arise for inclusive decays, however [16], which we therefore describe here.

For states like our hypothetical scalars, which are much more massive than the QCD scale, the total hadronic decay rates are well approximated by the perturbative sum over the partial rates for decays into all possible quarks and gluons. In the present instance

this implies:

$$\Gamma(h \rightarrow \text{hadrons}) = \Gamma_{qq'} + \Gamma_{qt} + \Gamma_{tt} + \Gamma_{\text{gluons}}, \quad (30)$$

where we divide the sum over quarks into those involving two, one or no top quarks, since the top-quark contributions can arise only for sufficiently massive scalars.

Neglecting light quark masses, the quark decays are given by eq. (24):

$$\begin{aligned} \Gamma_{qq} &= \frac{3m_h}{8\pi} \sum_{qq'} \left(|y_{qq'}|^2 + |z_{qq'}|^2 \right), \\ \Gamma_{qt} &= \Gamma(h \rightarrow q\bar{t}) + \Gamma(h \rightarrow t\bar{q}) = \frac{3m_h}{4\pi} \sum_q \left(|y_{qt}|^2 + |z_{qt}|^2 \right) \left(1 - \frac{m_t^2}{m_h^2} \right)^2, \\ \Gamma_{tt} &= \frac{3m_h}{8\pi} \left[|y_{tt}|^2 \left(1 - \frac{4m_t^2}{m_h^2} \right) + |z_{tt}|^2 \right] \left(1 - \frac{4m_t^2}{m_h^2} \right)^{\frac{1}{2}}. \end{aligned} \quad (31)$$

where the expression for Γ_{qt} uses the Hermiticity property $y_{qt} = y_{tq}^*$, which follows from the reality of \mathcal{L}_{eff} .

Keeping in mind the gluon colour factor, $N = 8$, the decay to gluons is given by the analogue of eq. (28):

$$\Gamma_{\text{gluons}} = \frac{2m_h^3}{\pi} \left(|c_g|^2 + |\tilde{c}_g|^2 \right). \quad (32)$$

Clearly, depending on the size of the various effective couplings, decay processes such as these can be used to determine the magnitudes of the couplings to gauge bosons and leptons, as well as some information about the Yukawa couplings to quarks. Disentangling the couplings to different quark flavours requires a separation of the hadronic decays into specific exclusive decay modes. Although this can be cleanly done for heavy quarks — c, b, t , say — it will inevitably be complicated by hadronic matrix-element uncertainties for light quarks and gluons.

3.2) Scalar Production (Electron Colliders)

Scalar particle detection will provide information about the effective couplings which contribute to the scalar production, in addition to the information which may be extracted

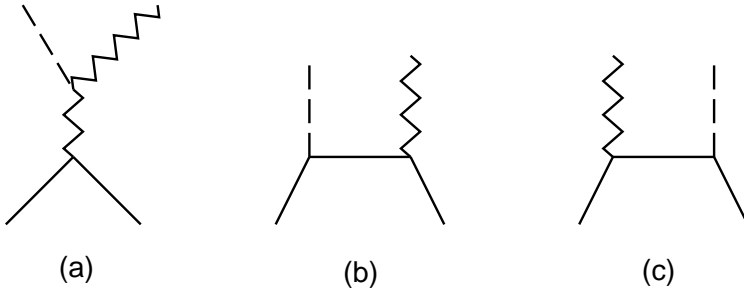


Figure (3):

The Feynman graphs which contribute the leading contribution to the reaction $f\bar{f} \rightarrow hV$, for $V=Z,\gamma$. For $V=Z$ the hZZ vertex is as given by eq. (2), while for $V=\gamma$ the $h\gamma\gamma$ vertex comes from eq. (6).

by studying the scalar decays. This section is devoted to summarizing the production rates which arise if the scalars are produced in electron (or muon) colliders, like LEP or SLC.

In electron machines neutral scalars can be emitted by any of the participants in the basic SM reaction. Since we imagine the scalars to be too heavy to be themselves directly produced in Z^0 decays, or to be produced in association with two gauge bosons, the main mode of single-scalar production is then due to the reactions $e^+e^- \rightarrow hZ$ or $e^+e^- \rightarrow h\gamma$, with the subsequent decay of the final h (and Z). The lowest order contributions to these processes arising within the effective theory correspond to the Feynman graphs of Fig. (3).

Since the reactions differ in their detailed features depending on whether it is a γ or Z which accompanies the scalar, we now consider each case separately. In order to use these results in later applications, we do not immediately specialize to electrons in the initial state, quoting instead our expressions for the more general process $f\bar{f} \rightarrow Vh$ (with $V = Z$ or γ), with an arbitrary initial fermion.

3.2.1) The Reaction $f\bar{f} \rightarrow Zh$

We give the results from evaluating the graphs of Fig. (3) using the dimension-three effective coupling, of eqs. (2), for the ZZh vertex.² We also work in the limit of vanishing

² We do not include graph (a) with an intermediate photon, using interaction (7) because this interaction has higher dimension than the one used. For many models it is also suppressed by loop factors. This neglect should be borne in mind when handling models for which the couplings a_Z^i are suppressed to be of the same order of $c_{Z\gamma}^i$.

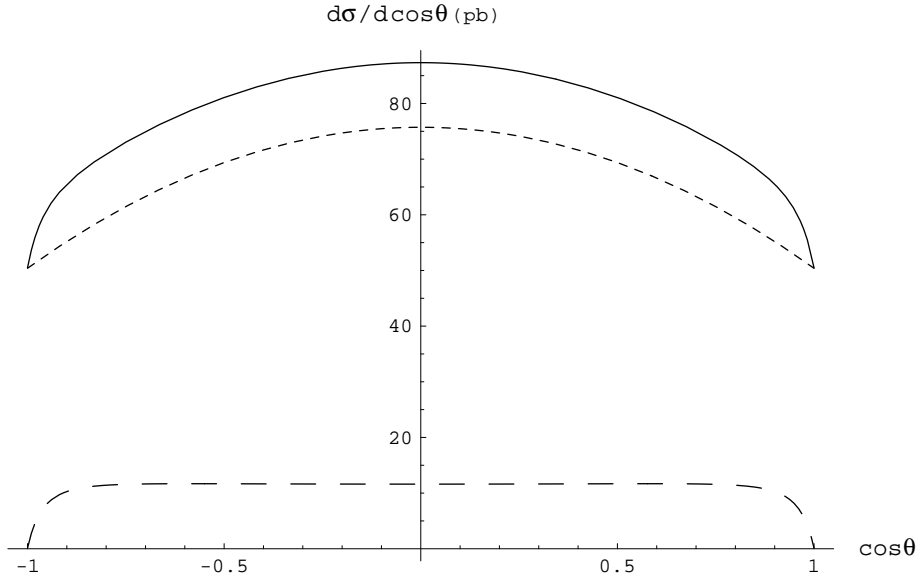


Figure (4):

The differential production cross section for the reaction $e^+e^- \rightarrow Z h$, showing the dependence on the CM scattering angle, θ , between the direction of the incoming electron and outgoing Z boson. The figure assumes the electron has 140 GeV in the CM frame, as well as SM fermion- Z couplings, a scalar mass $m_h=120$ GeV, and the effective couplings $a_Z=eM_Z/s_w c_w$, and $|\mathcal{Y}|^2=|y|^2+|z|^2=0.01 e^2$. The short-dashed line shows the contribution where the h is emitted from the Z line, and the long-dashed line gives the same with emission from either of the initial fermions. Their sum is represented by the solid line.

mass for the initial-state fermion, and use unitary gauge for the internal Z boson. (Notice that in the present context vanishing fermion mass is *not* equivalent to vanishing scalar Yukawa couplings.) In the approximation that we neglect the fermion masses, graph (a) does not interfere with graphs (b) and (c) due to their differing helicity structure. We find therefore:

$$\frac{d\sigma}{dudt} (f\bar{f} \rightarrow hZ) = \frac{d\sigma_a}{dudt} + \frac{d\sigma_{bc}}{dudt}, \quad (33)$$

with

$$\frac{d\sigma_a}{dudt} = \frac{\alpha |a_Z|^2 (g_L^2 + g_R^2)}{16s_w^2 c_w^2 s^2} \left[\frac{s + (t - M_Z^2)(u - M_Z^2)/M_Z^2}{|s - M_Z^2 + i\Gamma_Z M_Z|^2} \right] \delta(s + t + u - m_h^2 - M_Z^2), \quad (34)$$

and

$$\frac{d\sigma_{bc}}{dudt} = \frac{\alpha |\mathcal{Y}|^2}{8s_w^2 c_w^2} \left\{ \frac{(g_L - g_R)^2}{M_Z^2 s} + (g_L^2 + g_R^2) \left(\frac{1}{t^2} + \frac{1}{u^2} \right) \left(\frac{ut - m_h^2 M_Z^2}{s^2} \right) + \frac{4g_L g_R}{uts^2} \left[ut + m_h^2 (s - M_Z^2) \right] \right\} \delta(s + t + u - m_h^2 - M_Z^2). \quad (35)$$

Here s, t and u are the usual Mandelstam variables, with $t = -(p - k)^2$ where p^μ and k^μ are the 4-momenta of the incoming electron and outgoing Z boson. The constants g_L and g_R are the effective couplings of the fermion to the Z , normalized so that their SM values would be: $g_L^{SM} = T_{3f} - Q_f s_w^2$ and $g_R^{SM} = -Q_f s_w^2$. a_Z and $\mathcal{Y} = y_{ff} + iz_{ff}$ similarly denote the relevant effective couplings of h to the Z and the fermion.

These imply the following expressions for the integrated cross section, $\sigma = \sigma_a + \sigma_{bc}$:

$$\sigma_a = \frac{\alpha |a_Z|^2 (g_L^2 + g_R^2)}{96s_w^2 c_w^2 M_Z^2} \left[\frac{\lambda^{1/2} (\lambda + 12s M_Z^2)}{s^2 (s - M_Z^2)^2} \right], \quad (36)$$

and

$$\begin{aligned} \sigma_{bc} = & \frac{\alpha |\mathcal{Y}|^2}{8s_w^2 c_w^2} \left\{ \left[\frac{(g_L - g_R)^2 s}{M_Z^2} - 4(g_L^2 + g_R^2 - g_L g_R) \right] \frac{\lambda^{1/2}}{s^2} \right. \\ & \left. - \frac{2}{s^2} \left[(g_L^2 + g_R^2)(s - m_h^2 - M_Z^2) + \frac{4g_L g_R m_h^2 (s - M_Z^2)}{s - m_h^2 - M_Z^2} \right] \ln \left| \frac{M_Z^2 + m_h^2 - s + \lambda^{1/2}}{M_Z^2 + m_h^2 - s - \lambda^{1/2}} \right| \right\}, \end{aligned} \quad (37)$$

where $\lambda = (s - m_h^2 - M_Z^2)^2 - 4M_Z^2 m_h^2$.

Some of the implications of these expressions are illustrated by Figures (4) and (5), which plot the dependence of the cross section on the electron's centre-of-mass (CM) energy and on the CM scattering angle between the outgoing Z and the incoming electron. Inspection of these plots reveals the following noteworthy features:

1. *In general all three graphs, (a), (b) and (c), are required.*

It is common practice to only consider graph (a) when computing the Zh production rate within the Standard Model and many of its popular extensions. This is because the electron-scalar coupling in these models is proportional to the electron mass, and so is negligibly small. Indeed, expressions (34) and (36) reproduce the SM results once the replacement for a_Z from eq. (14) is made. The neglect of diagrams (b) and (c), which have

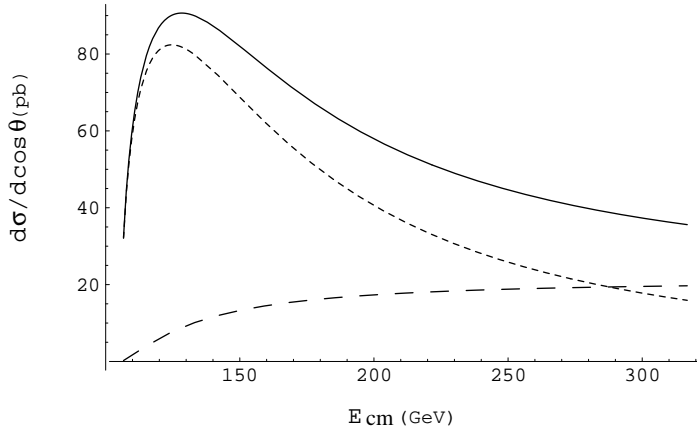


Figure (5):

The production cross section for the reaction $e^+e^- \rightarrow Z h$, as evaluated from the graphs of Fig. (3), evaluated at $\cos \theta=0$. The figures assume SM fermion- Z couplings, a scalar mass $m_h=120$ GeV, as well as the effective couplings $a_Z=eM_Z/s_w c_w$, and $|\mathcal{Y}|^2=|y|^2+|z|^2=0.01 e^2$. The significance of the dashed and solid lines is the same as in Fig. (4).

scalar emission occurring from the electron lines, in comparison with graph (a) is not always *a priori* justified, however, since models exist for which the electron Yukawa couplings are not so small. Since one of the central issues requiring addressing should a new scalar be found is precisely the question of whether its Yukawa couplings are related to masses, we do not prejudge the result here, and so keep all of graphs (a), (b) and (c).

2. Graphs (a) and (b), (c) differ in the $\cos \theta$ dependence they predict.

According to Fig. (4), graphs (a) and graphs (b) and (c) differ in the dependence on CM scattering angle they predict for the $Z h$ production cross section. In principle, given sufficient accuracy, this difference could be used to distinguish the two kinds of contributions from one another experimentally. The nature of this difference depends on the value of m_h , with scalar-*strahlung* from the initial fermions peaking more strongly about $\cos \theta = \pm 1$ for smaller scalar masses.

3. Graphs (b) and (c) predict strongly rising dependence on energy.

It can happen that energy dependence furnishes a more useful discriminator between the two kinds of production processes, as is illustrated by Fig. (5). The high-energy limit of the Zh production cross section depends sensitively on the form of the Yukawa couplings, as may be seen from the growth of the cross section which σ_{bc} predicts for $s \gg M_z^2, m_h^2$.

This strongly-rising cross section is typical of theories which involve massive spin-one particles which are not gauge bosons for linearly-realized gauge symmetries [6], [5]. Notice, for instance, that it would not arise in γh production (as we shall shortly see explicitly) because the singular term at high energies is proportional to $(g_L - g_R)^2$, which vanishes for photons. The singular behaviour does not arise in the SM because of a cancellation between the contribution of graphs (b) and (c) with the fermion-mass dependence — which is neglected here — of graph (a). Such a cancellation is possible within the SM because the linearly-realized $SU_L(2) \times U_Y(1)$ gauge invariance relates the Higgs yukawa coupling, y_f , to the fermion masses.

Since we do not assume *a priori* that our hypothetical new scalar falls into a simple $SU_L(2) \times U_Y(1)$ multiplet with the other known particles, we cannot assume that similar cancellations occur between eq. (36) and (37) in our effective theory when $s \gg M_z^2$. Indeed, the failure of these cancellations, if seen, would be good news. The unitarity violations which follow from this failure at sufficiently high energies mean that the low-energy approximation used to make sense of the effective lagrangian is breaking down. And this means that the threshholds for the production of more new particles must be encountered before this occurs. If we should find ourselves lucky enough to experimentally see such strongly rising cross sections, we could confidently expect the discovery of further new particles to follow the new scalar particle under discussion here.

3.2.2) The Reaction $f\bar{f} \rightarrow \gamma h$

Under certain circumstances the contributions to γh production may be computed by evaluating Figs. (3) using couplings taken from eqs. (4) and (6). In this section we state the necessary circumstances for these equations to apply, and give simple expressions for

the result which follows in many cases of interest.

Generally, use of effective couplings is justified provided the momentum flowing into the effective vertex is sufficiently small compared with the scale of the physics which was integrated out to produce the effective theory. For example, if the effective operators of eq. (6) are obtained by integrating out a loop involving a particle of mass m_f , then use of the effective coupling in low energy processes amounts to the neglect of corrections of order (external momenta)/ m_f .

If all of the external scalar and photons (or gluons) are on shell, then the only invariant external mass scale is set by m_h , permitting an effective calculation so long as relative contributions of order m_h^2/m_f^2 are negligible. This is the case for the h decays considered earlier, for example, as well as for gluon-gluon or photon-photon fusion within hadron colliders in some regimes of energy and scattering angle. For $h\gamma$ production in e^+e^- machines, however, the virtual boson can be strongly off-shell and so a calculation in terms of an effective operator is only justified up to corrections of order Q^2/m_f^2 , where Q^2 is the invariant momentum transfer carried by the virtual particle.

The contributions to $f\bar{f} \rightarrow h\gamma$ of effective operators like c_γ^i , \tilde{c}_γ^i , $c_{z\gamma}^i$ and $\tilde{c}_{z\gamma}^i$ are more difficult to compute in a model-independent way if it happens that they can interfere with other graphs. Indeed, experience with specific models shows that this often happens, since the couplings of these dimension-five effective interactions are usually suppressed by loop factors, and so embedding them into tree graphs gives results which can interfere with other one-loop graphs. For instance, even though the contribution to $f\bar{f} \rightarrow h\gamma$ of a heavy top quark in the SM is well described by inserting the effective coupling c_γ^h of eq. (19) into graph (a) of fig. (3), the result interferes with other amplitudes, such as loop graphs involving γh emission from a virtual W boson [17], [18]. This same interference can happen more generally, such as with a loop graph involving $h\gamma$ emission from a virtual W (using the effective coupling a_W , say).

There are important cases for which this kind of interference does not occur, and so where a simpler statement of the $c_{g,\gamma}^i$ and/or $\tilde{c}_{g,\gamma}^i$ contributions to $f\bar{f} \rightarrow h\gamma$ can be made. Interference might be forbidden, for example, by approximate symmetries like CP

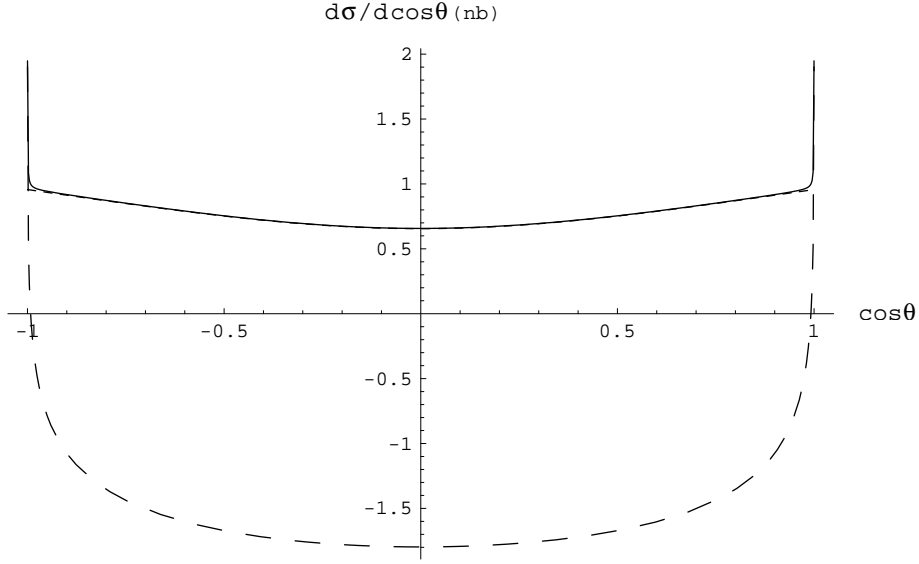


Figure (6):

The new-physics part of the differential production cross section (\tilde{c}_γ and yukawa) for the reaction $e^+e^-\rightarrow\gamma h$, as a function of CM scattering angle $\cos\theta$ (where θ is the angle between the incoming electron and the outgoing photon), evaluated at a CM energy of 140 GeV. The figure assumes QED fermion-photon couplings, a scalar mass $m_h=120$ GeV, as well as the effective couplings $\tilde{c}_\gamma=1/(246\text{ GeV})$, $\tilde{c}_{Z\gamma}=0$ and $|\mathcal{Y}|^2=|y|^2+|z|^2=0.01\text{ e}^2$. The short-dashed line corresponds to the $h-\gamma$ vertex contribution, long-dashed is the bremsstrahlung contribution and the solid line stands for the total.

invariance. As we shall see, CP invariance generally requires the vanishing of the couplings y_{fg}^h , a_w^h , a_z^h and $c_{g,\gamma}^h$ for a CP-odd pseudoscalar, h , but permits nonzero couplings of the type z_{fg}^h and $\tilde{c}_{g,\gamma}^h$. In this case only the graphs of fig. (3) play any role in $f\bar{f}\rightarrow h\gamma$, and so the cross section may be directly evaluated from these with the result $d\sigma(f\bar{f}\rightarrow\gamma h)=d\sigma_V+d\sigma_{\text{yuk}}$, where

$$\begin{aligned} \frac{d\sigma_V}{dt du} = & \frac{\alpha(t^2+u^2)}{s^3} \left[\left| Q_f \tilde{c}_\gamma + \left(\frac{g_V \tilde{c}_{Z\gamma}}{s_w c_w} \right) \frac{s}{s - M_Z^2 + i\Gamma_Z M_Z} \right|^2 \right. \\ & \left. + \left(\frac{g_A^2 \tilde{c}_{Z\gamma}^2}{s_w^2 c_w^2} \right) \left| \frac{s}{s - M_Z^2 + i\Gamma_Z M_Z} \right|^2 \right] \delta(s+t+u-m_h^2), \end{aligned} \quad (38)$$

and we have included the contributions of both virtual photon and virtual Z exchange.

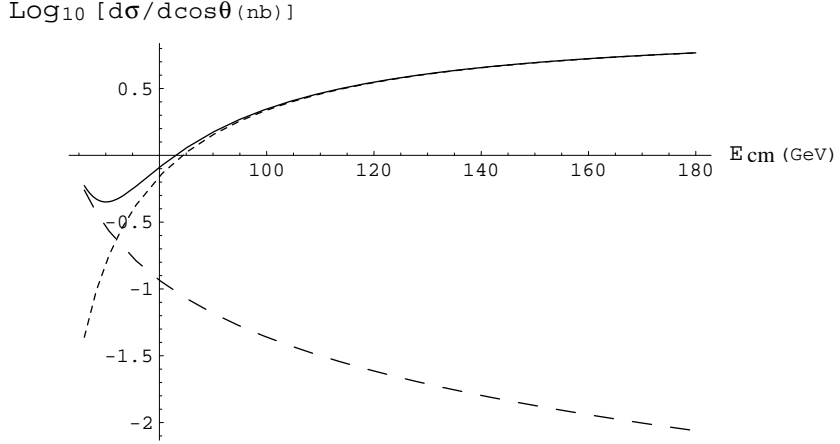


Figure (7):

The new-physics contribution to the differential production cross section for the reaction $e^+e^-\rightarrow\gamma h$, as a function of CM energy, evaluated at CM scattering angle $\cos\theta=0$. The figure assumes QED fermion-photon couplings, a scalar mass $m_h=120$ GeV, as well as the effective couplings $\tilde{c}_\gamma=1/(246$ GeV), $\tilde{c}_{Z\gamma}=0$ and $|\mathcal{Y}|^2=|y|^2+|z|^2=0.01 e^2$. The same interpretation of dashed and solid lines applies here as for the lines as in Fig. (6).

Here the effective Z -fermion couplings are $g_V=\frac{1}{2}(g_L+g_R)$ and $g_A=\frac{1}{2}(g_L-g_R)$, normalized so that their SM values would be $g_V^{SM}=\frac{1}{2}T_{3f}-Q_f s_w^2$ and $g_A^{SM}=\frac{1}{2}T_{3f}$.

Evaluating graphs (b) and (c) of the same figure – which do not interfere with graph (a) for massless initial fermions – gives the following result for $d\sigma_{\text{yuk}}$:

$$\frac{d\sigma_{\text{yuk}}}{dt du} = \frac{\alpha |\mathcal{Y}|^2 Q_f^2}{4 s^2} \left[\frac{u}{t} + \frac{t}{u} + 2 \left(1 + \frac{m_h^2 s}{u t} \right) \right] \delta(s + t + u - m_h^2). \quad (39)$$

Although interference makes the analogous results for the production of a CP-even scalar more difficult to compute it may still be done, such as by judiciously modifying the analytic SM contributions of ref. [18]. We do not pursue this observation further here, however, concentrating instead on the properties of expressions (38) and (39). These results are plotted for illustrative choices for the parameters in Figs. (6) and (7). We make the following observations:

1. Graph (a) differs strongly from graphs (b) and (c) on the dependence on CM scattering angle it predicts.

Fig. (6) shows that graphs (b) and (c) imply the well-known strong forward-peaking of the bremstrahlung cross section. This contrasts with the flatter dependence on scattering angle which follows if the h is emitted from the virtual boson line. These two properties make the differential cross section near $\theta = \frac{\pi}{2}$ a good probe of the effective couplings, c_γ , \tilde{c}_γ , $c_{z\gamma}$ and $\tilde{c}_{z\gamma}$.

2. For γh production graphs (b) and (c) do not have a rising high-energy limit.

Because the photon is massless, its gauge symmetry must be linearly realized (on peril of violations of unitarity and/or Lorentz invariance), and so the cross section, σ_{bc} , for γh production does not share the rising high-energy limit found for Zh production. For photons it is instead the cross section due to h emissions from the γ line, σ_a , which rises at high energies, eventually implying a breakdown of the low-energy approximation. In either case it is clear that the high-energy behaviour of both the Zh and γh production cross sections depends sensitively on whether the new scalars assemble into a linear realization of the electroweak $SU_L(2) \times U_Y(1)$ gauge symmetry.

3.3) Scalar Production (Hadron Colliders)

If the scalar mass is much heavier than 100 GeV, then its discovery will most likely be made at a hadron collider, rather than in an e^+e^- machine. In this case its production cross section can be more involved to compute than in the previous section. This is because the possibly large size of the scalar Yukawa couplings makes more graphs important at the parton level than is the case, say, for a SM Higgs. Unfortunately, a complete discussion of all parton processes using the couplings of the general effective lagrangian goes beyond the scope of this paper.

We instead content ourselves to recording expressions for the production processes in the case that these Yukawa couplings can be neglected. This is sufficiently general a situation to still include a great many of the most popular models. In this case production

is dominated by one or two parton processes, depending on the CM energy at which the collision occurs. We next consider the most important of these.

3.3.1) Gluon Fusion

Gluon-gluon fusion [19] is by far the dominant production mechanism for scalar bosons at the LHC (with $\sqrt{s} = 14$ TeV) throughout the scalar mass range of current interest, and in particular for very low scalar masses. For the lower energies of the next Tevatron run ($\sqrt{s} = 2$ TeV) scalar-emission processes like $q\bar{q}' \rightarrow hW$ and $q\bar{q} \rightarrow hZ$ are also important, and indeed may be preferred [20], [21] due to the large QCD background which can swamp the dominant gluon-fusion production mechanism, to the extent that the produced scalar dominantly decays through the $b\bar{b}$ channel (which need not be true in a generic model). We present results for the parton-level cross section for Wh and Zh production below, after first discussing gluon fusion.

The parton-level cross section of the gluonic process $gg \rightarrow h$, mediated by the effective interactions of eq. (6) is $\hat{\sigma} = \sigma_0 \delta(\hat{s} - m_h^2)$, with

$$\sigma_0 = \frac{\pi}{4} (|c_g|^2 + |\tilde{c}_g|^2), \quad (40)$$

where \hat{s} is the parton-level Mandelstam invariant. The lowest-order contribution to c_g by a heavy fermion is given by eq. (17) (or, as specialized to the SM top quark contribution – which is dominant – by eq. (19)).

Eq. (40) implies the following lowest-order cross section for scalar particle production by gluon fusion in pp collisions:

$$\sigma_{LO}(pp \rightarrow h + X) = \frac{\pi}{4} (|c_g|^2 + |\tilde{c}_g|^2) \tau_H \frac{d\mathcal{L}^{gg}}{d\tau_H}, \quad (41)$$

where $\tau_H = m_h^2/s$, \sqrt{s} is the total CM energy of the proton collider and $d\mathcal{L}^{gg}/d\tau_H$ is the gluon luminosity [19]:

$$\frac{d\mathcal{L}^{gg}}{d\tau_H} = \int_{\tau_H}^1 \frac{dx}{x} g(x, M^2) g(\tau_H/x, M^2). \quad (42)$$

Here M denotes the factorization scale at which the gluon structure function, $g(x, M)$, is defined.

Because this process is strongly enhanced by next-to-leading-order (NLO) QCD corrections (50 – 100%), these effects must be incorporated into any realistic calculation. A consistent treatment of the gluon-gluon parton process to next order in α_s requires the contributions of gluon emission from the initial gluon lines and internal fermion loops, in addition to virtual gluon exchange between any colour carrying lines. This must be added to other subprocesses, like gluon-quark and quark-antiquark collisions, which can also contribute to scalar production at the same order.

Combining all of these contributions, the cross section at next-to-leading order is then [11],[12],[22]:

$$\sigma(pp \rightarrow h + X) = \sigma_1 \tau_H \frac{d\mathcal{L}^{gg}}{d\tau_H} + \Delta\sigma_{gg} + \Delta\sigma_{gq} + \Delta\sigma_{q\bar{q}} \quad (43)$$

where

$$\sigma_1 = \frac{\pi}{4} \left(\left| c_g^{(1)} \right|^2 + \left| \tilde{c}_g^{(1)} \right|^2 \right) \left(1 + \frac{\alpha_s}{\pi} C_{re} \right). \quad (44)$$

Here $c_g^{(1)}$ and $\tilde{c}_g^{(1)}$ are defined to include the gluon-loop corrections to the effective couplings, c_g and \tilde{c}_g . The infrared singular part of these virtual-gluon contributions cancel the infrared singular part of real gluon emission, which is denoted in the above by C_{re} . For instance, when integrating out the top quark in the SM, $\tilde{c}_g^{(1)} = 0$ and

$$c_g^{(1)} = \frac{1}{4v} \left(\frac{\beta(\alpha_s)}{1 + \gamma_m(\alpha_s)} \right) \approx \frac{\alpha_s}{12\pi v} \left(1 + \frac{11\alpha_s}{4\pi} \right) \quad (45)$$

where $\beta(\alpha_s) = \frac{\alpha_s}{3\pi} (1 + \frac{19\alpha_s}{4\pi} + \dots)$ is the QCD beta function and $\gamma_m(\alpha_s) = \frac{2\alpha_s}{\pi} + \dots$ is the anomalous dimension for the quark mass operators. (Notice that this reproduces eq. (19) up to second order in α_s .) The SM contribution from real gluon emission is [22]:

$$C_{re} = \pi^2 + \frac{(33 - 2N_F)}{6} \ln \left(\frac{\mu^2}{m_h^2} \right) \quad (46)$$

with μ the renormalization scale.

The remainder of the contributions to eq. (43) — coming from the finite part of $\hat{\sigma}_{gg}$, $\hat{\sigma}_{gq}$ and $\hat{\sigma}_{q\bar{q}}$) — are [22]:

$$\Delta\sigma_{gg} = \int_{\tau_H}^1 d\tau \frac{d\mathcal{L}^{gg}}{d\tau} \frac{\alpha_s}{\pi} \sigma_0 \left\{ -z P_{gg}(z) \ln \left(\frac{M^2}{\tau s} \right) - \frac{11}{2}(1-z)^3 + 12 \left[\frac{\ln(1-z)}{(1-z)} - z(2-z(1-z)) \ln[1-z] \right] \right\} \quad (47)$$

$$\Delta\sigma_{gq} = \int_{\tau_H}^1 d\tau \sum_{q,\bar{q}} \frac{d\mathcal{L}^{gq}}{d\tau} \frac{\alpha_s}{\pi} \sigma_0 \left\{ \left[-\frac{1}{2} \ln \left(\frac{M^2}{\tau s} \right) + \ln(1-z) \right] z P_{gq}(z) - 1 + 2z - \frac{1}{3}z^2 \right\} \quad (48)$$

$$\Delta\sigma_{q\bar{q}} = \int_{\tau_H}^1 d\tau \sum_q \frac{d\mathcal{L}^{q\bar{q}}}{d\tau} \frac{\alpha_s}{\pi} \sigma_0 \frac{32}{27} (1-z)^3 \quad (49)$$

where these expressions assume that the particles whose loops generate the effective couplings c_k and \tilde{c}_k are much heavier than $m_h/2$. As before, M is the factorization scale of the parton densities, and P_{gg} , P_{gq} are the standard Altarelli-Parisi splitting functions [23]. Finally the remaining collinear singularities are absorbed into the renormalized parton densities [22].

The beauty of these expressions lie in their generality. Since the parton expressions use the large-mass limit for the particle in the loop responsible for the effective couplings, the decoupling of this particle from lower-energy partonic QCD is explicit in the appearance of the new physics contribution only inside the effective parton-level cross section, σ_0 and σ_1 , which are fixed in terms of c_g and \tilde{c}_g by eqs. (40) and (44). As a result, the above expressions hold for any new physics for which the process $gg \rightarrow h$ dominates the h production cross section in hadron collisions. Different kinds of new heavy particles can alter their predictions for the gluon-fusion contribution to the $pp \rightarrow hX$ cross section only through their differing contributions to σ_0 and σ_1 .

3.3.2) W, Z Fusion

To the extent that W or Z fusion processes are important, the contributions of effective scalar couplings to these processes may also be incorporated into simulations using the parton-level cross sections for $WW \rightarrow h$ or $ZZ \rightarrow h$. The differential cross section in the case of W or Z fusion can be obtained at first approximation directly from eq.(2) of ref. [24],

by multiplying this equation by a factor $s_w^2|a_w|^2/e^2M_w^2$ or $s_w^2c_w^2|a_z|^2/e^2M_z^2$ respectively.

We do not explore the detailed implications of these processes here because W and Z fusion are not expected to dominate in hadron colliders for the small scalar masses which are of interest to us.

3.3.3) Zh and Wh Production

It has been argued [20], [21] that the parton processes $\bar{q}q \rightarrow Zh$ and $\bar{q}q' \rightarrow Wh$ may prove to be more important mechanisms for h production at the Tevatron because of the difficulty in pulling the gluon fusion signal out of the backgrounds. We record here the cross sections for these parton-level processes using the effective couplings of §2.

The cross section for $\bar{q}q \rightarrow Zh$ production is directly given by eqs. (34) and (35) (or their integrated versions, eqs. (36) and (37)) provided one uses in them the couplings, g_L , g_R , y_{qq} and z_{qq} , appropriate to the quark in question. The same is true for the contribution to $\bar{q}q' \rightarrow Wh$ of graph (a) of Fig. (3) – with the scalar emitted from the W line – provided one makes the replacements

$$M_z \rightarrow M_w, \quad \Gamma_z \rightarrow \Gamma_w \quad \text{and} \quad \frac{\alpha |a_z|^2 (g_L^2 + g_R^2)}{16s_w^2 c_w^2} \rightarrow \frac{\alpha |a_w|^2}{32s_w^2} \quad (50)$$

in eq. (34) or (36).

The cross section for $\bar{q}q' \rightarrow Wh$ coming from graphs (b) and (c) of Fig. (3) – with the scalar emitted from the fermion line – requires a less trivial generalization of eqs. (35) and (37). The result for the differential cross section is:

$$\frac{d\hat{\sigma}_{bc}}{d\hat{u}d\hat{t}} = \frac{\alpha}{16s_w^2} \left\{ \frac{|\mathcal{Y}_q|^2 + |\mathcal{Y}_{q'}|^2}{2M_w^2 \hat{s}} + \left(\frac{|\mathcal{Y}_{q'}|^2}{\hat{t}^2} + \frac{|\mathcal{Y}_q|^2}{\hat{u}^2} \right) \left(\frac{\hat{u}\hat{t} - m_h^2 M_w^2}{\hat{s}^2} \right) \right\} \delta(\hat{s} + \hat{t} + \hat{u} - m_h^2 - M_w^2). \quad (51)$$

4. Connecting to Observables: The Influence of Virtual Scalars

After scalar decays and production, the next most important class of observables to consider consists of scattering processes involving only familiar SM fermions as external

states. These have the advantage of often being well measured, and since they can receive contributions from virtual scalar exchange, they provide an important source of constraints on scalar couplings.

Constraints of this type organize themselves into four broad categories according to whether they involve high- or low-energy processes (compared to the QCD scale, say), and whether they do or do not change fermion flavour. Only two of these are of interest for the present purposes since we have chosen to restrict our attention to flavour-diagonal processes. We therefore divide our discussion into two sections, which respectively describe constraints coming from high- and low-energy observables.

For the present purposes, it suffices to work at lowest order in the effective couplings when computing the implications of the new scalar for high-energy processes. The same need not be true for the low-energy observables, however. Since the decoupling of the heavy scalar ensures that its effects generically become weaker and weaker for lower energies, only the best measured observables imply significant bounds on its interactions. But precisely because these observables are so well measured, their analysis within the effective theory proves to be one of those few situations in which it is necessary to go beyond tree level in the effective interactions.

4.1) High-Energy Flavour-Diagonal Scattering

We focus in this section on two-body fermion scattering, to which virtual scalars may contribute through the Feynman graphs of Fig. (8). To these must be added the usual SM contributions, which at lowest order are also of the form of Fig. (8), but involving exchanged spin-one vector bosons (W , Z , γ and gluons). Before evaluating these cross sections in detail, we first draw some general conclusions which follow for all such processes in the (excellent) approximation in which external fermion masses are neglected.

4.1.1) Helicity Considerations

In the absence of masses for the initial and final fermions, the scalar-exchange graphs of Fig. (8) do not interfere with the vector-exchange graphs of the SM because of their

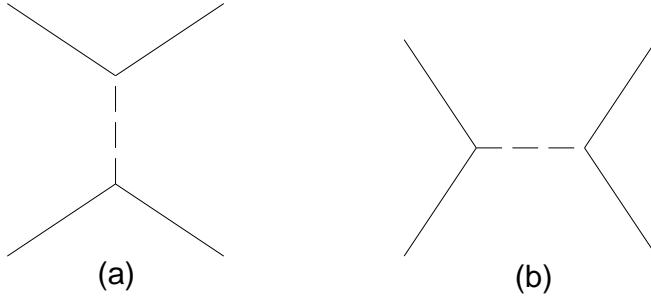


Figure (8):

The Feynman graphs which contribute the leading scalar contribution to the reactions $f\bar{f} \rightarrow g\bar{g}$ and $ff \rightarrow gg$, for light fermions f and g .

different helicity properties. This is because in the absence of fermion masses the initial and final fermions may be labelled by their helicities, which are conserved along any fermion line by vector emission, but which are flipped along fermion lines by scalar emission.

For example, in $f\bar{f}$ annihilation processes, SM vector-exchange graphs contribute only to the scattering of left- (right-) handed fermions with right- (left-) handed antifermions. The only nonzero scalar-exchange processes, on the other hand, are to the scattering of left- (right-) handed fermions with left- (right-) handed antifermions. Since processes mediated by the exchange of SM particles and virtual scalars only contribute to different helicity configurations, it follows that their contributions to the cross section cannot interfere, permitting the SM and scalar-exchange cross sections to be simply summed: *e.g.* $\sigma_{\text{tot}} = \sigma_{\text{SM}} + \sigma_h$. It therefore suffices to give explicit expressions here for the cross section due to scalar exchange only.

We now present these cross sections, doing so in steps of increasing complexity. We start by considering the particularly simple case of scattering of different flavours of fermions, since in this case only the single Feynman graph (a) or (b) of Fig. (8) contributes to the process. We describe the s -channel process, graph (a) first, followed by the t -channel process, graph (b). We then extend our conclusions to processes in which *both* graphs (a) and (b) can contribute at once.

4.1.2) s -Channel Scattering: $f\bar{f} \rightarrow g\bar{g}$

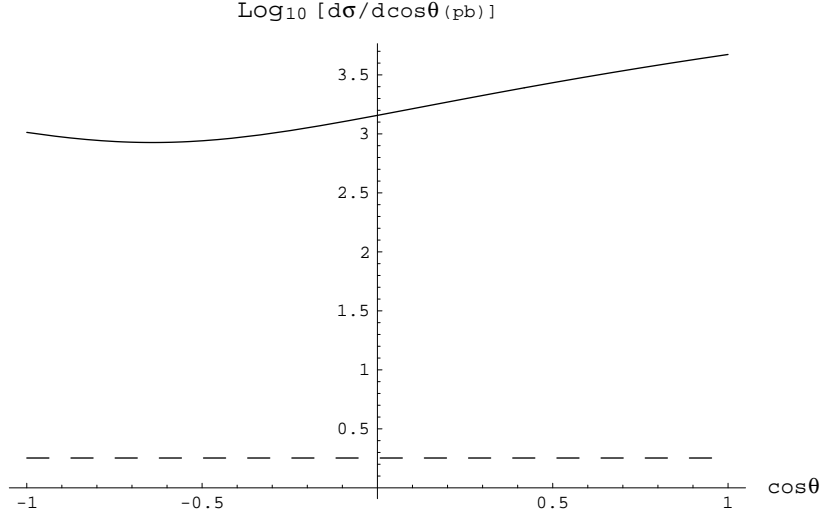


Figure (9):

A comparison of the tree-level SM (solid line) and scalar-mediated (dashed line) contributions to the differential cross section for the reaction $e^+e^- \rightarrow \mu^+\mu^-$, showing the dependence on the CM scattering angle, θ , between the direction of the incoming electron and outgoing muon. The figure assumes an electron CM energy of 100 GeV, a scalar mass $m_h=120$ GeV, and the effective couplings $|\mathcal{Y}_e|^2=|\mathcal{Y}_\mu|^2=0.01 e^2$.

Consider, then, the reaction $f\bar{f} \rightarrow g\bar{g}$ with $f \neq g$, and suppose that the flavour-changing Yukawa couplings, y_{fg} and z_{fg} , are too small to significantly contribute. With these assumptions only the s -channel diagram (a) of Fig. (8) contributes, giving the result:

$$\left(\frac{d\sigma}{du dt} \right)_{s-ch} = \frac{|\mathcal{Y}_f|^2 |\mathcal{Y}_g|^2}{16\pi} \frac{1}{(s - m_h^2)^2} \delta(s + t + u), \quad (52)$$

where $\mathcal{Y}_f = y_{ff} + iz_{ff}$ and $t = (p_f - p_g)^2$ is the Mandelstam variable defined using the 4-momenta of the initial and final fermions. Eq. (52) trivially integrates to give the total cross section:

$$\sigma_{s-ch} = \frac{|\mathcal{Y}_f|^2 |\mathcal{Y}_g|^2}{16\pi} \frac{s}{(s - m_h^2)^2}. \quad (53)$$

Figures (9) and (10) compare these expressions for the reaction $e^+e^- \rightarrow \mu^+\mu^-$ with their tree-level SM counterparts. We restrict the comparison to scattering angles $|\cos\theta| < 0.9$ — where θ is the angle between the directions of the incoming electron and

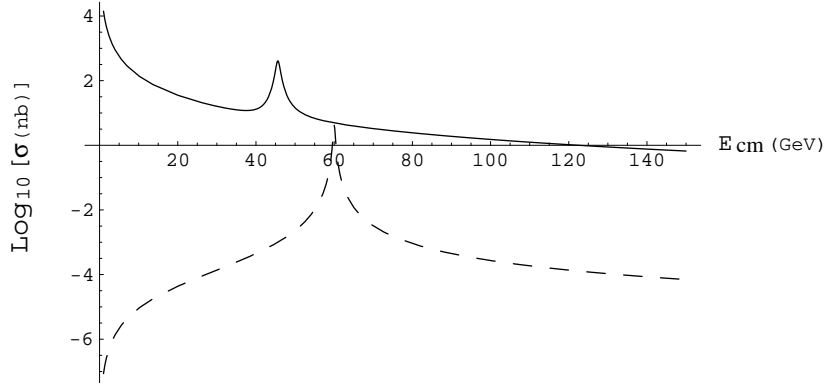


Figure (10):

A comparison of the CM energy dependence of the tree-level SM (solid line) and scalar-mediated (dashed line) cross sections for the reaction $e^+e^- \rightarrow \mu^+\mu^-$. (The cross sections are integrated only over scattering angles $|\cos \theta| < 0.9$ in order to exclude the small-angle scattering region, for which SM radiative corrections are most important.) The figure assumes a scalar mass $m_h = 120$ GeV, and the effective couplings and $|\mathcal{Y}_e|^2 = |\mathcal{Y}_\mu|^2 = 0.01 e^2$.

outgoing muon — in order to minimize configurations for which SM radiative corrections are important.

Since neither cross section grows at high energies, they must be distinguished in practice by their differing shapes as functions of both energy and scattering angle. In practice this requires resolving the potentially narrow scalar resonance from the energy dependence of the cross section. Interestingly, since the high-energy e^+e^- annihilation cross section is known only for several energies, it would be easy to miss a narrow scalar state even if the scalar mass were comparatively low.

Bounds nevertheless exist, but are comparatively weak. They are obtained by examining small-angle scattering processes, for which radiative corrections can be important because initial-state radiation can allow scattering at energies greater than resonance to profit from the large on-resonance cross section. The best current limits obtained in this

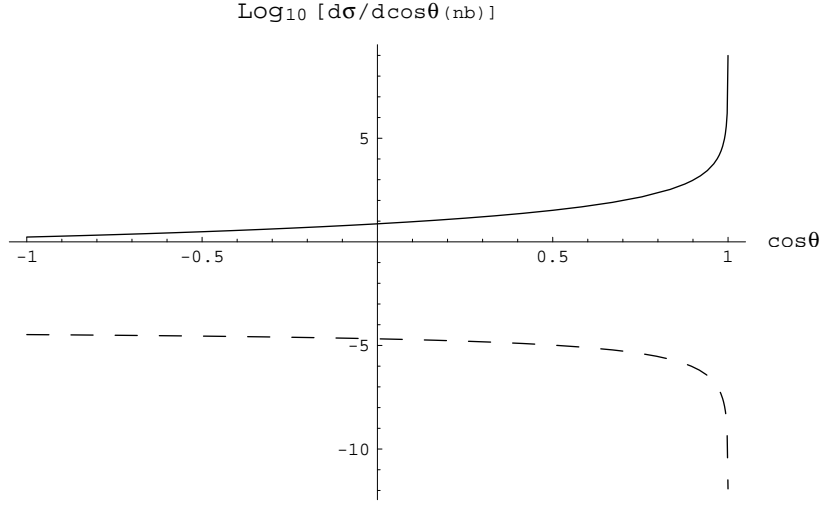


Figure (11):

A comparison of the tree-level SM (solid line) and scalar-mediated (dashed-line) contributions to the differential cross section for the reaction $e^- \mu^- \rightarrow e^- \mu^-$, showing the dependence on the CM scattering angle, θ , between the direction of the incoming and outgoing electron. The figure assumes an electron CM energy of 100 GeV, a scalar mass $m_h = 120$ GeV, and the effective couplings $|\mathcal{Y}_e|^2 = |\mathcal{Y}_\mu|^2 = 0.01 e^2$.

way from the reaction $e^+ e^- \rightarrow \mu^+ \mu^-$ [25] constrain

$$\begin{aligned} \sqrt{|\mathcal{Y}_e \mathcal{Y}_\mu|} &\lesssim 0.07 & \text{if} & \quad m_h \sim 100 \text{ GeV,} \\ &\lesssim 0.02 & \text{if} & \quad m_h \sim 190 \text{ GeV.} \end{aligned} \tag{54}$$

These bounds deteriorate sharply with larger m_h , weakening to $\sqrt{|\mathcal{Y}_e \mathcal{Y}_\mu|} \lesssim 0.3$ when $m_h \sim 300$ GeV.

4.1.3) *t*-Channel Scattering: $fg \rightarrow fg$

Consider next the reaction $fg \rightarrow fg$, again under the assumption that the flavour-changing Yukawa couplings, y_{fg} and z_{fg} , are negligibly small. As usual, neglect of fermion masses permits the SM contribution to be summed with the cross section due to scalar exchange. At tree level the scalar-mediated contribution arises only from the *t*-channel graph, (b), of Fig. (8). The result obtained from this graph is easily found by crossing the

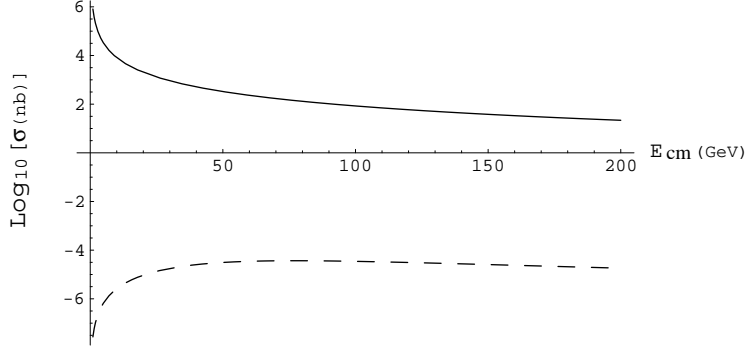


Figure (12):

A comparison of the tree-level SM (solid line) and scalar-mediated (dashed-line) contributions to the integrated cross section for the reaction $e^- \mu^- \rightarrow e^- \mu^-$, showing the dependence on the CM energy. The angular integrals are restricted to the region $|\cos \theta| < 0.9$ in order to reduce the sensitivity to initial-state radiation effects. The figure assumes a scalar mass $m_h = 120$ GeV, and the effective couplings $|\mathcal{Y}_e|^2 = |\mathcal{Y}_\mu|^2 = 0.01 e^2$.

external lines of the s -channel result, giving:

$$\left(\frac{d\sigma}{du dt} \right)_{t-ch} = \frac{|\mathcal{Y}_f|^2 |\mathcal{Y}_g|^2}{16\pi s^2} \frac{t^2}{(t - m_h^2)^2} \delta(s + t + u). \quad (55)$$

The total cross section which follows from this is:

$$\sigma_{t-ch} = \frac{|\mathcal{Y}_f|^2 |\mathcal{Y}_g|^2}{16\pi s} \left[\frac{s + 2m_h^2}{s + m_h^2} - \frac{2m_h^2}{s} \ln \left(\frac{s + m_h^2}{m_h^2} \right) \right]. \quad (56)$$

Figure (11) displays the dependence of this cross section on the CM-frame scattering angle, with the tree-level SM result plotted for the purposes of comparison. They differ significantly, with the SM result showing the characteristically strong forward scattering due to the exchange of the massless photon. The energy dependence of the integrated cross section is similarly displayed in Fig. (12).

This kind of scattering would contribute to the interaction cross section of electron-nucleon collisions, such as is measured at HERA, by modifying the parton level process

$eq \rightarrow eq$ or $e\bar{q} \rightarrow e\bar{q}$. This contribution is in addition to any others, such as to modifications of the process $\gamma\gamma \rightarrow h$ or $gg \rightarrow h$ which can be mediated by the effective couplings $c_g, \tilde{c}_g, c_\gamma$ or \tilde{c}_γ .

To date, experimental searches for scalars at HERA appear to have been restricted either to flavour-changing leptoquarks or to supersymmetry-motivated models with two Higgs doublets (2HDMs), for which relatively weak bounds exist [26], [27]. Unfortunately, these analyses are not directly applicable to the general possible scalar couplings, since they either presuppose negligible Yukawa couplings to electrons and light quarks, or assume more dramatic flavour-changing couplings.

Even though their signatures differ, a rough indication of the strength of the bounds which are possible for the neutral scalars considered here may be had by comparing with the results of the leptoquark searches, for which sensitivity is claimed to scalars in the mass range of several hundred GeV if their Yukawa couplings are electromagnetic in strength: $|\mathcal{Y}| \sim e$. It would clearly be valuable to have a more detailed, model-independent study of the effects of scalar exchange at ep colliders.

4.1.4) Scattering of Identical Fermions: $ff \rightarrow ff$

When the initial and final fermion pairs are all of the same flavour graph (b) of Fig. (8) must be summed with the same graph with the final fermions interchanged. Besides contributing to electron-electron collisions, this kind of scattering process also plays a role in high-energy hadron collisions through parton process like $qq \rightarrow qq$. Unfortunately, as we found for scalar production at hadron colliders, one cannot simply adapt existing studies of scalar-mediated scattering in hadron machines to infer bounds on the quark-scalar Yukawa couplings, because the light-quark Yukawa couplings are typically assumed to be negligible in these papers. We regard a detailed simulation of hadron collisions to be beyond the scope of this paper, and so do not pursue these processes more closely in what follows.

Summing the two relevant graphs gives the contribution of scalar exchange to elastic

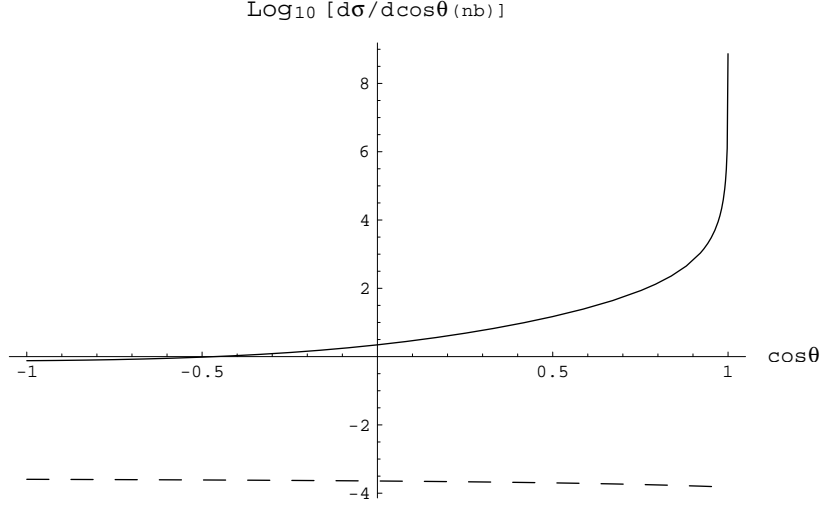


Figure (13):

A comparison of the tree-level SM (solid line) and scalar-mediated (dashed-line) contributions to the differential cross section for Bhabha scattering, $e^+e^- \rightarrow e^+e^-$, showing the dependence on the CM scattering angle, θ , between the direction of the incoming and outgoing electron. The figure assumes an electron CM energy of 100 GeV, a scalar mass $m_h=120$ GeV, and the effective couplings $|\mathcal{Y}_e|=0.1$ e.

ff scattering:

$$\begin{aligned}
 \frac{d\sigma_{\text{sc}}}{dt du}(ff \rightarrow ff) &= \frac{|\mathcal{Y}_f|^4}{16\pi s^2} \left[\frac{3}{4} \left(\frac{t}{t-m_h^2} + \frac{u}{u-m_h^2} \right)^2 + \frac{1}{4} \left(\frac{t}{t-m_h^2} - \frac{u}{u-m_h^2} \right)^2 \right] \delta(s+t+u) \\
 &= \frac{|\mathcal{Y}_f|^4}{16\pi s^2} \left[\frac{t^2}{(t-m_h^2)^2} + \frac{ut}{(u-m_h^2)(t-m_h^2)} + \frac{u^2}{(u-m_h^2)^2} \right] \delta(s+t+u).
 \end{aligned} \tag{57}$$

The first expression in eq. (57) has a simple interpretation, since the interchange $t \leftrightarrow u$ corresponds to exchanging the momenta of the final-state fermions. Since statistics dictate that the complete amplitude must be antisymmetric under the interchange of both momenta and spin, the two terms in the first of eq. (57) correspond to the scattering rates with the initial two fermions prepared in an overall spin-triplet or spin-singlet state.

The total cross section is obtained by integrating eq. (57) over t and u and dividing

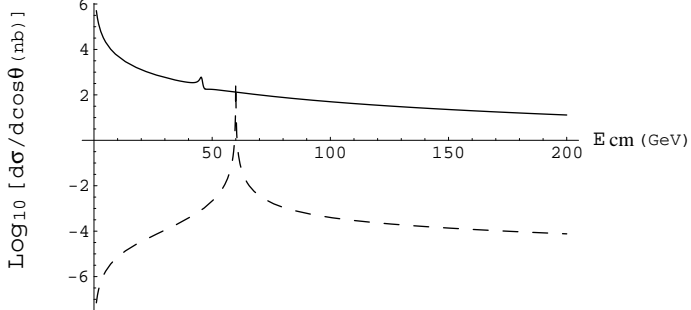


Figure (14):

A comparison of the tree-level SM (solid line) and scalar-mediated (dashed-line) contributions to the integrated cross section for Bhabba scattering, $e^+e^- \rightarrow e^+e^-$, showing the dependence on the CM energy. The differential cross section is integrated only over the region $|\cos\theta| < 0.9$ in order to reduce the size of radiative corrections. The figure assumes a scalar mass $m_h = 120$ GeV, and the effective couplings $|\mathcal{Y}_e| = 0.1$ e. by 2 to account for identical fermions in the final state:

$$\sigma_{\text{sc}}(ff \rightarrow ff) = \frac{|\mathcal{Y}_f|^4}{32\pi s} \left[\frac{3s + 5m_h^2}{s + m_h^2} - \frac{2m_h^2}{s} \left(\frac{3s + 5m_h^2}{s + 2m_h^2} \right) \ln \left(\frac{s + m_h^2}{m_h^2} \right) \right]. \quad (58)$$

4.1.5) Scattering of Identical Fermions: $f\bar{f} \rightarrow f\bar{f}$

The final high-energy process we consider is the reaction $f\bar{f} \rightarrow f\bar{f}$, whose cross section may be obtained from the result of the previous section by crossing symmetry. One finds in this way $\sigma(f\bar{f} \rightarrow f\bar{f}) = \sigma_{\text{SM}} + \sigma_{\text{sc}}$, with:

$$\frac{d\sigma_{\text{sc}}}{dt du}(f\bar{f} \rightarrow f\bar{f}) = \frac{|\mathcal{Y}_f|^4}{16\pi s^2} \left[\frac{t^2}{(t - m_h^2)^2} + \frac{st}{(s - m_h^2)(t - m_h^2)} + \frac{s^2}{(s - m_h^2)^2} \right] \delta(s + t + u). \quad (59)$$

The integrated cross section then becomes:

$$\begin{aligned} \sigma_{\text{sc}}(f\bar{f} \rightarrow f\bar{f}) = & \frac{|\mathcal{Y}_f|^4}{16\pi s} \left[\frac{s + 2m_h^2}{s + m_h^2} + \frac{s^2}{(s - m_h^2)^2} + \frac{s}{s - m_h^2} \right. \\ & \left. - \frac{m_h^2}{s} \left(\frac{3s - 2m_h^2}{s - m_h^2} \right) \ln \left(\frac{s + m_h^2}{m_h^2} \right) \right]. \end{aligned} \quad (60)$$

The dependence of these results on CM scattering angle and energy are summarized in Figs. (13) and (14). Searches for scalar contributions to the process $e^+e^- \rightarrow e^+e^-$ at LEP furnish the best existing bounds on the strength of the electron Yukawa couplings, which depend in detail on the scalar mass [25]. The constraints inferred for the size of potential electron Yukawa couplings improve as m_h increases from 100 to 190 GeV, and then decrease with still higher scalar masses. The 95% CL exclusion limits at a few representative energies are

$$\begin{aligned}
 |\mathcal{Y}_e| &\lesssim 0.12 & \text{if} & \quad m_h \sim 100 \text{ GeV,} \\
 &\lesssim 0.01 & \text{if} & \quad m_h \sim 190 \text{ GeV,} \\
 &\lesssim 0.16 & \text{if} & \quad m_h \sim 300 \text{ GeV.}
 \end{aligned} \tag{61}$$

4.2) Expressions for Low-Energy Observables

Besides contributing directly to high-energy scattering, scalar particle exchange can induce various observable effects at energies, E , much smaller than m_h . Even though the size of these effects are typically suppressed by small powers like E/m_h , the high precision of low-energy measurements can sometimes lead to strong constraints on combinations of couplings.

Precisely because the applications envisaged are to energies much smaller than m_h , it is again fruitful to employ an effective-lagrangian approach. To do so we imagine successively integrating out all particles, starting with the new scalar and proceeding down to very low energies. Of the many effective interactions amongst the ordinary SM particles which are generated by integrating out the scalar, those of lowest dimension are most important, being least suppressed by powers of $1/m_h$. A complete list of these is easily made, and here we follow the notation of ref. [7] (which also gives expressions for how these effective couplings contribute to observables, as well as numerical bounds which experiments imply for their size).

The following three classes of operators emerge as being of most interest (and are examined in more detail in the remainder of this section):

1. *Dimensions 2, 3 and 4:* The lowest-dimension effective couplings which are well measured describe W and Z propagation (most notably through the parameter $\rho = M_W^2/M_Z^2 c_w^2$) as well as W and Z couplings to fermions, and so are constrained by precision electroweak data. Because these receive contributions at loop level in the scalar effective theory, the bounds they imply for the scalar effective couplings are comparatively weak. Other operators like fermion masses and trilinear and quartic gauge-boson self-couplings also arise at this dimension, but do not provide practical constraints on scalar couplings because they are much less accurately measured. (For example, to see possible contributions of h loops to m_e would require independent precise measurements of the electron mass at low and high energies, and the latter of these is practically impossible.)
2. *Dimensions 5:* Of the larger number of dimension-5 effective interactions, anomalous photon and gluon couplings to fermions are the best measured, and so furnish the best bounds on the scalar couplings. Of these the CP-violating electric- and chromoelectric-dipole operators provide the best limits, because they cannot be confused with SM CP violation.
3. *Dimensions 6:* Some four-fermi interactions are the best measured of the many dimension-six operators which are possible. This is particularly true for those operators which break exact or approximate SM conservation laws, like flavour conservation or CP symmetry.

Before turning to the more detailed discussion of these categories, a general remark is required concerning the nature of the bounds which can be obtained in this way. Since the generic Lagrangian presented in §2 is effective, it is imagined to have been obtained after integrating out other heavier degrees of freedom having mass Λ , say. In general this integration generates many effective couplings which do not involve the scalar h at all, in addition to the h -dependent ones which are our focus here. The main point to be made is that we disregard any possible conspiracy between these two classes of contributions to low-energy observables, and treat the experimental limits as applying solely to the h -mediated contributions. This is reasonable so long as the bound obtained is quite

strong, since then the cancellation which would be required between the scalar-mediated and direct contributions in order to evade this bound would be unnatural. It is a less believable assumption if the bounds are weak, since then partial cancellations between these contributions to observables could be plausible.

4.2.1) Integrating Out the Scalar (Tree Level)

We now integrate out the scalar at tree level. There are two types of new interactions which are induced by scalar particle exchange: effective quartic gauge boson self-couplings and effective four-fermion interactions. We find the following quartic boson couplings:

$$\mathcal{L}_b^{(\text{tree})} = \frac{a_w^2}{2m_h^2} (W_\mu^* W^\mu)^2 + \frac{a_z^2}{8m_h^2} (Z_\mu Z^\mu)^2. \quad (62)$$

Unfortunately deviations of these couplings from their SM values are not strongly constrained experimentally, and so the limits derived from them are very weak.

The four-fermion interactions arising at tree level are

$$\begin{aligned} \mathcal{L}_f^{(\text{tree})} &= -\frac{1}{m_h^2} \sum_{ff'gg'} \bar{f}(y_{ff'} + i\gamma_5 z_{ff'}) f' \bar{g}(y_{gg'} + i\gamma_5 z_{gg'}) g', \\ &= -\frac{1}{m_h^2} \sum_{fg} \bar{f}(y_f + i\gamma_5 z_f) f \bar{g}(y_g + i\gamma_5 z_g) g + (\text{flavour-changing terms}), \end{aligned} \quad (63)$$

where $y_f = y_{ff}$, $z_f = z_{ff}$ and the sum runs over light fermions having masses $m_f \ll m_h$. The terms not written explicitly in the second equality involve the flavour-changing couplings, y_{fg} and z_{fg} , which we assume to be negligibly small.

Low-energy loop corrections to this Lagrangian can be important, largely due to the strength of the strong interactions at low energies. Thus, the interactions of eqs. (62) and (63) should be evolved using the renormalization group (RG) down to the energy scales at which a specific low-energy process occurs (e.g. m_B , m_D , m_K , m_n , etc.). This can be done perturbatively unless the low-energy scale lies below the QCD scale. In what follows we incorporate the resulting leading-order perturbative anomalous dimensions into our expressions when computing implications for observables.

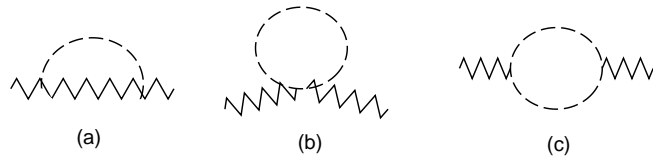


Figure (15):

The Feynman graphs which contribute at one loop to gauge boson vacuum polarizations.

4.2.2) Integrating Out the Scalar (One Loop)

At one-loop level a much wider variety of effective operators is possible, although with effective couplings which necessarily involve small loop-suppression factors. These can nevertheless be important if the reactions they mediate can be cleanly predicted in the SM and are very well measured. With a few exceptions – such as precision tests of QED – this requirement focuses our attention onto low-dimension effective operators which violate exact or approximate SM selection rules or conservation laws.

Since we do not consider flavour-changing scalar Yukawa couplings, we become restricted to violations of other approximate conservation laws (like mass suppressions due to approximate helicity conservation, or CP violation), and to precision measurements like anomalous magnetic moments. We are led in this way to consider loop-generated contributions to gauge-boson vacuum polarizations as well as to effective fermion-photon and fermion-gluon effective interactions.

- *Oblique Corrections:*

The graphs of fig. (15) give the one-loop scalar-mediated contributions to the electroweak vacuum polarizations. All three graphs are ultraviolet divergent, implying that the scalar/gauge-boson couplings mix under renormalization with effective spin-one mass and kinetic operators. This mixing introduces a logarithmic dependence on the renormalization point, μ , of these effective couplings, which are the effective theory's way of keeping track of potentially large logarithms of mass ratios in any underlying theory.

For instance, integrating out a single scalar field, h , gives the following contributions

to the W and Z effective mass terms, renormalized at $\mu = m_h$:

$$\delta m_V^2 = \frac{1}{16\pi^2} \left[-a_V^2 + b_V m_h^2 + \frac{g_V^2}{4} (m_h^2 + M_V^2) \right] \ln \left(\frac{\Lambda^2}{m_h^2} \right), \quad (64)$$

where we neglect all masses in comparison with m_h , $V = W, Z$ and Λ is the scale at which the original scalar effective lagrangian of §2 is defined. (In practice Λ can be taken as the mass of the lightest particle which generated \mathcal{L}_{eff} once it was integrated out.) The quantity g_V requires some explanation: g_z denotes the trilinear coupling of eq. (5) between the new scalar, h , and the unphysical scalar, z , which would have been absorbed into the longitudinal Z polarization in unitary gauge, but which arises in the renormalizable gauges we use to evaluate figs. (15). g_w denotes the analogous coupling between h , W and the electrically charged unphysical scalar, w . The SM contribution is obtained from (64) by substituting the couplings of eqs. (14) and (15), and using $g_z = e/(s_w c_w)$ and $g_w = e/s_w$.

Although these mass shifts are not themselves detectable, they contribute to measurable ‘oblique’ corrections to W and Z vacuum polarizations [28], [29].³ For example, they contribute to the parameter $\rho = M_w^2/(M_z^2 c_w^2)$ as follows:

$$\begin{aligned} \Delta\rho = \rho - 1 = & -\frac{1}{16\pi^2} \left\{ \left[\left(\frac{a_w}{M_w} \right)^2 - \left(\frac{a_z}{M_z} \right)^2 \right] - m_h^2 \left[\left(\frac{b_w}{M_w^2} \right) - \left(\frac{b_z}{M_z^2} \right) \right] \right. \\ & \left. - \frac{1}{4} \left[(m_h^2 + M_w^2) \left(\frac{g_w}{M_w} \right)^2 - (m_h^2 + M_z^2) \left(\frac{g_z}{M_z} \right)^2 \right] \right\} \ln \left(\frac{\Lambda^2}{m_h^2} \right). \end{aligned} \quad (65)$$

Although all terms proportional to m_h^2 in this equation vanish when specialized to the couplings of the SM Higgs, the others do not. The resulting nonzero value precisely cancels the divergent ($\ln \Lambda^2$) contributions to $\Delta\rho$ which arise from other SM graphs, not involving the physical Higgs, h . Once the Λ dependence of these other graphs has cancelled in this way, what remains is the well-known SM logarithmic m_h dependence of $\Delta\rho$ [28]:

$$\Delta\rho = -\frac{3\alpha}{16\pi c_w^2} \ln \left(\frac{m_h^2}{M_z^2} \right) + (\text{non logarithmic terms}). \quad (66)$$

³ If powers of M_Z^2/m_h^2 cannot be neglected then a generalization of the usual parameterization of these oblique corrections is required [30].

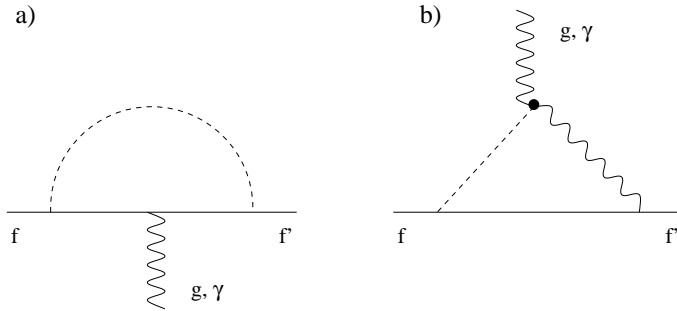


Figure (16):

The Feynman graphs which contribute at one loop to low energy effective interactions between light fermions and massless gauge bosons.

Contributions to the other oblique parameters may be computed along similar lines, although we do not do so here because the bounds which follow on the effective scalar couplings are not particularly strong.

- *Vertex Corrections:*

Another class of well-measured effective operators are the dimension-five modifications to the fermion-photon and fermion-gluon interactions, which we consider in detail next.

Evaluating the scalar-fermion and scalar-gauge boson exchange diagrams of Fig. (16), we consider separately the contribution of graphs (a) and (b). It is useful to group the results of evaluating graph (a) according to whether they are proportional to the internal fermion mass, the external fermion mass, or neither. That is: $\mathcal{L}^a = \mathcal{L}_{\text{int}}^a + \mathcal{L}_{\text{ext}}^a + \mathcal{L}_{\text{neith}}^a$. Neglecting all external momenta and masses in comparison with m_h we find, for flavour-

changing Yukawa couplings:

$$\begin{aligned}
\mathcal{L}_{\text{int}}^a &= \frac{eF_{\mu\nu}}{32\pi^2 m_h^2} \sum_{fkf'} Q_k m_k G_1 \left(\frac{m_k^2}{m_h^2} \right) \bar{f} \sigma^{\mu\nu} [y_{fk} y_{kf'} - z_{fk} z_{kf'} + i\gamma_5 (y_{fk} z_{kf'} + z_{fk} y_{kf'})] f', \\
\mathcal{L}_{\text{ext}}^a &= \frac{eF_{\mu\nu}}{32\pi^2 m_h^2} \sum_{fkf'} Q_k G_2 \left(\frac{m_k^2}{m_h^2} \right) \bar{f} \sigma^{\mu\nu} [(m_f + m_{f'}) (y_{fk} y_{kf'} + z_{fk} z_{kf'}) \\
&\quad + i\gamma_5 (m_f - m_{f'}) (y_{fk} z_{kf'} - z_{fk} y_{kf'})] f' \\
\mathcal{L}_{\text{neith}}^a &= \frac{e\partial^\mu F_{\mu\nu}}{32\pi^2 m_h^2} \sum_{fkf'} Q_k G_3 \left(\frac{m_k^2}{m_h^2} \right) \bar{f} \gamma^\nu [y_{fk} y_{kf'} + z_{fk} z_{kf'} + i\gamma_5 (y_{fk} z_{kf'} - z_{fk} y_{kf'})] f',
\end{aligned} \tag{67}$$

The result for the case of external gluons is obtained from this by a simple substitution: $eQ_f F_{\mu\nu} \rightarrow g_s G_{\mu\nu}^a t^a$. Furthermore, since one is free to simplify an effective lagrangian using the lowest-order equations of motion, the derivative $\partial^\mu F_{\mu\nu}$ can be eliminated in favour of the electromagnetic (or colour) current by using the equations of motions for the electromagnetic (gluon) field. Expressions (67) follow for light external fermions if only terms linear in m_f and $m_{f'}$ are retained. The (possibly large) mass, m_k , of the intermediate fermion is not neglected, and appears through the invariant functions $G_k(a)$, given by

$$\begin{aligned}
G_1(a) &= \frac{1}{2(1-a)^2} (-3 + 4a - a^2 - 2\ln a) \\
G_2(a) &= \frac{1}{12(1-a)^4} (20 - 39a + 24a^2 - 5a^3 + 12\ln a - 6a\ln a) \\
G_3(a) &= -\frac{1}{18(1-a)^4} (38 - 81a + 54a^2 - 11a^3 + 24\ln a - 18a\ln a).
\end{aligned} \tag{68}$$

For flavour-diagonal couplings, $f = f' = k$ we have significant simplifications and the results are given by

$$\mathcal{L}^a = e \sum_f \left[-\frac{1}{2} F_{\mu\nu} \bar{f} \sigma^{\mu\nu} \left(d_f^a + i\gamma_5 \tilde{d}_f^a \right) f + A_f^a \partial^\mu F_{\mu\nu} \bar{f} \gamma^\nu f \right], \tag{69}$$

with the leading contributions to these effective couplings being given (for large m_h^2/m_f^2)

by:

$$\begin{aligned}
d_f^a &= \frac{Q_f m_f}{16\pi^2 m_h^2} \ln\left(\frac{m_h^2}{m_f^2}\right) (y_f^2 + 3z_f^2), \\
\tilde{d}_f^a &= -\frac{Q_f m_f}{8\pi^2 m_h^2} \ln\left(\frac{m_h^2}{m_f^2}\right) y_f z_f \\
A_f^a &= \frac{Q_f m_f}{24\pi^2 m_h^2} \ln\left(\frac{m_h^2}{m_f^2}\right) (y_f^2 + z_f^2).
\end{aligned} \tag{70}$$

Unlike graph (a), graph (b) of Fig. (16) diverges (logarithmically) in the ultraviolet implying a mixing between the operators of eq. (6) and the (chromo-) magnetic- and electric-dipole moment operators we are considering here. As was the case for the vacuum polarization graphs considered earlier, this mixing tracks potentially large logarithms, through the logarithmic dependence on the renormalization point which it implies for these effective couplings. For example, if in the SM we regard c_g and c_γ to be generated by integrating out the t quark, then the effective couplings are defined by matching conditions at scale $\mu = m_t$. Renormalization of the effective couplings down to $\mu = m_h$, where the scalar particle is integrated out, generates the logarithmic factor $\ln(m_t^2/m_h^2)$, which directly appears in a full SM calculation.

To the extent that such logarithms are large, it makes sense to keep track of only the divergent term, and this is most easily done simply by cutting off the integral at the scale of new physics responsible for the generation of the c_i . Although this misses terms which are subdominant to the logarithm, which can be dangerous if the mass ratio is not enormous (as m_t/m_h is not for a light SM Higgs), it suffices for our present purposes wherein we look only for order-of-magnitude limits. For the same reasons, it suffices for numerical purposes to evaluate the large logarithm itself as being order unity, which we do in what follows. Thus we have

$$\begin{aligned}
\mathcal{L}^b &= \frac{e F_{\mu\nu}}{16\pi^2} \ln\left(\frac{\Lambda^2}{m_h^2}\right) \sum_{f,f'} Q_f \bar{f} \sigma^{\mu\nu} (y_{ff'} c_\gamma + z_{ff'} \tilde{c}_\gamma + i\gamma_5 (y_{ff'} \tilde{c}_\gamma + z_{ff'} c_\gamma)) f' \\
&= -\frac{e}{2} F_{\mu\nu} \sum_f \bar{f} \sigma^{\mu\nu} (d_f^b + i\gamma_5 \tilde{d}_f^b) f + (\text{flavour-changing terms}),
\end{aligned} \tag{71}$$

with

$$d_f^b = -\frac{Q_f}{16\pi^2} (y_f c_\gamma + z_f \tilde{c}_\gamma) \ln\left(\frac{\Lambda^2}{m_h^2}\right), \quad \tilde{d}_f^b = -\frac{Q_f}{16\pi^2} (y_f \tilde{c}_\gamma + z_f c_\gamma) \ln\left(\frac{\Lambda^2}{m_h^2}\right). \quad (72)$$

These expressions have the noteworthy feature of not being suppressed by inverse powers of m_h , making them more sensitive in the limit of large scalar masses.

- *Four-Fermion Interactions:*

Effective four-fermion interactions receive non-trivial contributions at one loop level which may contain more information about various scalar-fermion couplings. In particular, the box diagrams, involving either hh or hW exchange, may induce some structures not already contained in the tree-level terms. Since we neglect flavour-changing couplings for h , it turns out that only the hW -exchange diagram produces significant bounds:

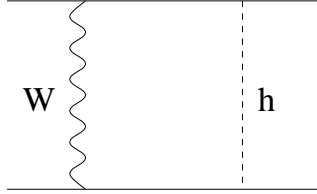


Figure (17):

The Feynman graph (plus those obtained through various permutations of the bosonic lines) which contribute into a low energy four-fermion interaction

$$\mathcal{L}_{box} = -\frac{G_F}{\sqrt{2}} \frac{V_{ff'} V_{gg'}^*}{16\pi^2} \frac{M_W^2}{m_h^2 - M_W^2} \ln\left(\frac{m_h^2}{M_W^2}\right) \times \sum \left[(\bar{f} \Gamma_{ff'} f') (g \Gamma_{gg'} g') + (\bar{f} \sigma_{\mu\nu} \Gamma_{ff'} f') (g \sigma^{\mu\nu} \Gamma_{gg'} g') \right] + h.c.. \quad (73)$$

In this expression $V_{ff'}$ are the elements of the Kobayashi-Maskawa mixing matrix and $\Gamma_{ff'}$ denotes the following combination of couplings:

$$\Gamma_{ff'} = y_f - y_{f'} - iz_f - iz_{f'} - \gamma_5(y_f + y_{f'} - iz_f - iz_{f'}) \quad (74)$$

As in the previous cases, the box graphs are computed in the limit of small external masses and momenta. We also use an explicitly renormalizable gauge for the W -propagator.

4.2.3) Comparison with Precision Measurements

We now turn to constraints on the couplings of the effective low-energy Lagrangians we have just constructed.

- *Anomalous Magnetic Moments:*

The quantities $d_e = d_e^a + d_e^b$ and $d_\mu = d_\mu^a + d_\mu^b$ contribute directly to the anomalous magnetic moment of the electron and muon, with

$$\delta a_i = 2m_i d_i \quad (75)$$

where the anomalous moment is defined as $a_i = (g_i - 2)/2 = (\mu_i/\mu_{B_i}) - 1$, where $\mu_{B_i} \equiv e_i/2m_i$ is the Bohr magneton (in units for which $\hbar = c = 1$) and $i = e, \mu$.

A bound is obtained by requiring δa_μ to be smaller than the 1.6σ experimental error of the present experimental value [31], $a_\mu^{\text{exp}} = 1\ 165\ 923\ 0(84) \times 10^{-10}$. The strong $(m_\mu/m_h)^2$ dependence of $m_\mu d_\mu^a$ implies that only a weak bound on the scalar Yukawa couplings is obtained from this constraint:

$$\left(\frac{100 \text{ GeV}}{m_h}\right)^2 \left(y_\mu^2 + 3z_\mu^2\right) < 0.07. \quad (76)$$

For this limit we have used $m_h = 100$ GeV to evaluate the logarithm of eq. (70). The same bound as applied to d_μ^b in eq. (72) (evaluated at $\mu = m_\mu$) gives a stronger limit, due to its weaker dependence on m_h :

$$\left(y_\mu c_\gamma + z_\mu \tilde{c}_\gamma\right) < 5 \cdot 10^{-4}. \quad (77)$$

Although eq. (77) looks quite restrictive, in order to limit y_μ and z_μ some information about the effective couplings c_γ and \tilde{c}_γ is necessary. To get a rough estimate we use the SM t -quark value of eq. (19): $\tilde{c}_\gamma^{SM} = 0$ and $c_\gamma^{SM}(t) = 2\alpha/(9\pi v) = 2.25 \cdot 10^{-6} \text{ GeV}^{-1}$, to learn that

$$y_\mu \left(\frac{c_\gamma}{c_\gamma^{SM}(t)}\right) \lesssim 2. \quad (78)$$

Clearly only weak limits are obtained from these observables.

- *Electric Dipole Moments:*

The presence of both scalar and pseudoscalar couplings of h to fermions breaks CP invariance. In the flavour-conserving channel this should lead to the generation of electric dipole moments (EDMs) for elementary particles and atoms. This can be used to usefully constrain the effective couplings because SM CP-violation due to the Kobayashi-Maskawa matrix is known to produce EDMs many orders smaller than are the current experimental limits (see, e.g. ref. [32]).

The best experimental constraints come from the searches for the EDMs of the neutron [33], paramagnetic [34] and diamagnetic atoms [35]. Although the results of the experiments with paramagnetic atoms are often interpreted as limits on the electron EDM, there are often many other possible contributions to the EDM of paramagnetic atoms from other effective low-energy couplings, such as from CP-odd semi-leptonic four-fermion operators like $\bar{e}\gamma_5 e \bar{q}q$ and the like. Because of the potentially large number of effective operators in eqs. (63) and (67) which can contribute to the EDMs of the neutron and diamagnetic atoms, closed form expressions for these moments are problematic, if not impossible, to obtain.

At the same time, there could be direct contributions to EDMs generated at the scale Λ , without direct participation of the scalar h . These cannot be taken into account in our approach unless the underlying theory is more fully specified. In fact, for some models these direct contributions can be more important than h -mediated terms. In view of this, we follow the strategy outlined earlier of treating every operator as giving an independent contribution to EDM, which is separately constrained from experiment, assuming no cancellations with other terms. We must keep in mind when so doing not to trust weak bounds that arise in this way.

To obtain constraints we combine the theoretical analysis performed in refs. [36] and [37] with the experimental results of [33], [34] and [35]. The limits found in this way are presented in Table 1. The rows of this table are labelled by flavour-diagonal parity odd

(pseudoscalar) couplings, while its columns are labelled by parity even (scalar) ones. All CP-violating effective couplings involve products of one of each of these. For example, the quantity \tilde{d}_e represents a contribution to the electron EDM, which is strongly constrained by atomic EDM measurements. Eq. (70) gives this quantity in terms of the product $z_{ee} y_{ee}$, and the bound which follows on this product may be read from the $z_{ee} - y_{ee}$ element of the table.

Electron-quark cross terms in the table represent limits imposed by atomic EDMs on the operators of the form $\bar{e}\gamma_5 e \bar{q}q$ and $\bar{e}e \bar{q}\gamma_5 q$, while those involving cross terms of the form $z_f c_\gamma$ and $y_f \tilde{c}_\gamma$ come from bounds on effective couplings like those of eq. (72). Finally those involving products of the form $c_g \tilde{c}_g$, $c_\gamma \tilde{c}_\gamma$, etc., are obtained by estimating their contribution either to the CP-odd three gluon operator [38] or to quark dipole moments, induced by these combinations at two loops.

All limits are given for $m_h = 100$ GeV and should be quadratically rescaled for different values of m_h except for the limits in two last rows and columns which are sensitive to m_h only logarithmically. The effective coupling constants $c_{\gamma(g)}$ and $\tilde{c}_{\gamma(g)}$ are taken in units of $(100 \text{ GeV})^{-1}$, and one-loop QCD RG evolution coefficients have been taken into account where necessary, with all couplings taken at the renormalization point of 100 GeV.

-	y_{ee}	y_{uu}	y_{dd}	y_{ss}	c_γ	c_g
z_{ee}	$1 \cdot 10^{-5}$	$3 \cdot 10^{-9}$	$3 \cdot 10^{-9}$	$6 \cdot 10^{-9}$	$1.5 \cdot 10^{-9}$	$1.5 \cdot 10^{-6}$
z_{uu}	$5 \cdot 10^{-9}$	$1.5 \cdot 10^{-7}$	$1.5 \cdot 10^{-7}$	$3 \cdot 10^{-7}$	$2 \cdot 10^{-7}$	$1 \cdot 10^{-8}$
z_{dd}	$5 \cdot 10^{-9}$	$1.5 \cdot 10^{-7}$	$1.5 \cdot 10^{-7}$	$3 \cdot 10^{-7}$	$1 \cdot 10^{-7}$	$1 \cdot 10^{-8}$
z_{ss}	$1 \cdot 10^{-6}$	$7 \cdot 10^{-7}$	$7 \cdot 10^{-7}$	$\sim 10^{-6}$	$\sim 10^{-5}$	$\sim 10^{-6}$
\tilde{c}_γ	$1.5 \cdot 10^{-9}$	$2 \cdot 10^{-7}$	$1 \cdot 10^{-7}$	$\sim 10^{-5}$	~ 1	$\sim 10^{-1}$
\tilde{c}_g	$1 \cdot 10^{-6}$	$1 \cdot 10^{-8}$	$1 \cdot 10^{-8}$	$\sim 10^{-6}$	$\sim 10^{-1}$	$\sim 10^{-4}$

Table 1:

The limits on the couplings of scalar h with light fermions, photons and gluons imposed by various EDM experiments.

A few comments about these limits are in order. First, we implicitly assume the absence of dangerous CP-violating operators like $G_{\mu\nu}\tilde{G}^{\mu\nu}$, such as might be assured by existence of a PQ symmetry, for example. Second, several entries marked with the symbol ‘~’ represent at best an order-of-magnitude estimate, since their extraction from the observables involves hadronic matrix elements which cannot be reliably estimated. The same symbol marks the entries which give rise to EDMs at two-loop level, which we estimate here simply on dimensional grounds, although more refined calculations are feasible. This is the case for the $c_\gamma\tilde{c}_\gamma$ entry, for example, which generates a quark EDM at two loops. The combination $c_g\tilde{c}_g$, which we bound by estimating the three-gluon CP-odd operator, $\text{Tr}(GG\tilde{G})$ [38], which it generates, has in addition a large matrix-element uncertainty which further complicates the estimate for the size it implies for nucleon and atomic EDMs.

These constraints can be further generalized to give bounds on the yz -combinations of heavy-quark/scalar couplings. Thus, $y_{bb}z_{bb}$ contributes at two-loop order to the operator, $\text{Tr}(GG\tilde{G})$, leading to the approximate bound, $y_{bb}z_{bb} < 10^{-2} - 10^{-3}$.

What might be the implications of these limits for collider physics? Let us imagine a situation in which the scalar-electron coupling y_{ee} is taken at the edge of the limit coming from Bhabha scattering, eq. (61), and so which conceivably might be seen in the decay of the new scalar. Then the limit $y_{ee}z_{ee} \lesssim 10^{-5}$ coming from the electron EDM data is so strong that it requires very high statistics to detect any spin correlations in the decay $h \rightarrow e^+e^-$. The EDM constraints cannot similarly exclude measurable spin correlations in h decays into heavier fermions, however. For example, even the bound $y_{bb}z_{bb} \lesssim 10^{-2}$ quoted earlier is not sufficient to rule out spin correlations in $h \rightarrow \bar{b}b$, because it permits $y_{bb} \sim z_{bb}$ to be as large as $|y_{bb}| \sim 0.1$.

- *Pion Decays:*

In this subsection we consider the decays of the neutral and charged pions induced by scalar exchange at tree or one-loop level. Leptonic pion decay is sensitive to scalar couplings because of the well-known suppression its SM contribution receives from powers of the final-state lepton masses. Here we study what may be learned from these decays about the couplings of h -particles to light fermions.

We start with the decay $\pi^0 \rightarrow e^+ e^-$, whose amplitude is tremendously suppressed in the SM by electromagnetic loop factors and the electron mass. It has been measured only recently to have branching ratio $B = (7.5 \pm 2.0) \cdot 10^{-8}$. The effective coupling of eq. (63), induced by scalar exchange, contributes to this decay with the rate

$$\Gamma_{\pi^0 \rightarrow ee} = \eta^2 \frac{m_\pi}{8\pi} \left(\frac{m_\pi}{m_h} \right)^4 \left(\frac{F_\pi}{m_u + m_d} \right)^2 (z_{uu} - z_{dd})^2 (z_{ee}^2 + y_{ee}^2), \quad (79)$$

where $\eta \simeq 5$ is a QCD RG coefficient. Here we evaluate the relevant strong matrix element, $\langle \text{vac} | (z_{uu} \bar{u} \gamma_5 u + z_{dd} \bar{d} \gamma_5 d) | \pi^0 \rangle$ using chiral perturbation theory, with $F_\pi = 92$ MeV and current quark masses defined at the renormalization point $\mu = 1$ GeV.

Although the observed branching ratio agrees in order of magnitude with SM predictions, a detailed comparison is complicated by theoretical uncertainties in the SM amplitude. We therefore obtain our bound by requiring eq. (79) to be of order the SM process, which we take to be $\lesssim 10^{-7}$ of the total width. This produces the following limit:

$$\left(\frac{100 \text{ GeV}}{m_h} \right)^4 (z_{uu} - z_{dd})^2 (z_{ee}^2 + y_{ee}^2) \lesssim 10^{-4}. \quad (80)$$

The decays of charged pions can be even more restrictive. In this case the hadronic uncertainties can be cancelled by considering a ratio of two branching ratios, such as $R = \Gamma_{\pi^+ \rightarrow \nu_e e^+} / \Gamma_{\pi^+ \rightarrow \nu_\mu \mu^+}$. Although this process proceeds at tree level if charged scalars exist, it cannot do so given only neutral scalars, such as is the present focus. Instead it is mediated by the effective interaction, eq. (73), induced by the box graph involving hW exchange. This effective Lagrangian generates a decay amplitude which interferes with the SM result, giving the following correction to the $\nu_e e$ partial width:

$$\delta \Gamma_{\pi^+ \rightarrow \nu_e e^+} = \eta \frac{m_\pi^3 F_\pi^2 G_F^2 |V_{ud}|^2}{16\pi^3} \left(\frac{M_W^2}{m_h^2 - M_W^2} \right) \ln \left(\frac{m_h^2}{M_W^2} \right) \frac{m_e}{m_u + m_d} (y_e(z_d - z_u) + z_e(y_d + y_u)) \quad (81)$$

This correction can be quite significant since the SM decay width is suppressed by the small electron mass.

Measurements of the ratio R constrain the Yukawa coupling combination in eq. (81) provided that these couplings break lepton universality (as is often true in models having large Yukawa couplings). If so, then the experimental bound $\delta R \approx \delta\Gamma_{\pi^+ \rightarrow \nu e^+}/\Gamma_{\pi^+ \rightarrow \nu_\mu \mu^+} < 8 \cdot 10^{-7}$, implies an important limit:

$$y_e(z_d - z_u) + z_e(y_d + y_u) < 4 \cdot 10^{-5}. \quad (82)$$

In summary, we see that while there are important limits on scalar/fermion and scalar/gauge-boson couplings coming from low- and high-energy processes, they are relatively weak in that they do not cover much of parameter space. In particular, they are insufficient as yet to significantly constrain the best-motivated models of new scalar physics, and they are very far from being sensitive to the Higgs-fermion couplings predicted by the SM. This is true even for electron couplings, about which the strongest limits are known.

5. Predictions for Effective Couplings in Specific Models

Whereas the previous sections are dedicated to identifying the possible low-energy scalar interactions and their implications for experiment in as model-independent a way as possible, in this section we change gears and explore what form the effective couplings take in a number of representative models. Because it is more model-specific, this section more closely follows results that appear in many places throughout the literature.

Our main motivation for making contact with models is to profit from the interplay between the generality of the effective lagrangian approach, and the predictiveness of the underlying models. By comparing how different classes of models contribute to the effective couplings, and combining this with the previous sections' expressions for their implications for observables, we intend to learn which observables best discriminate between the various models on the market. Indeed, the detailed discussion of this discrimination is the climax of this paper, and is the topic of the next section.

Partially motivated by the next section's comparison, the models are discussed in this section in the order of increasing similarity with the Standard Model. We start with a

very brief discussion of a particular kind of composite scalar which does not carry a linear realization of the electroweak gauge group, but then devote most of our attention to models involving scalars in various electroweak representations.

5.1) Strong Electroweak Symmetry Breaking

Models for new physics broadly divide into two classes, according to whether or not the sector which breaks the electroweak gauge symmetries is strongly or weakly coupled. Unfortunately, the predictions of models in which this sector is strongly coupled [40] are difficult to accurately obtain, precisely because of these strong couplings. Partly because of this there is no canonical reference model which involves well-understood dynamics and which is known to satisfy all experimental constraints. This makes a general survey of their properties more difficult to perform, since these properties are less definitively understood.

For the present purposes we content ourselves with focussing on some of the properties of the lightest scalar states, which typically arise as pseudo-Goldstone bosons for spontaneously broken approximate flavour symmetries [41]. Since the low-energy couplings of such particles are more constrained by the symmetry-breaking pattern itself, their properties may be predicted more robustly.

In particular, since the Goldstone boson for any exact symmetry must decouple at low energies, variables can always be chosen to ensure that these bosons are derivatively coupled in the low-energy action [42]. Of course, strictly massless bosons are not of realistic interest in the present context, so the relevant spontaneously broken symmetries are usually taken to be only approximate. Nonzero masses and nonderivative couplings are then permitted, but they are suppressed by the small symmetry-breaking parameters which must be present if the symmetry limit is to be a good approximation. Unfortunately, to the extent that the low-energy scalar couplings do depend on these parameters they also become more model dependent.

One feature which often distinguishes such pseudo-Goldstone bosons (pGBs) [43] is their absence of direct tree-level couplings to electroweak gauge bosons. This is because the electroweak gauge group is typically a subgroup of the larger flavour group whose

spontaneous breaking produces the pGBs in the first place. But because pGBs quite generally transform in the adjoint representation of this group, they typically must transform as either singlets or doublets of $SU_L(2)$. Since electroweak interactions typically raise the masses of the doublet states, one often finds the lowest-energy neutral scalar to be an electroweak singlet, which does not couple to W 's and Z 's at tree level [44].

W and Z couplings can be generated once loops are taken into account, however. For instance, an analogy with QCD suggests one class of effective couplings which can be phenomenologically significant, and yet also is reasonably model independent. This class consists of the parity-violating dimension-five interactions of eqs. (6), since these are often determined purely by the anomalies of the global symmetries of interest. For instance, in QCD pions are pGBs for approximate chiral $SU_L(2) \times SU_R(2)$ transformations, and the $U(1)$ subgroup to which the π^0 corresponds has an electromagnetic anomaly. In the effective theory of pions obtained at energies below the chiral-symmetry breaking scale, $\Lambda_\chi \sim 4\pi F_\pi \sim 1$ GeV, this anomaly is represented by an effective interaction of the form

$$\mathcal{L}_{\text{eff}} = -\tilde{c}_{\gamma\pi} \pi^0 F_{\mu\nu} \tilde{F}^{\mu\nu} \quad \text{with} \quad \tilde{c}_{\gamma\pi} = \frac{\alpha N_c}{12\pi F_\pi} = \frac{\alpha}{4\pi F_\pi}, \quad (83)$$

which is well known to correctly describe neutral pion decay once inserted into eq. (28).

For models with strongly-coupled electroweak-breaking sectors, electromagnetic (or QCD) anomalies amongst the approximate global symmetries generically arise, so interactions of the above form coupling light scalar states to photons (or gluons and electroweak bosons) are expected to arise, but with

$$\tilde{c}_\gamma \sim O\left(\frac{\alpha}{4\pi v}\right) \quad \text{and/or} \quad \tilde{c}_g \sim O\left(\frac{\alpha_s}{4\pi v}\right). \quad (84)$$

c_γ and c_g might also be expected to be of the same order of magnitude.

5.2) Linearly Realized Electroweak Multiplets: Generalities

The rest of the models we consider contain scalars which acquire their coupling to gauge bosons because they arise as explicit members of (linearly-realized) representations

of the electroweak gauge group. We will call scalars of this type *elementary* scalars. Although scalars are elementary (in this sense) in models where the electroweak symmetry breaking is due to perturbative physics, they need not be restricted to this case. For instance electroweak symmetry breaking might arise dynamically within a strongly-coupled supersymmetric model which also contains other ‘elementary’ scalars.

It proves to be useful divide models with elementary scalars into two subcategories when discussing how experiments can differentiate them from one another. We therefore distinguish between: (i) light scalars which arise as part of a multiplet whose nonzero *v.e.v.* breaks the electroweak symmetries, and so contributes to the mass to ordinary SM particles; and (ii) light scalars arising within multiplets which do not acquire *v.e.v.s.* and so whose couplings are not significantly connected to particle masses. In this paper we reserve the name *Higgs* particle only for scalars in class (i).

Before quoting expressions for effective couplings in some specific models, we first concentrate on what features are generic to the tree-level couplings in all models where the light scalar is elementary. We do so for the scalar/gauge-boson and scalar/fermion interactions.

Consider, then, a collection ($k = 1, \dots, n$) spinless particles transforming under various representations of the $SU_L(2) \times U_Y(1)$ electroweak gauge group. We may without loss of generality choose to represent these particles using real scalar fields, ϕ_k , in which case the gauge generators represented on the scalars, T_a, Y , are imaginary and antisymmetric $n \times n$ matrices. With these choices the tree-level scalar-gauge boson couplings come from the scalar kinetic terms

$$\mathcal{L}_{\text{kin}} = -\frac{1}{2} \sum_{k=1}^n \mathcal{D}_\mu \phi_k \mathcal{D}^\mu \phi_k \quad (85)$$

where the covariant derivative is defined in the usual way:

$$\mathcal{D}_\mu = \partial_\mu - igW_\mu^a T^a - \frac{i}{2} g' Y B_\mu. \quad (86)$$

Since tree-level scalar-gauge boson couplings arise purely from the scalar kinetic term in the lagrangian, their form may be relatively cleanly specified in terms of the electroweak

representation content of the scalar sector.

5.2.1) Gauge Boson Masses

The electroweak gauge bosons acquire their masses once some of the scalars acquire nonzero *v.e.v.s.*, v_k . If we assume negligible mixing between the $SU_L(2) \times U_Y(1)$ gauge bosons and other spin-one particles, then the W_μ^a and B_μ are related to the physical gauge bosons through the usual rotation $A_\mu = W_\mu^3 s_w + B_\mu c_w$, $Z_\mu = W_\mu^3 c_w - B_\mu s_w$ and $W_\mu^\pm = (W_\mu^1 \mp iW_\mu^2)/\sqrt{2}$, where (as before) c_w and s_w are the cosine and sine of the weak mixing angle, θ_w , which relates the couplings g and g' to the electric charge e via the relations $g = e/s_w$ and $g^2 + (g')^2 = e^2/(s_w^2 c_w^2)$. In terms of these quantities (and, as stated earlier, neglecting any mixing with a Z' or W') the tree-level gauge boson masses become:

$$M_W^2 = \frac{e^2}{2s_w^2} v^T (\vec{T}^2 - T_3^2) v \quad \text{and} \quad M_Z^2 = \frac{e^2}{s_w^2 c_w^2} v^T T_3^2 v. \quad (87)$$

In these expressions the superscript ‘ T ’ denotes the transpose of the n -component column vector of scalar fields, and the charge neutrality of the vacuum, $Q v = 0$, has been used, where in our conventions the electric charge is given by $Q = T_3 + \frac{Y}{2}$. The vector sum \vec{T}^2 denotes the quadratic Casimir operator for $SU_L(2)$, with eigenvalues $t(t+1)$ for non-negative integer or half-integer t . A second observable combination of these quantities is given by the tree-level expression for Fermi’s constant:

$$\frac{1}{\sqrt{2}G_F} = \frac{4s_w^2 M_W^2}{e^2} = 2 v^T (\vec{T}^2 - T_3^2) v. \quad (88)$$

A basic constraint which must be imposed on any realistic model is the success of the SM tree-level prediction, $\rho = M_W^2/(M_Z^2 c_w^2) = 1$, since deviations from this prediction are currently limited by experiment to be $\lesssim O(10^{-3})$ [31]. Inspection of eq. (87) shows that this constrains the scalar expectation values, through their connection to ρ :

$$\rho = 1 + \Delta\rho = \frac{v^T (\vec{T}^2 - T_3^2) v}{2 v^T T_3^2 v}. \quad (89)$$

We may read off the contribution of each multiplet to this expression: $\Delta\rho = \sum_k (\Delta\rho)_k$ with

$$\Delta_k \rho = \frac{(t_k(t_k+1) - 3t_{3k}^2) v_k^2}{2\mathcal{V}}, \quad (90)$$

where t_k and t_{3k} are the weak isospin and the eigenvalue of T_3 on scalar field ϕ_k , and $\mathcal{V} = \sum_k t_{3k}^2 v_k^2$, with all multiplets included in the sum.

At tree level the experimentally ‘safe’ representations are therefore those for which the neutral scalars satisfy $t_{3k}^2 = \frac{1}{3} t_k(t_k+1)$ [3]. Clearly this only has solutions with integer or half-integer t_{3k} for particular values for t . Besides the standard simple solutions – $t = 0$ or $t = \frac{1}{2}$ with $t_3 = \pm\frac{1}{2}$ – the next smallest solutions are $t = 3, y = 4$, or $t = \frac{25}{2}, y = 15$, etc.. Barring unnatural cancellations, for any other representations, $\Delta\rho \neq 0$ at tree level, and so agreement with experiment implies an upper bound on each scalar’s *v.e.v.*.

5.2.2) Scalar-Gauge Boson Vertices

With these preliminaries in hand, the tree-level scalar-gauge couplings involving the electrically neutral scalars may be written in terms of the mass eigenfields quite generally, as follows.

The physical scalar states are obtained by first shifting all fields by their *v.e.v.s*, and then rotating the result to diagonalize the scalar mass matrix:

$$\phi_k \rightarrow v_k + A_{kl} h_l, \quad (91)$$

where A is an $n \times n$ orthogonal matrix. For electrically neutral scalars, and in the absence of W and Z boson mixing, the dimension-three scalar-vector couplings of eq. (2) then become

$$\begin{aligned} a_w^i &= \frac{e^2}{s_w^2} \left[A^T \left(\vec{T}^2 - T_3^2 \right) v \right]^i, \\ a_z^i &= \frac{2e^2}{s_w^2 c_w^2} \left[A^T T_3^2 v \right]^i. \end{aligned} \quad (92)$$

The dimension-four scalar-vector couplings of eq. (5) are similarly given by:

$$\begin{aligned} b_w^{ij} &= \frac{e^2}{s_w^2} \left[A^T \left(\vec{T}^2 - T_3^2 \right) A \right]^{ij} \\ b_z^{ij} &= \frac{2e^2}{s_w^2 c_w^2} \left[A^T T_3^2 A \right]^{ij} \\ g_z^{ij} &= \frac{ie}{s_w c_w} \left[A^T T_3 A \right]^{ij}. \end{aligned} \quad (93)$$

These expressions clearly reduce to the usual SM formulae, eqs. (14) and (15), in the special case of a lone doublet scalar field, for which $n = 1$, $A = 1$, $t = \frac{1}{2}$ and $t_3 = -\frac{1}{2}$. They also lend themselves to the derivation of general relations amongst the coupling constants, which can be used to discriminate amongst the various kinds of models.

For instance, suppose $k = 1$ represents the lightest scalar state, which we assume has been observed. Comparison of eqs. (87) and (92) show that the WWh trilinear couplings for this scalar are related to the W mass by:

$$\frac{a_w^1}{e M_w / s_w} = \frac{\sqrt{2} \sum_k A_{k1} \lambda_k v_k}{\sqrt{\sum_l \lambda_l v_l^2}}, \quad (94)$$

where the sum is over all neutral scalars in the electroweak basis, and λ_k denotes the eigenvalue, $\lambda_k = t_k (t_k + 1) - t_{3k}^2$, for each multiplet.

The ratio of coupling to mass of eq. (94) is unity at tree level in the Standard Model: $(a_w s_w / e M_w)_{SM} = 1$. By contrast, in a model containing only doublets and singlets we have $\lambda_k = 0$ or $\frac{1}{2}$ for *all* electrically neutral scalars, and so eq. (94) reduces to

$$\frac{a_w^1}{e M_w / s_w} = \frac{\sum_k A_{k1} v_k}{\sqrt{\sum_l v_l^2}} \leq 1, \quad (95)$$

where the final inequality follows because eq. (95) may be interpreted as the inner product of two unit vectors, $\vec{e} \cdot \vec{f}$, with components $e_k = A_{k1}$ (which has unit length because A is orthogonal) and $f_k = v_k / \sqrt{\sum_k v_k^2}$. As a result the ratio $a_w^1 s_w / (e M_w)$ is always smaller than one for any model involving only doublets and singlets.

The same need *not* be true once other representations are included, as we make clear in detail with examples once we examine individual models in subsequent sections. In particular, the lower bound $t(t+1) - t_3^2 \geq t$ implies that $\lambda_k > \frac{1}{2}$ for all representations other than singlets or doublets. The general statement is this: the ratio $a_W^1/(eM_W/s_w)$ *must* be smaller than one for a model containing only doublets and singlets, but can be either larger or smaller than unity when other multiplets also appear, depending on the details of the scalar *v.e.v.s*, and their mixing matrix, A_{ij} . Although no definite conclusions are possible if this ratio should be experimentally found to be smaller than one, singlet/doublet models may be ruled out if it should be greater than unity.

Comparing the trilinear ZZh vertex with the Z mass only permits somewhat weaker conclusion. The argument is identical to the one presented above

$$\frac{a_Z^1}{e M_Z/s_w c_w} = \frac{2 \sum_k A_{k1} t_{3k}^2 v_k}{\sqrt{\sum_l t_{3l}^2 v_l^2}}, \quad (96)$$

We see that the conclusion $a_Z^1 s_w c_w / e M_Z \leq 1$ follows inevitably for any model having negligible W and Z mixing, and for which the only scalars with nonzero *v.e.v.s* have $t_3 = \pm \frac{1}{2}$ or $t_3 = 0$ (regardless of the total isospin, t , carried by each multiplet).

5.2.3) Fermion-Scalar Vertices

Since the overwhelming majority of experiments are performed using light fermions as initial or final particles, the fermion Yukawa couplings are perhaps the most crucial interactions to measure once a scalar particle is discovered. In this section we collect general tree-level results concerning these couplings.

Imagine coupling an arbitrary collection of scalar fields, ϕ_i , to a general set of fermion fields, χ^r . We are free to choose, without loss of generality, all scalar fields to be real and all spinor fields to be majorana. (With this choice electrically charged particles like electrons are represented by two spinor fields – *e.g.*: one for e_L^- and one for e_R^- – just as electrically charged spinless particles are represented by one complex, and so two real, scalar fields.) If the particles are organized into linear representations of the electroweak gauge group, then we must require their interactions to be invariant under the variation

$\delta\phi = i\omega^a T_a \phi$ and $\delta\chi = i\omega^a \mathcal{T}_a \gamma_L \chi - i\omega^a \mathcal{T}_a^* \gamma_R \chi$, where γ_L and γ_R denote the projection matrix onto left- and right-handed spinors.

The most general fermion mass terms and renormalizable scalar/fermion interactions which are possible are given by:

$$-\mathcal{L}_{\text{yuk}} = \frac{m_{rs}}{2} \bar{\chi}^r \gamma_L \chi^s + \frac{\Gamma_{rs}^i}{2} \bar{\chi}^r \gamma_L \chi^s \phi_i + \text{h.c.}, \quad (97)$$

where the coefficient matrices, Γ_{ab}^i are required by electroweak gauge invariance to satisfy $\Gamma_{rs}^j (T_a)_j^i + \Gamma_{rt}^i (\mathcal{T}_a)_s^t + (\mathcal{T}_a)_r^t \Gamma_{ts}^i = 0$. Once the scalars acquire nonzero *v.e.v.s*, v_i , the left-handed fermion mass matrix therefore becomes $M = m + \Gamma^i v_i$.

The rotation from an interaction basis to a mass basis is accomplished by performing an orthogonal rotation, A_{ij} , amongst the scalars, as well as a unitary rotation, $U^r{}_s$, amongst the left-handed fermion fields: $\chi^r = U^r{}_s \gamma_L \eta^s + U^{r*}{}_s \gamma_R \eta^s$. The matrix U is chosen to ensure that the fermion masses are diagonal and nonnegative: $U^T M U = \text{diag}(m_1, m_2, m_3, \dots)$.

The Yukawa couplings amongst the physical propagation eigenstates therefore become:

$$y_{rs}^i = \left(U^T \Gamma^j U \right)_{rs} A_j^i. \quad (98)$$

The main observation concerning these couplings, which drives much of the model building, is that they need not be diagonal in their fermionic indices (r, s) when expressed in terms of mass eigenstates. If not, then scalar emission changes fermion flavour, a prospect which in many circumstances is very strongly precluded by experiment.

Of course, the SM provides an important example where such flavour changes do not arise. They do not because the model has only one Higgs particle and its *v.e.v.* is the only source of mass in the entire model. As a result we have $M = \Gamma v$ and so the same rotation which diagonalizes the fermion masses automatically also diagonalizes $y = U^T \Gamma U = \text{diag}(y_1, y_2, \dots)$.

Electroweak gauge invariance has further implications for such Yukawa couplings. Since all of the SM fermions transform as doublets or singlets under $SU_L(2)$, they can

form Yukawa couplings (without also requiring new exotic fermions) only with a scalar multiplet which transforms as a triplet, doublet or singlet. These representations therefore play a special role in the models which follow. $U_Y(1)$ hypercharge invariance further restricts which fermions can couple to which scalars, as we explore in more detail for various models.

5.2.4) Contributions to c_k and \tilde{c}_k

The effective couplings, c_k and \tilde{c}_k vanish at tree level in all renormalizable models of elementary scalars. Because these couplings can nevertheless contribute significantly to observables, we record here general expressions for their one-loop contributions, which we will use for particular models in subsequent sections.

The general result for the CP-invariant photon and gluon effective couplings due to a loop of spinless, spin-half or spin-one particles may be written:

$$c_k = \frac{\alpha_k}{6\pi} \sum_{s=0,\frac{1}{2},1} (-1)^{2s+1} \sum_{R_s} \frac{\mathcal{C}_k(R_s)y(R_s)}{m(R_s)} I_s \left[\frac{m^2(R_s)}{m_h^2} \right], \quad (99)$$

where R_s denotes the various representations on spin- s fields of the colour or electromagnetic gauge group which is carried by the particle content of the model. $m(R_s)$ represents the mass of the particle in the loop, and $\mathcal{C}_k(R_s)$ is the quadratic Casimir for this particle's representation, defined by $\text{Tr}(T_a T_b) = \mathcal{C}(R_s) \delta_{ab}$. The spin-dependent functions, $I_s(r)$, are given explicitly by expressions (21) of section 2. Specializing this result to the SM particle content and couplings reproduces eq. (20).

In eq. (99) $y(R_s)$ is the relevant trilinear coupling to scalars enjoyed by the particle circulating in the loop. These couplings are normalized so that y is the Yukawa coupling, y_f , for spin-half particles; $y_w = a_w/(2M_w)$ for spin-one particles, and $y_s = \nu_{SSH}/m_s$ for spin-zero particles (here denoted by S).

The result for the CP-odd effective couplings, \tilde{c}_k , is obtained by omitting the bosons ($s = 0, 1$) and simply replacing the axial coupling, $z(R_s)$ for $y(R_s)$ in the fermion contribution to eq. (99).

We now turn to the examination of some particular models in more detail. The models we present are chosen either because they are theoretically well motivated (and hence popular) or because they illustrate particular points we wish to emphasize.

5.3) Models With Higher Scalar Multiplets

The main feature which distinguishes the various models of elementary scalars is the representation content which is chosen for the scalar fields. Although the majority of the best-motivated models involve only doublets, our goal here is to assess the extent to which the field content can be inferred from experiments.

As just discussed, scalars which are not electroweak triplets, doublets or singlets cannot form Yukawa couplings involving just the known SM fermions. All scalars of this type can therefore be distinguished in principle by their prediction of vanishing tree-level fermion-scalar couplings, but nonvanishing scalar-gauge boson interactions [3].

5.3.1) The $3 - 4$ Model

We pause here to examine one such model in slightly more detail. We do so — even though the model we consider is not particularly attractive — for two reasons. First, it illustrates within a simple context most of the issues which arise later when we discuss better-motivated models. Second, it furnishes the existence proof for models having $a_w s_w / e M_w$ potentially significantly larger than unity.

In this model we supplement the usual SM particle content, including its doublet Higgs, ϕ , with a single complex scalar multiplet, S , transforming in a $T = 3$ multiplet of $SU_L(2)$ and carrying hypercharge $y = 4$. These quantum numbers are chosen to ensure the vanishing of the new scalar's tree-level contribution to $\Delta\rho$, as given by eq. (90).

There are two new neutral scalar particles in this model, and for the present purposes it is sufficient to assume that the scalar potential does not break CP spontaneously (renormalizability and gauge invariance in this model together preclude explicit CP violation in the scalar potential). In this case the CP-odd state neither mixes nor acquires a nonzero *v.e.v.*, while both of these are possible the two CP-even states. Denoting the mixing angle

by α , we have

$$\begin{pmatrix} A_{1h} \\ A_{2h} \end{pmatrix} = \begin{pmatrix} \cos \alpha \\ -\sin \alpha \end{pmatrix}, \quad (100)$$

where 1 denotes the doublet scalar, 2 labels the CP-even neutral scalar from the S multiplet and h is the mass eigenstate which is assumed to have been observed.

- *Yukawa Couplings:*

Because of its unorthodox charge assignments, the two neutral scalars in the new multiplet cannot couple renormalizably with SM fermions at all. So if the light Higgs is the CP-odd state it does not couple to SM fermions, and if it is one of the CP-even ones its coupling is as given by the usual SM expressions up to an overall mixing-angle factor:

$$y_{fg} = \delta_{fg} \frac{m_f}{v_\phi} \cos \alpha, \quad z_{fg} = 0. \quad (101)$$

- *Gauge Boson Couplings:*

Of more direct interest here is the tree-level prediction: $\Delta\rho = 0$, as well as the prediction for G_F and the trilinear WWh and ZZh couplings. These vanish for the CP-odd scalar but take the following nonzero values for the CP-even case:

$$\begin{aligned} \frac{1}{\sqrt{2} G_F} &= v_\phi^2 [1 + 16r^2], \\ \frac{a_W^h}{eM_W/s_w} &= \frac{a_Z^h}{eM_Z/s_w c_w} = \frac{\cos \alpha - 16r \sin \alpha}{\sqrt{1 + 16r^2}}, \end{aligned} \quad (102)$$

where $r = v_s/v_\phi$. Clearly, because the condition $\Delta\rho \ll 1$ does not require r to be small (unlike what we shall find in some of the other models we consider), in this model both of the ratios $\left| \frac{a_W^h}{eM_W/s_w} \right|$ and $\left| \frac{a_Z^h}{eM_Z/s_w} \right|$ can be much larger than one.

- *Loop Effects:*

It is important to ask whether predictions for small effective couplings are not merely artifacts of the tree approximation. For this theory tree-level Yukawa couplings are very small because they are suppressed by small fermion masses. It is easy to see that this

remains true once radiative corrections are included, for the same reasons as were given in §2 for the SM.

As noted earlier, if the observed light scalar should be CP-odd, then it cannot mix with the SM doublet, and so its Yukawa couplings vanish. The absence of Yukawa couplings then rules out nonzero values for \tilde{c}_g and \tilde{c}_γ . CP itself also directly forbids a nonzero c_g and c_γ , so all four of these loop couplings are zero.

On the other hand, should the observed scalar be one of the CP-even states, then the predicted c_k 's differ from the SM results for two reasons. First, the scalar/fermion and scalar/ W couplings are modified by mixing in the scalar sector. Next, c_γ acquires a new contribution due to the existence of new charged scalars. In this case we find $\tilde{c}_g = \tilde{c}_\gamma = 0$ and

$$\begin{aligned} c_g &= c_g(\text{SM}) \cos \alpha, \\ c_\gamma &= c_g \left(\text{SM-spin } \frac{1}{2} \right) \cos \alpha && \text{if } \text{CP}(h) = +1 \\ &+ c_g(\text{SM-spin 1}) \frac{\cos \alpha - 16r \sin \alpha}{\sqrt{1 + 16r^2}} + \frac{\alpha}{24\pi} \sum_S Q_s^2 \frac{\nu_{SSH}}{m_s^2}. \end{aligned} \quad (103)$$

5.4) Models with Extra Scalar Singlets

The simplest extensions of the SM in the scalar sector would add electroweak singlet scalars, S , to the usual SM field content. Our assumption of electric neutrality for these scalars then further implies that their hypercharge is zero, so they have no tree-level couplings at all to the W , Z or photon.

- *Tree Level Couplings:*

Electroweak gauge invariance also precludes forming tree-level Yukawa couplings involving these scalars and only ordinary SM fermions, making them not particularly interesting for experiments unless more light fermions beyond those of the SM are also included. In fact, there is an important class of such fermions which arise in theoretically well-motivated models, and could plausibly have avoided detection to date: right-handed neutrinos (*i.e.*

electroweak singlet fermions, N) [45]. Such singlet fermions can couple to scalar singlets, and transfer these couplings to SM fermions through mixing with left-handed neutrinos in the neutrino mass matrix.

In this scenario only the new singlet fermions acquire tree-level Yukawa couplings to the new scalars, and so ordinary fermions only learn about these through neutrino mixing with these new fermions, which arise due to Yukawa couplings with the SM-type Higgs. As a result the scalar phenomenology is intimately tied up with neutrino properties, and depends crucially on whether or not any of the lepton numbers, L_i , remain conserved.

If the interactions conserve all lepton numbers, then the singlet scalar must carry $L_i = 2$ (if it couples at all to generation ‘ i ’). If S does not acquire an expectation value, then neutrinos cannot oscillate and there are no observable new-scalar effects unless the new scalar’s mass is small enough (less than roughly the QCD scale) to contribute to big-bang nucleosynthesis.

More interesting possibilities arise if some or all of the lepton numbers are broken, since then both the neutrinos and the scalars can mix in more interesting ways. If the symmetries are broken spontaneously, strong bounds arise on the resulting Goldstone boson, and so we disregard this possibility here. If they are instead explicitly broken and all scalar masses are reasonably heavy (larger than Λ_{QCD} , say), then the main constraints come from experiments on the light neutrino states, such as searches for oscillations or double- β decay.

In these types of models, the expected properties of an observed scalar depend on how much overlap this state has with the SM Higgs and with the new singlet states. If there is only a single, real new singlet then there are two neutral scalar states, and these can mix according to eq. (100). If, on the other hand, the new scalar is complex, there are three neutral scalar states. If CP is conserved then the pseudoscalar doesn’t mix with the two scalars, and so the mixing proceeds as for the 3 – 4 model, with the CP even states again mixing according to eq. (100). If CP is broken, then all three neutral scalars can

mix, generalizing eq. (100) to

$$\begin{pmatrix} A_{1h} \\ A_{2h} \\ A_{3h} \end{pmatrix} = \begin{pmatrix} \cos \alpha \cos \beta \\ -\sin \alpha \cos \beta \\ -\sin \beta \end{pmatrix}, \quad (104)$$

where h denotes the observed light scalar state, and we take ‘1’ to label the doublet scalar, ‘2’ to be what would have been the CP-even scalar in the absence of CP violation. ‘3’ denotes what becomes the CP-odd state in this limit.

If $\sin \alpha$ and $\sin \beta$ are both small, then the observed scalar shares the usual properties of the SM Higgs. On the other hand, if the observed scalar has much singlet overlap, then its Yukawa couplings to all electrically-charged fermions remain proportional to mass, although with mixing-dependent strength. Its couplings to neutrinos, however, need not be small, and so this kind of h could be relatively long-lived, and dominantly decay through invisible neutrino modes. Of course for the same reasons it would be also difficult to detect within accelerator experiments.

- *Loop Effects:*

The size of c_k in these models depends dramatically on whether the observed scalar is dominantly SM Higgs or singlet. If dominantly a Higgs, the c_k differs from the SM result purely through the effects of scalar mixing on the coupling strengths to charged fermions and the W . Notice there is no scalar contribution to the c_k ’s because there are no new electrically-charged scalars in these models. If the new scalar is dominantly a singlet, then all of the c_k ’s vanish at one loop, regardless of whether it is CP odd or even or if CP is broken.

5.5) Triplet Models

Consider next a model containing one standard isodoublet, ϕ , (with hypercharge $y_2 = 1$) and one scalar isotriplet, ψ [46]. In order that the triplet contain electrically neutral components, its hypercharge eigenvalue must be $y_3 = 0$ or $y_3 = 2$ (with the neutral scalar then having $t_3 = 0$ or -1 respectively).

Since the perturbative spectrum and couplings of the model depend in detail on whether $y_3 = 0$ or $y_3 = 2$, we consider each case separately.

5.5.1) The Case $y_3 = 0$

If $y_3 = 0$ then the triplet may be chosen to be real. In this case there are only two neutral spinless particles, and one scalar with charge $q = 1$.

- *Tree-level Couplings:*

Since hypercharge conservation precludes coupling the triplet to fermions, only the doublet has Yukawa couplings, which therefore take the same form as in the Standard Model. Both neutral scalar mass eigenstates can participate in these interactions inasmuch as the triplet mixes with the doublet. Since the scalar mixing matrix is a two-by-two rotation, it is given by eq. (100), implying the following relations between the Yukawa couplings, fermion masses and scalar mixing angle:

$$y_{fg} = \delta_{fg} \frac{m_f}{v_\phi} \cos \alpha, \quad z_{fg} = 0. \quad (105)$$

Triplets contribute to $\Delta\rho$ at tree level, so we must ensure the ratio of triplet to doublet *v.e.v.s*, $r = v_\psi/v_\phi$, is sufficiently small. From eq. (90):

$$\Delta\rho = 4r^2 \lesssim O(10^{-3}), \quad (106)$$

so v_ϕ is to good approximation related to Fermi's constant in the same way as in the SM:

$$\frac{1}{\sqrt{2} G_F} = \frac{4 s_w^2 M_w^2}{e^2} = v_\phi^2 [1 + 4r^2] \approx v_\phi^2. \quad (107)$$

The trilinear WWh and ZZh couplings become:

$$\begin{aligned} \frac{a_w^h}{e M_w / s_w} &= \frac{\cos \alpha - 4r \sin \alpha}{\sqrt{1 + 4r^2}}, \\ &= \frac{\cos \alpha - 2 \sin \alpha \sqrt{\Delta\rho}}{\sqrt{1 + \Delta\rho}}, \\ &\approx \cos \alpha - 2 \sin \alpha \sqrt{\Delta\rho} + O(\Delta\rho) \end{aligned} \quad (108)$$

and $\frac{a_z^h}{e M_z / s_w c_w} = \cos \alpha.$

Clearly the SM expression, $a_W s_w / eM_W = a_Z s_w c_w / eM_Z$ holds here, to within an accuracy of a few percent, even though both of these quantities can differ appreciably from the corresponding SM predictions.

Although $a_Z^h s_w c_w \leq eM_Z$ quite generally in this model, $a_W^h s_w$ can be larger or smaller than eM_W depending on the value of α . For example, it is larger if α lies in the range $|\sin \alpha| \lesssim \sqrt{3\Delta\rho}$. Even though the ratio $a_W^h s_w / eM_W$ can be bigger than 1 in this way, the constraints on $\Delta\rho$ do not permit it be much bigger. In this model it is never larger than $\sqrt{(1+4\Delta\rho)/(1+\Delta\rho)} \approx 1 + \frac{3}{2}\Delta\rho$. This is not likely to be measurable. Of course this conclusion is not generally true for all models, as the above discussion of the 3 – 4 model explicitly illustrates.

- *Loop Effects:*

The same arguments as were given for the SM in §2 imply that loops do not ruin the tree-level prediction that Yukawa couplings are suppressed by small fermion masses.

In this model the contributions to the effective couplings c_k and \tilde{c}_k are similar to what was found earlier for the 3 – 4 model. Fermion and gauge boson contributions are identical to those of the SM, weighted by the corresponding effective couplings — $y_f/y_f(\text{SM})$ and $a_w/a_w(\text{SM})$ — as required by scalar mixing. To these must be added the contribution of the heavy $Q = 1$ scalar, in the case of c_γ .

5.5.2) The Case $y_3 = 2$

If $y_3 = 2$ then the triplet must be complex, implying a total of three neutral scalars, plus one charged and one doubly-charged state. In general all three neutral scalars can get *v.e.v.s* — which we denote v_ϕ, v_R, v_I — and mix with one another, but if the scalar interactions are CP-preserving then the three neutral states break up into two CP-even ones which do not mix with the third, which is CP-odd. Mixing in the general case is therefore given by eq. (104), with the CP-conserving limit corresponding to either $\sin \beta = 0$ or $\cos \beta = 0$.

In this case hypercharge conservation only permits couplings of the neutral component of the triplet to the left-handed neutrinos [47], and these preserve overall lepton number

provided $L(\psi) = -2$. In the presence of such couplings there are three possibilities: (i) L is broken by the scalar potential V (*e.g.* through a term of the form $\phi^T \sigma_2 \vec{\sigma} \phi \cdot \vec{\psi}^*$); (ii) L is not broken by V and ψ gets a *v.e.v.*, so one of the neutral scalars is a massless Goldstone mode; or, (iii) L is neither broken by V nor spontaneously. Each of these options presents its own potential phenomenological difficulties (although arguably, none are fatal), whose pursual goes beyond the scope of the present paper.

- *Tree-level Couplings:*

All fermions apart from neutrinos have only Yukawa couplings to the doublet scalar, making their description similar to the $y_3 = 0$ case. In terms of the fermion masses and scalar mixing angles we have (for all fermions except neutrinos):

$$y_{fg} = \delta_{fg} \frac{m_f}{v_\phi} \cos \alpha \cos \beta, \quad z_{fg} = 0. \quad (109)$$

In this model $\Delta\rho$ can depend on the *v.e.v.s* of both of the (real) neutral scalar fields of the triplet. Defining $r_R = v_R/v_\phi$ and $r_I = v_I/v_\phi$ we have:

$$\Delta\rho = \frac{-2(r_R^2 + r_I^2)}{1 + 4(r_R^2 + r_I^2)} \lesssim O(10^{-3}), \quad (110)$$

Fermi's constant is:

$$\frac{1}{\sqrt{2} G_F} = v_\phi^2 [1 + 2(r_R^2 + r_I^2)] \approx v_\phi^2, \quad (111)$$

and the trilinear couplings with gauge bosons are:

$$\begin{aligned} \frac{a_W^h}{eM_W/s_w} &= \frac{\cos \alpha \cos \beta - 2(r_R \sin \alpha \cos \beta + r_I \sin \beta)}{\sqrt{1 + 2(r_R^2 + r_I^2)}}, \\ \frac{a_Z^h}{eM_Z/s_w c_w} &= \frac{\cos \alpha \cos \beta - 4(r_R \sin \alpha \cos \beta + r_I \sin \beta)}{1 + 4(r_R^2 + r_I^2)}. \end{aligned} \quad (112)$$

The limit of conserved lepton number corresponds to the limit $r_R = r_I = 0$ and absolutely no mixing amongst the three scalars — and so $(\alpha, \beta) = (0, 0), (\frac{3\pi}{2}, 0)$ or $(\alpha, \frac{3\pi}{2})$ depending on which scalar is the one observed. Similarly, if CP is not broken explicitly or

spontaneously then $r_I = 0$. If it happens that the observed scalar is one of the model's CP-even states in this limit, then we may take $\beta = 0$ in the above, in which case our results reduce to two-by-two mixing, as they must. Alternatively, the case where the observed light state is CP-odd corresponds to the limit $\beta = \frac{3\pi}{2}$, in which case all of the above couplings vanish (as they again must).

In the excellent approximation that we neglect quantities of order $O(\sqrt{|\Delta\rho|})$, the model predicts relations among the fermion and gauge-boson couplings of the light scalar: $y_f^2 = \sqrt{2}G_F m_f^2 (a_z^h)^2$. The same prediction also holds to good approximation with a_z^h replaced by a_w^h . This kind of prediction also holds for the $y_3 = 0$ model, and is reasonably robust, relying only on the absence of direct Yukawa couplings to the new scalar multiplet in the model of interest.

- *Loop Effects:*

As for the previously-studied models, the suppression of tree-level Yukawa couplings by small fermion masses survives loop corrections.

The contributions to c_k and \tilde{c}_k in the $y_3 = 2$ triplet models resemble those in the singlet models discussed above, both because of the potential for three-scalar mixing, and because of the triplet having tree-level Yukawa couplings exclusively to neutrinos. Fermion and gauge boson contributions get rescaled compared to the SM by the appropriate effective couplings, and both the $Q = 1$ and $Q = 2$ scalars contribute to c_γ .

5.6) Two-Higgs-Doublet Models (2HDM)

The scalar sector of a great many of the theoretically most plausible models, including prominently the Minimal Supersymmetric Standard Model (MSSM), fall into the general class of multi-doublet theories, consisting of several copies of the basic SM $Y = 1$ doublet. Besides being very well motivated, these models enjoy many attractive properties, such as having naturally vanishing tree level contributions to $\Delta\rho$.

In this section we consider the basic Two-Higgs Doublet Model (2HDM) [3],[48], which in many ways is the minimal archetype for the rest of the multi-doublet models. It

consists of the usual SM particle content, supplemented only by a second Higgs doublet.

The model predicts one $Q = 1$ electrically-charged spinless particle state in addition to a total of three electrically-neutral mass eigenstates. As usual, two of these – called h and H – are CP-even and one – called A – is CP-odd, if CP is not broken. (Conventionally h denotes the lighter of the two CP-even states.) Finally, if we write the *v.e.v.s* of the two would-be CP-even states by v_1 and $v_2 \cos \xi$, and denote the third *v.e.v.* by $v_2 \sin \xi$. These must satisfy the tree-level prediction for Fermi's constant, $1/(\sqrt{2} G_F) = v_1^2 + v_2^2$, but neither the ratio v_2/v_1 nor ξ are constrained by $\Delta\rho$. $\xi = 0$ if the scalar sector conserves CP.

In general all three of the neutral eigenstates mix among themselves (and with the would-be Goldstone mode which is eaten by the Z boson, in a non-unitary gauge), and so the interactions of the lightest scalar state are describable in terms of two mixing angles, as in eq. (104). In this section we do not adopt this earlier notation for the mixing angles, since the angles α and β are conventionally chosen differently when describing these models. Since it is not our purpose here to exhaustively explore the parameter space of the model, in the interests of brevity we quote expressions here for the effective couplings in the CP-conserving limit, where $\xi = 0$ and the CP-odd state A does not mix with h and H . We emphasize that we do *not* use this assumption in our later discussion of the properties of the low-energy scalar in these models.

Under the assumption of CP invariance, only two angles turn out to be required to diagonalize all of the scalar masses in a general gauge. This is because the CP-odd states (A and the would-be Goldstone boson, z) do not mix with the CP-even states (h and H) in the electrically neutral sector, and because the same rotation angle, $\tan \beta = v_2/v_1$, required to diagonalize the $A - z$ mass matrix also diagonalizes the mixing between the electrically-charged state and the charged Goldstone mode, w . The rotation required to diagonalize the two-by-two CP-even mass matrix defines the second mixing angle, α .

- *Gauge Boson Couplings:*

With these conventions the CP-odd state, A , does not participate in trilinear interac-

tions with two gauge bosons, and the trilinear gauge couplings to the light CP-even state, h , can be written:

$$\begin{aligned} a_w^h &= \frac{e^2}{2s_w^2} (v_2 \cos \alpha - v_1 \sin \alpha) = \frac{eM_w}{s_w} \sin(\beta - \alpha), \\ a_z^h &= \frac{e^2}{2s_w^2 c_w^2} (v_2 \cos \alpha - v_1 \sin \alpha) = \frac{eM_z}{s_w c_w} \sin(\beta - \alpha), \end{aligned} \quad (113)$$

which are clearly both bounded above by their SM counterparts, in accordance with the general results of the previous sections.

We record here also the tree-level trilinear Z -scalar-scalar coupling, the ZAh vertex, which is given by:

$$g_z^{Ah} = \frac{e}{2s_w c_w} \cos(\beta - \alpha), \quad (114)$$

and the tree-level quartic scalar/gauge-boson interactions, which are completely unchanged from the SM:

$$b_w^{ij} = \frac{e^2}{s_w^2} \delta^{ij}, \quad b_z^{ij} = \frac{e^2}{2s_w^2 c_w^2} \delta^{ij}. \quad (115)$$

- *Yukawa Couplings:*

We next turn to the neutral scalar Yukawa couplings. Because gauge invariance cannot rule out the couplings of either of these doublets to SM fermions, in the generic case we expect to find tree-level couplings between neutral scalars and fermions which change fermion flavour.

The desire to avoid these kinds of dangerous flavour-changing couplings motivates the definition of two particular subclasses of models for which these couplings are naturally forbidden by a discrete symmetry. That is, adopting the nomenclature of ref. [3]:

1. *Type I* models are defined in such a way as to arrange for one of the two doublets to not couple at all to fermions. This can be done, for instance, by imposing the discrete symmetry $(\phi_1, \phi_2) \rightarrow (-\phi_1, \phi_2)$, with none of the fermions transforming.

With this choice it is only the doublet ϕ_2 which generates all fermion masses, and so the resulting mass-eigenstate Yukawa couplings are diagonal and independent of γ_5 for the

same reason they are in the SM. The Yukawa couplings to the light CP-even state h are then related to fermion masses by the tree-level formulae: $z_{fg}^h = 0$ and

$$y_{fg}^h = \delta_{fg} \frac{m_f}{v_2} \cos \alpha = \delta_{fg} \left(\sqrt{2} G_F m_f^2 \right)^{\frac{1}{2}} \frac{\cos \alpha}{\sin \beta}. \quad (116)$$

This implies the well-known tree-level prediction that all *ratios* of Yukawa couplings are the same as they would be in the SM: $y_f/y_g = m_f/m_g$.

2. *Type II* models are defined in such a way as to ensure that only one doublet couples to ‘up-type’ ($t_3 = +\frac{1}{2}$) fermions, with the other doublet coupling only to ‘down-type’ ($t_3 = -\frac{1}{2}$) fermions. This can also be ensured using a discrete symmetry of the form $(\phi_1, \phi_2) \rightarrow (\phi_1, -\phi_2)$, although this time with all right-handed up-type fields also changing sign under the symmetry.

Since the fermions in any one charge sector couple only to one kind of scalar, all tree-level Yukawa couplings are again flavour diagonal, with $z_{fg}^h = 0$ and

$$\begin{aligned} y_{uu'}^h &= \delta_{uu'} \frac{m_u}{v_2} \cos \alpha = \delta_{uu'} \left(\sqrt{2} G_F m_u^2 \right)^{\frac{1}{2}} \frac{\cos \alpha}{\sin \beta}, \\ y_{dd'}^h &= -\delta_{dd'} \frac{m_d}{v_1} \sin \alpha = -\delta_{dd'} \left(\sqrt{2} G_F m_d^2 \right)^{\frac{1}{2}} \frac{\sin \alpha}{\cos \beta}. \end{aligned} \quad (117)$$

Although ratios involving only up-type (or only down-type) Yukawa couplings agree with the SM predictions – $y_u/y_{u'} = m_u/m_{u'}$ – mixed ratios differ from their SM predictions by a fixed factor: $y_u/y_d = (m_u/m_d)(\tan \alpha / \tan \beta)$.

- *Loop Effects:*

For the same reasons as for the other models examined to this point, the suppression of tree-level Yukawa couplings by small fermion masses also survives loop corrections in this model.

The contribution to c_γ in a 2HDM is obtained from eq. (99) by adding to the W and fermion contributions (using the a_W^h and y_{fg}^h of the 2HDM) the contribution of the new

charged Higgs [3],[11]. That is, we have for Type I models:

$$\begin{aligned} c_g^{2HDM}(\text{Type I}) &= \frac{\cos \alpha}{\sin \beta} c_g^{SM}, \\ c_\gamma^{2HDM}(\text{Type I}) &= \frac{\cos \alpha}{\sin \beta} c_\gamma^{SM}(\text{fermions}) - \sin(\beta - \alpha) c_\gamma^{SM}(W) + \frac{\nu_{cch}}{4m_c^2}, \end{aligned} \quad (118)$$

where the last term is due to the charged scalar, labelled ‘ c ’, for which the large-mass limit has been used. For Type II models, these quantities are instead:

$$\begin{aligned} c_g^h(\text{Type II}) &= \frac{\cos \alpha}{\sin \beta} c_g^{SM}(\text{up-type fermions}) - \frac{\sin \alpha}{\cos \beta} c_g^{SM}(\text{down-type fermions}), \\ c_\gamma^h(\text{Type II}) &= \frac{\cos \alpha}{\sin \beta} c_\gamma^{SM}(\text{up-type fermions}) - \frac{\sin \alpha}{\cos \beta} c_\gamma^{SM}(\text{down-type fermions}), \\ &\quad - \sin(\beta - \alpha) c_\gamma^{SM}(W) + \frac{\nu_{cch}}{4m_c^2}, \end{aligned} \quad (119)$$

For a comparatively light charged Higgs (around 200 GeV) we get a negative contribution of the order of $0.02\nu_{cch}/m_h^2$.

The CP-violating couplings, \tilde{c}_γ^h and \tilde{c}_g^h , are obtained by everywhere substituting z_{fg}^h for y_{fg}^h , and so vanish for Type I and II models, but need not do so for a generic 2HDM.

5.7) Left-Right Symmetric (LR) Models

Left-right symmetric models have also been extensively discussed in the literature [49], [50]. Their gauge group is $SU(2)_L \times SU(2)_R \times U(1)$, and so their treatment requires a generalization of our previous discussion because of the possibility which arises here of mixing amongst the LH and RH electroweak gauge bosons. The usual scalar sector of a left-right symmetric model (LRSM) contains a bidoublet and two triplets:

$$\phi = \begin{pmatrix} \phi_1^0 & \phi_1^+ \\ \phi_2^- & \phi_2^0 \end{pmatrix}, \quad \Delta_L = \begin{pmatrix} \frac{1}{\sqrt{2}}\delta_L^+ & \delta_L^{++} \\ \delta_L^0 & -\frac{1}{\sqrt{2}}\delta_L^+ \end{pmatrix}, \quad \Delta_R = \begin{pmatrix} \frac{1}{\sqrt{2}}\delta_R^+ & \delta_R^{++} \\ \delta_R^0 & -\frac{1}{\sqrt{2}}\delta_R^+ \end{pmatrix}. \quad (120)$$

whose neutral components acquire a non-zero vacuum expectation value, $\langle \phi_1^0 \rangle = k_1/\sqrt{2}$, $\langle \phi_2^0 \rangle = k_2/\sqrt{2}$ and $\langle \delta_{L,R}^0 \rangle = v_{L,R}/\sqrt{2}$. A large mass for the ‘other’ charged gauge boson,

W' , is required on phenomenological grounds [51], and this requires a large value for v_R . The preference is for vanishing v_L , on the other hand, to avoid possible generation of large Majorana masses for left-handed neutrinos.

- *Gauge Boson Couplings:*

The kinetic part of the lagrangian from which our scalar/gauge-boson vertices arise is

$$-\mathcal{L} = \text{Tr}(\mathcal{D}_\mu \phi)^\dagger (\mathcal{D}^\mu \phi) + \text{Tr}(\mathcal{D}_\mu \Delta_L)^\dagger (\mathcal{D}^\mu \Delta_L) + \text{Tr}(\mathcal{D}_\mu \Delta_R)^\dagger (\mathcal{D}^\mu \Delta_R) \quad (121)$$

where the covariant derivatives are defined by

$$\begin{aligned} \mathcal{D}_\mu \phi &= \partial_\mu \phi + \frac{ig_L}{2} \vec{W}_{L\mu} \cdot \vec{\sigma} \phi - \frac{ig_R}{2} \phi \vec{W}_{R\mu} \cdot \vec{\sigma} \\ \mathcal{D}_\mu \Delta_{L,R} &= \partial_\mu \Delta_{L,R} + \frac{ig_{L,R}}{2} [\vec{W}_{L,R\mu} \cdot \vec{\sigma}, \Delta_{L,R}] + ig' B_\mu \Delta_{L,R} \end{aligned} \quad (122)$$

Here σ^i are the Pauli matrices, while g_L , g_R and g' are the coupling constants for the factors of the gauge group $SU_L \times SU_R \times U(1)$.

The most important difference from our previous discussions arises when we rotate the gauge fields to diagonalize their mass matrix. There are three mixing angles which are generated in this way. In order to recover the SM relation $e = g_L \sin \theta_W$, the weak mixing angle is conventionally defined as $\sin \theta_W = xy/\sqrt{x^2 + z^2 + x^2 z^2}$, where $x = g_R/g_L$ and $z = g'/g_L$ denote ratios of the gauge couplings. The other two mixing angles are α_c , used to diagonalize the charged gauge-boson sector, and α_0 which describes the rotation amongst the two massive neutral gauge bosons, Z and Z' (see, for instance, [50]). In what follows we liberally use the small-mixing-angle approximation, $\alpha_c, \alpha_0 \ll 1$, since typically $\alpha_c \sim M_W^2/M_{W'}^2$, when $M_W \ll M_{W'}$, and similarly for α_0 .

The ρ parameter in this model gets two contributions at leading order in the mixing angles: $\rho = 1 + \Delta\rho_W + \Delta\rho_Z$, where

$$\Delta\rho_W = -\alpha_c^2 \frac{M_{W'}^2 - M_W^2}{M_W^2} \quad \Delta\rho_Z = \alpha_0^2 \frac{M_{Z'}^2 - M_Z^2}{M_Z^2}. \quad (123)$$

The expression for the Fermi coupling constant, defined at tree level from muon decay, also differs in these models from our earlier treatment, because it receives contribution from both charged gauge bosons

$$\frac{G_F}{\sqrt{2}} = \frac{g_L^2}{8} \left(\frac{\cos^2 \alpha_c}{M_W^2} + \frac{\sin^2 \alpha_c}{M_{W'}^2} \right) \approx \frac{g_L^2}{8M_W^2} \left(1 + \alpha_c^2 \frac{M_W^2}{M_{W'}^2} \right). \quad (124)$$

The composition of the lightest Higgs in terms of initial neutral fields ϕ_1^0 , ϕ_2^0 , δ_L^0 and δ_R^0 can be absolutely arbitrary, since the scalar potential may have very many different terms with unspecified coefficients [52]. It should be noted at this point that an unattractive feature of these types of left-right models is the tree-level FCNC — mediated by a linear combination of the ϕ_1^0 and ϕ_2^0 fields — which they generically have. As a result, limits on the masses of scalars having a strong overlap with these FCNC states are generally stronger than are the limits for $M_{W'}$ [53]. Unfortunately there is no natural way of giving these scalars such a large mass, apart from simply fine tuning the appropriate scalar couplings [52]. We assume here that this problem is solved in some way (a possible solution was proposed in [50] by considering a fermiophobic model), so that all FCNC scalars are very heavy, with the lightest scalar having flavour-conserving couplings.

With these assumptions and notational choices, the WWh and ZZh vertices, in the limit of very small mixing angle [50], are

$$\begin{aligned} a_w^h &\approx g_L \left(M_W - \alpha_c^2 \frac{3M_{W'}^2}{2M_W} \right) \\ a_z^h &\approx \frac{g_L}{c_w} \left(M_Z - \alpha_0^2 \frac{3M_{Z'}^2}{2M_Z} \right). \end{aligned} \quad (125)$$

We see that left-right symmetric models always reduce a_w^h and a_z^h relative to the SM result, as was the case for extra doublets. Notice also that the second term in each of these expressions is directly related to the corresponding contributions $\Delta\rho_W$ and $\Delta\rho_Z$, so (assuming no fine-tuned cancellations in ρ) they can be at most of order $\Delta\rho \sim 10^{-3}$.

- *Yukawa Couplings:*

The Yukawa couplings of the model are similar to the triplet model discussed above. The neutral components of the bidoublet can have Yukawa couplings to all fermions except neutrinos, and so their *v.e.v.s* are responsible for the masses of all of these particles. As mentioned earlier, we suppose these couplings to be flavour diagonal for the lightest scalar, assumed to be the one observed. The triplet has ordinary weak hypercharge $y = 2$ and so can only have tree-level Yukawa couplings with the left-handed lepton doublet, implying a coupling of its neutral component only to neutrinos.

5.7.1) Loop Effects

The suppression of small Yukawa couplings persists into the loop expansion for the model considered here, but for reasons which differ from those of the models previously considered. In those models each fermion acquires a new chiral symmetry in the limit of vanishing mass, and it is this symmetry which forces corrections to mass-suppressed Yukawa couplings to remain proportional to the same small masses.

It turns out that the argument differs for the LR models because of the presence of both LH and RH fermion- W couplings in the model. (The connection between these couplings and the chiral symmetry argument is explained in detail in §6, below.) In this case W loop corrections to fermion self-energies and fermion-scalar vertices can give corrections to down-type fermions which are proportional to up-type fermion masses. Since they are also proportional to the RH W -fermion coupling, which is of order $\alpha_c \ll 1$ in these models, these mass corrections are nonetheless negligible in practice.

Other corrections which take advantage of flavour-changing scalar interactions are also possible, but can be ignored here because we assume the absence of flavour-changing neutral-scalar couplings, and because the flavour-changing Yukawa couplings to charged scalars are themselves small.

In the absence of flavour-changing Yukawa couplings for the light scalar, h , the one-loop contributions to c_g^h are proportional to the SM results, rescaled by the mixing angle between h and the bidoublet components, ϕ_1^0 and ϕ_2^0 . The contributions to \tilde{c}_g^h and \tilde{c}_γ^h are given by the same expressions with z_{ff}^h replacing y_{ff}^h .

The contributions to c_γ^h are more complicated since this coupling receives contributions from boson loops. In addition to the usual SM terms, with fermion and W contributions rescaled by y_{ff}^h/y_f^{SM} and a_w^h/a_w^{SM} , we have contributions from the electrically charged scalars and from the heavy gauge boson, W' . Using the large-mass limit for both the charged scalars and W' we find:

$$c_\gamma^{LR} = \frac{\alpha}{6\pi v} \left[\sum_q 3Q_q^2 \eta_q I_{\frac{1}{2}} \left(\frac{m_q^2}{m_h^2} \right) + \sum_\ell Q_\ell^2 \eta_\ell I_{\frac{1}{2}} \left(\frac{m_\ell^2}{m_h^2} \right) - \left(1 - \alpha_c^2 \frac{3M_{W'}^2}{2M_w^2} \right) I_1 \left(\frac{M_w^2}{m_h^2} \right) - a_{W'}^h I_1 \left(\frac{M_{W'}^2}{m_h^2} \right) + \frac{1}{4} \sum_c \frac{Q_c^2 \nu_{cch}}{m_c^2} \right]. \quad (126)$$

Here $\eta_f = y_{ff}^h / (\sqrt{2}G_F m_f^2)^{\frac{1}{2}}$ denotes the relevant fermion Yukawa coupling, normalized by the SM result, and the final sum over c runs over all of the heavy charged scalar states.

Naively, since $I_1(r)$ is a slowly varying function of r one might expect a large contribution to c_γ from W' , however this would only be true if its coupling to h , $a_{W'}^h$, were proportional to the gauge boson mass, $M_{W'}$, as is the case for W in the SM. In left-right models, however, $a_{W'}^h$ is instead proportional to M_w [54], implying a W' contribution approximately proportional to

$$a_{W'}^h I_1 \left(\frac{M_{W'}^2}{m_h^2} \right) \sim \left(\frac{M_w}{M_{W'}} \right)^2 I_1 \left(\frac{M_w^2}{m_h^2} \right) \approx \frac{21}{4} \left(\frac{M_w}{M_{W'}} \right)^2. \quad (127)$$

This suppression of the W' contribution, whose mass is constrained to be heavier than 1.6 TeV [51] in standard left-right models, makes it numerically insignificant.

5.8) The Minimal Supersymmetric Standard Model

Supersymmetric extensions of the SM are probably the best motivated of the theoretical alternatives we discuss, because of the well-known merits of supersymmetry for protecting the hierarchy between the electroweak and higher scales. The minimal such variant of the SM — the so-called Minimal Supersymmetric Standard Model (MSSM) — has accordingly been the subject of considerable theoretical and experimental efforts

[3], [31]. Here we wish only to emphasize several features of the model, relating to the properties of its neutral scalars.

In fact, a variety of models are all called ‘the’ MSSM, and although all such models agree on the supersymmetric generalization of the SM particle content, they can differ on the precise way in which supersymmetry is spontaneously broken. Luckily enough, these differences do not have much impact on the interactions of the most interest here, such as Yukawa and trilinear gauge-boson/scalar couplings. The same cannot be said for other couplings, such as trilinear and quadratic interactions in the scalar potential, and so these (in general) imply some model dependence for the scalar mixing matrices.

The model requires two doublet chiral Higgs supermultiplets, H_1 and H_2 , with opposite hypercharges. The three neutral scalar states which emerge from these multiplets after the breaking of the electroweak gauge group are denoted h , H and A , as in the 2HDM. There are, in addition, scalar $y = -1$ doublets arising as superpartners to the lepton doublets, the neutral elements of which contain three more (complex) sneutrinos, denoted $\tilde{\nu}_k$, for $k = 1, 2, 3$. The sneutrinos share the lepton number of their spin-half superpartners, and so they cannot mix with the Higgs sector unless lepton number is broken (as is the case in some R -parity violating models, for instance [55]⁴). All of these scalars can be produced at colliders, in principle.

The validity of our effective Lagrangian approach presupposes that the masses of the at-present-undiscovered superpartners are sufficiently large. We might assume here, for instance, that squarks, sleptons and gauginos are all as heavy as several hundred GeV. To the extent that sneutrino masses must be as large as are those of their charged slepton partners, they would also be too heavy to include within the effective Lagrangian as well. However, since scalar masses are among the parameters which depend in detail on supersymmetry breaking, we entertain the possibility that the hypothetically-observed new particle could be a sneutrino.

On the other hand, since the Higgs scalars must acquire nonzero expectation values,

⁴ The formula $R=(-)^{3B+L+F}$ relates R parity to baryon number, B , lepton number, L and fermion number, F , and so its conservation is automatic if baryon and lepton number are both conserved.

their masses are connected to quartic scalar interactions, and so are more robustly constrained. In particular, an important MSSM prediction is that the mass of the lightest Higgs boson cannot be made too large. At the tree level it must be smaller than M_Z , with this upper bound rising to 130 GeV once radiative corrections to m_h are taken into account [56]. Given this upper limit, a betting man's prejudice would be to expect a single light scalar to be a Higgs, within the MSSM framework.

- *Scalar/Gauge-boson Couplings:*

The general expression for the trilinear and quartic scalar/gauge-boson couplings as functions of the neutral-scalar mixing matrix, A_{ij} , are found by specializing eqs. (92) and (93) to the pure-doublet case:

$$a_w^i = a_z^i c_w^2 = \frac{e^2}{2s_w^2} A_{ji} v_j, \quad b_w^{ij} = b_z^{ij} c_w^2 = \frac{e^2}{2s_w^2} \delta_{ij}. \quad (128)$$

It follows that the quartic couplings are unchanged from the SM, regardless of how the observed scalar mixes with Higgses and sneutrinos. The trilinear couplings depend on this mixing in more detail, and this is the only place where supersymmetry-breaking details enter.

An important special case, where statements can be made independent of the details of supersymmetry breaking, is when lepton number is conserved, since then none of the sneutrinos can acquire a lepton-number breaking *v.e.v.*. In this case all of the tree-level trilinear sneutrino/gauge-boson couplings vanish, and those of the remaining three neutral Higgses, h , H , A , can be expressed in terms of the scalar mixing angles of the 2HDM. These are particularly simple if CP is also unbroken, since they then reduce to the dependence on two angles, α and β . Decomposing the neutral components of the doublets, H_1 and H_2 , as in the previous section

$$\begin{aligned} H_2^0 &= v_2 + H \sin \alpha + h \cos \alpha + iA \cos \beta + iz \sin \beta \\ H_1^0 &= v_1 + H \cos \alpha - h \sin \alpha + iA \sin \beta - iz \cos \beta, \end{aligned} \quad (129)$$

leads to the prediction, eqs. (113) and (114), for these trilinear couplings.

- *Tree-Level Yukawa Couplings:*

Because Yukawa couplings are dimension-four interactions they get no direct contribution from soft supersymmetry-breaking interactions, making them sensitive to the details of supersymmetry breaking only to the extent that they depend on the mixing amongst scalars (or amongst neutral fermions). In particular, the tree-level Yukawa couplings of the Higgs states are determined by the model’s superpotential, which is required to be a holomorphic function of the (complex) superfields. For instance, the terms relevant to Yukawa couplings are

$$W = \mu H_1 H_2 + \mathcal{Y}_{ij}^d Q_i^T D_j H_1 + \mathcal{Y}_{ij}^u Q_i^T U_j H_2, \quad (130)$$

where $i = 1, 2, 3$ is a generation label, $Q_i = \begin{pmatrix} u_i \\ d_i \end{pmatrix}$ represents the left-handed quark supermultiplets, while U_j and D_j are left-handed antiquark supermultiplets. The important point about eq. (130) is that gauge invariance forces each Higgs doublet to couple to either up-type or down-type fermions, but not to both. The tree-level Yukawa couplings of the scalar doublets which emerge from this therefore take the form of a Type II 2HDM, eq. (117).

Sneutrino Yukawa interactions with SM fermions are more model dependent than are those of the Higgs states, even though they are also determined at tree level by the holomorphic superpotential. (Unlike the SM, the symmetry and field content of the MSSM admit renormalizable lepton- and baryon-number violating interactions.) The model dependence arises because the sneutrino couplings necessarily break lepton number, and so the corresponding couplings are only bounded by experiment to be consistent with zero, and are not related to other known parameters, like SM fermion masses. The experimental constraints on the size of these couplings originate from fermion-fermion scattering and from low energy precision measurements [55]. If parameters are chosen to ensure the proton is stable, then the limits obtained from these experiments are numerically similar to the bounds of eqs. (54) (61).

- *Loop Effects (Yukawa Couplings):*

Supersymmetric models represent a case where loop corrections to Yukawa couplings can be important [57] – [59]. This is because the superpartner particle content permits the existence of strong interactions which couple light flavours to heavy flavours, and so can ruin the chiral symmetry protecting Yukawa couplings to light fermions. Indeed, these radiative corrections can be dangerous, since if squark masses have non-trivial flavour dependence, then Higgs exchange generates effective FCNC interactions. (In this paper we assume no such FCNC contributions to be present.)

In the most likely scenario, the lightest scalar in the MSSM is a Higgs particle. At tree level it was supersymmetry itself which forced the Yukawa couplings of this scalar to be of Type II, but since supersymmetry is broken, the loop-corrected effective Yukawa couplings need not respect this Type II form. The size of these corrections as well as their flavour structure strongly depends on the assumptions that are made about how supersymmetry breaks. In the absence of FCNCs, we may write the one-loop-corrected effective Yukawa couplings to neutral scalars as

$$\begin{aligned} y_{uu'}^h &= \delta_{uu'} \left[\cos \alpha \left(y_u^{(0)} + y_u^{(1)} + \dots \right) - \sin \alpha \left(\tilde{y}_d^{(1)} + \dots \right) \right] \\ y_{dd'}^h &= \delta_{dd'} \left[-\sin \alpha \left(y_d^{(0)} + y_d^{(1)} + \dots \right) + \cos \alpha \left(\tilde{y}_u^{(1)} + \dots \right) \right], \end{aligned} \quad (131)$$

where $y_{u,d}^{(0)}$ denote the tree level Yukawa couplings (which are found by diagonalizing the couplings $\mathcal{Y}^{(u,d)}$ of the superpotential, eq. (130)) and $y_{u,d}^{(1)}$ represent their one-loop corrections. $\tilde{y}_{u,d}^{(1)}$ denotes a new type of radiatively generated correction which couples up-type quarks to the H_1^* field and down-type quarks to H_2^* . These couplings do not exist in the initial formulation of the theory because they break supersymmetry. However, they do arise below the scale of superpartners, as the supersymmetry is effectively broken there.

Now comes the main point. The quark Yukawa couplings can receive QCD-strength radiative corrections, due to graphs in which the quark splits into a squark-gluino pair. The order of magnitude for down-type quarks is given by

$$y_d^{(1)} \simeq \frac{\alpha_s}{3\pi} \frac{m_\lambda A_d}{m_{squark}^2}, \quad (132)$$

where A_d is a trilinear scalar coupling appearing amongst the soft supersymmetry-breaking interactions. Equation (132) has two noteworthy features. First, $y_d^{(1)}$ remains finite even in the limit of vanishing $y_d^{(0)}$, because the trilinear breaking parameter, A_d , breaks protective chiral symmetry. Second, the corrections do not ‘decouple’ in the sense that they do not go to zero in the limit of heavy superpartners, provided that the ratios A_d/m_{squark} and m_λ/m_{squark} are kept fixed. This property is natural as the Yukawa coupling corresponds to an operator of dimension four which is protected by supersymmetry, and so does not have to be suppressed as the splitting in a supermultiplet gets large. In many of the versions of the supersymmetry-breaking terms of the MSSM this kind of chiral-symmetry breaking is suppressed by hand, by setting $A_i \equiv A y_i^{(0)}$ when writing the soft supersymmetry-breaking terms.

A different type of coupling, $\tilde{y}_{u,d}^{(1)}$, can be generated due to the same diagram, when the μ -dependent interaction of the Higgs field with squarks is taken into account:

$$\tilde{y}_d^{(1)} \simeq y_d^{(0)} \frac{\alpha_s}{3\pi} \frac{\mu m_\lambda}{m_{squark}^2}, \quad (133)$$

Even though this result is proportional to the “initial” tree-level couplings $\simeq y_d^{(0)}$, it is still important as it gives a new type of interaction, which does not exist in the type II 2HDM. The loop corrections to fermion masses in the down-quark sector become numerically significant in the large- $\tan\beta$ regime [57], when the loop suppression of $\tilde{y}_d^{(1)}$ is compensated by large ratio v_2/v_1 , so that $\tilde{y}_d^{(1)} v_2$ and $y_d^{(0)} v_1$ are comparable. In this regime the interaction of the lightest Higgs h to the down-type quarks is also significantly modified with respect to the usual type II 2HDM expectations of $y_d/y_{d'} = m_d/m_{d'}$ [58]. This picture requires the other neutral scalars, A and H , to be in an intermediate range, as the relation of masses and couplings becomes indistinguishable from the SM ones in the limit $m_A, m_H \rightarrow \infty$. Large corrections to masses and Higgs-fermion couplings may also arise at $\tan\beta \sim 1$ if the trilinear soft-breaking terms include new non-holomorphic structures [59].

Thus a large value of $\tan\beta$ and/or the presence of unorthodox trilinear soft-breaking terms (of unusual form or unusual size) may be detected through the deviation from the $y_d/y_{d'} = m_d/m_{d'}$ relation. This is one way to distinguish SUSY models from other models

having a similar low-energy particle content and scalar sector, like the Type II 2HDM. It is clear, however, that the MSSM cannot be distinguished from a completely generic 2HDM, simply based on measurements of Higgs-fermion couplings, simply because the Yukawa couplings of the low-energy scalar are essentially arbitrary in a general 2HDM.

5.8.1) Loop Effects (Contributions to c_k)

If the light scalar is one of the neutral Higgs states, then these effective couplings receive loop contributions which are very much like those of the 2HDM. There are some differences, though, due to the contributions of the various superpartners which might be hoped to distinguish the MSSM from the 2HDM. We focus here on contributions which are beyond those already in the 2HDM.

Only the coloured superpartners – *i.e.* squarks and gluinos – can contribute to c_g and \tilde{c}_g , but since light scalars don't couple at tree level to gluinos only the squarks actually contribute, by an amount

$$\Delta c_g^h(\text{squarks}) \approx \frac{\alpha_s}{48\pi} \sum_{\tilde{q}} \frac{\nu_{\tilde{q}\tilde{q}h}}{m_{\tilde{q}}^2}, \quad (134)$$

in the large-squark-mass limit. The trilinear coupling in this expression gets contributions both from the supersymmetric part of the lagrangian, $\nu_{\tilde{q}\tilde{q}h} \sim y_q^h \mu$, and from the soft supersymmetry-breaking terms, $\nu_{\tilde{q}\tilde{q}h} \sim A_q$.

Similarly, the electromagnetic vertex receives contributions from both charginos, higgsinos and charged squarks and sleptons. For instance the contributions of heavy squarks are given by [3], [11]:

$$\Delta c_\gamma^h(\text{squarks}) \approx \frac{\alpha}{8\pi v} \sum_{\tilde{q}} \frac{Q_{\tilde{q}}^2 \nu_{\tilde{q}\tilde{q}h}}{m_{\tilde{q}}^2}. \quad (135)$$

Heavy charginos similarly give

$$\Delta c_\gamma(\text{charginos}) \approx \frac{\alpha}{6\pi} \sum_\chi \eta_\chi^h, \quad (136)$$

where $\eta_\chi = 2M_Z (S_{ii} \cos \alpha - Q_{ii} \sin \alpha) / m_\chi$, with S_{ii} and Q_{ii} defined as in [11].

One could hope that c_γ and c_g are indeed the most important couplings of the lightest scalar, h , since then a measurement of its size would be very sensitive to the existence of new charged particles. More detailed analysis shows, however, that even a mild decoupling of superpartners ($m_{chargino} \sim 250$ GeV) leads to SUSY corrections which are less than 10% of the SM values for c_γ and c_g [60].

6. Summary: The Decision Tree

We now come to the nub of this paper, which is a discussion of what experiments involving a newly discovered scalar can ultimately tell us about its underlying nature. Provided the framework we have assumed in this paper indeed holds – *viz* all other hitherto undiscovered particles are sufficiently massive to justify their neglect in a low-energy effective-lagrangian description – then we have seen that there is nothing more we can hope to learn about the properties of the new scalar than what are its effective couplings.

Clearly, then, any model-independent discussion of the properties of a new scalar must therefore come in two parts. First, we must turn to experiments to learn the values of the effective couplings; and second, we can ask what these inferred values tell us about the nature of new physics which has thrown this new scalar up for our inspection. We discuss these two issues separately in the following sections.

6.1) Experimentally Determining the Effective Couplings

Immediately after the discovery of a new scalar, only limited information can be expected to be available. The first information will undoubtedly be the kind of reaction in which the scalar was produced (*e.g.*: Is it produced in e^+e^- or at hadron collisions? At what CM energy? What other particles are produced in the production and decay reactions?), and into what kinds of particles it decays. Only later can we be expected to have more detailed information (*e.g.*: What are the detailed angular distributions of the production process? What are the precise branching ratios into each daughter particle?), from better measurements of the various effective coupling constants. Because most of

the interesting conclusions are relatively obvious, but impossible to draw until the data arrives, we confine ourselves to comparatively few remarks in this subsection.

In principle, those effective couplings which contribute to the production process may be disentangled from those appearing in the decay by examining the total reaction rate as a function of the independent variables, such as CM energy, scattering angle, *etc.*. Some qualitative conclusions may be drawn simply by considering the kinds of reactions which are involved. For example, if the new scalar is only pair-produced, then perhaps it carries an approximately conserved quantum number. If it is singly produced in e^+e^- collisions, then couplings to electrons, photons and/or Z bosons are indicated. Which of these is actually present, or dominates, depends on which other kinds of particles are produced in association with the new scalar. Comparison with the cross sections of Section 3 permits the inference of which effective couplings are involved from the measurement of the dependence on CM energy or the angular distribution of the produced scalar in the CM frame.

Observation of the decay products gives immediate information about the relative strength of the scalar couplings to its potential daughter particles. For example, decay into W pairs likely indicates that the coupling a_W is more important than are the Yukawa couplings, an hypothesis which might be tested by looking for $W - h$ production in hadron colliders.

6.2) *Using Effective Couplings to Discriminate Amongst Models*

Once the existence of a new scalar is established, the most interesting interpretational issue is to discover what it is trying to tell us. That is, given the values for the effective couplings which are inferred from its production and decay (as well as from the absence of other lower-energy processes), what can be said to distinguish the relative likelihood that it is a harbinger of supersymmetry, the first of many strongly-coupled resonant bound states, or an indication of something else?

Organizing the discussion using the effective lagrangian permits a systematic approach to the problem of distinguishing models. Since the only possible information which may be

used to distinguish them is the size of the effective couplings they predict, we may use the relative size of couplings to broadly characterize models. Sixteen categories immediately suggest themselves, depending on the answers a model gives to the following four yes/no questions:

1. Can the effective couplings to the W and Z be at least $O(e)$ in size?
2. Are there any fermions for which the effective Yukawa couplings can be $O(e)$ in size?
3. Can the effective couplings to two photons be at least $O(\alpha/2\pi v)$ in size?
4. Can the effective couplings to two gluons be at least $O(\alpha_s/2\pi v)$ in size?

In items 3 and 4, v denotes the quantity $(\sqrt{2}G_F)^{-1/2} = 246$ GeV.

Four of the possible sixteen categories which are obtained in this way are not of much interest, however, because models having $O(e)$ couplings to the W and Z bosons generally also have $O(\alpha/2\pi)$ couplings to the photon. The twelve remaining categories, together with some of the models which represent them, are listed in Table (2).

Several points about this table bear emphasis.

1. The most basic point is that the very first discovery experiments can do little more than identify which category of model is supported by the properties of the newly-discovered scalar.
2. The next most basic point is to observe that most of the models listed are distributed over a number of different categories, so the first experiments will immediately give nontrivial information, although they are unlikely to permit an immediate discrimination between theoretically popular alternatives — like multi-doublet models and supersymmetric models, for instance.
3. It should be remarked that the assignment of sample models to various categories can vary, depending on what other field content the underlying model is assumed to have. For instance, the entries for triplet models assume two features about the model. First, that the observed light neutral scalar is dominantly triplet, with any admixture with the usual SM-style doublet suppressed. Second, that the only new nonstandard electroweak multiplets in the model are the colour-singlet triplet field. If other fields

Class	Examples	Q1 (a_W, a_Z)	Q2 (y_f, z_f)	Q3 (c_γ)	Q4 (c_g)
I	SM, 2HDM (+) LRSM (+), SUSY (+)	Y	Y	Y	Y
II	Triplet ($\nu, +$)	Y	Y	Y	N
III		Y	N	Y	Y
IV	TechniPGBs, LRSM (-) 2HDM (-), SUSY (-)	N	Y	Y	Y
V	Higher Representation (+)	Y	N	Y	N
VI	Triplet ($\nu, -$)	N	Y	Y	N
VII		N	Y	N	Y
VIII		N	N	Y	Y
IX	Singlet with RH neutrino (ν) Conserved Q.No. (ν)	N	Y	N	N
X		N	N	Y	N
XI		N	N	N	Y
XII	Higher Representation (-)	N	N	N	N

Table (2):

The twelve categories of models, based on the size of their effective couplings. The positions of some representative models are indicated, where CP conserving scalar couplings are assumed for simplicity. (\pm) denotes the CP quantum number of the observed light scalar state. A ν in brackets indicates that the large Yukawa coupling may be restricted to neutrinos only. Categories XIII through XVI are not listed because models having $O(e)$ couplings to the W and generally also have $O(\alpha/2\pi)$ effective couplings to photons. Triplet indicates a doublet-triplet model for which the observed light scalar is dominantly from the triplet component.

were permitted, such as new exotic fermions, then loops of these new particles might generate a one-loop gluon coupling, forcing the recategorization of the model from either II or VI (depending on the CP quantum number of the light scalar) to either I or IV.

To make more refined decisions requires more precise measurements of the effective

couplings (or the discovery of more new particles!). This is possible because most of the above categories, including the most interesting ones – like I and IV – may be further subdivided according to the relative size of the various couplings within any given class. For example, inspection of eqs. (92) shows what information about the scalar quantum numbers can be gleaned from a comparison of the WWh to the ZZh coupling strengths. As was argued in section 5.2, a comparison of these to the W and Z boson masses can, in some circumstances, rule out the possibility that the new scalars are doublets or singlets.

More information is potentially available once the relative strengths of the Yukawa couplings become measured. We next summarize some of the conclusions which can follow from such more precise information.

6.2.1) Tree Level Relations Amongst Yukawa Couplings:

An obvious first test to perform is for the proportionality of the Yukawa coupling strength to the mass of the fermion involved. That is, tests of the prediction

$$\frac{y_f}{y_{f'}} = \frac{m_f}{m_{f'}}. \quad (137)$$

Although the SM predicts this relation to hold for all fermions, as we have seen it typically holds with modifications for other models. Some of the main subcategories of potential Yukawa coupling relations are:

- 1: If the new scalar is a Goldstone boson, then its couplings must vanish in the limit of vanishing momentum, and so its Yukawa couplings must strictly all vanish, although derivative scalar-fermion couplings need not do so. This makes a measurement of the energy dependence of the scalar-fermion coupling instructive, if performed over a large enough energy range.
- 2: Pseudo Goldstone bosons, and elementary scalar multiplets which do not acquire vacuum expectation values, need not couple to fermions with strength proportional to mass at all. Among the most striking experimental signatures would be a strong coupling to light fermions, like electrons or u, d quarks, since these are observable through their

implications for the differential production rates, for example, yet the direct experimental limits on their existence are quite weak.

- 3: Models of the Type II class of multi-doublet theories — including supersymmetric models — share the SM prediction (at tree level) so long as the ratio is made only between up-type fermions, or only among down-type fermions. In this case the ratio of ratios, $(y_u/y_d)/(m_u/m_d)$ is given by scalar mixing angles (*e.g.* by eq. (117)), and so this kind of model may be tested by comparing this ratio with predictions (like eq. (113)) for the scalar - gauge boson couplings, which also depends only on these mixing angles.
- 4: Multidoublet models of the Type I category share the SM prediction, eq. (137) for all fermions, but differ in their prediction for the constant of proportionality, y_f/m_f . The same is true for higher representation models which acquire their Yukawa couplings by mixing with the ordinary SM doublet. As eqs. (109) and (116) show, these two categories may be differentiated by comparing the mixing angles inferred from y_f/m_f with those inferred from the scalar - W, Z couplings of eqs. (108) and (113).

6.2.2) *Loop Corrections to Yukawa Coupling Relations:*

Because the tree-level Yukawa couplings and masses are often very small, it becomes important to consider also radiative corrections to these predictions. In particular large radiative corrections have recently been proposed as a means to distinguish supersymmetric from generic Type II 2HDMs [21],[58]. We here describe the logic of these tests within a more general framework.

Loop corrections to the tree-level predictions relating the effective couplings of dimension-4 or less interactions are particularly important in this regard because they do not decouple, in the sense that the contributions of heavy particles in loops need not be suppressed on dimensional grounds by inverse powers of the heavy particle mass.

As was discussed in Section 2, tree-level predictions of small Yukawa couplings can be prevented from being significantly changed by radiative corrections if the Yukawa coupling of interest is protected by a chiral symmetry. This is the case for the SM, for which the proportionality of y_f to m_f is not significantly modified by loops. It is instructive to ask in

more detail why this is true for the ratio y_b/m_b , since the b quark couples to the t quark *via* the charged-current weak interactions, and so any chiral symmetry involving a rephasing of the b quark must also require the t quark to rotate. But the large t quark mass then should strongly break the invariance of the SM lagrangian under chiral rotations of the top quark. Superficially one might therefore expect loop corrections to y_b to be proportional to y_t instead of y_b , and so to be significantly large.

The flaw in this reasoning is this: in order for the SM charged-current weak interactions to be invariant under $\delta b = i\epsilon \gamma_5 b$, provided it is sufficient to rotate the top quark by a *vectorlike* rotation: $\delta t = i\epsilon t$, which is also a symmetry of the top-quark mass term. A vectorlike t rotation suffices because the charged-current weak interactions are purely left-handed. And so SM loop corrections to y_b must indeed therefore be proportional to y_b .

We therefore see what is required in order to ruin the chiral symmetry protection of small Yukawa couplings in a model. One of two things is required:

1. Right-handed effective couplings of fermions to the ordinary W boson, together with nonzero Kobayashi Maskawa mixing with a heavy fermion like the top quark;
2. Direct chiral-symmetry breaking interactions, either through new kinds of Yukawa interactions whose couplings are not small, or through new flavour-changing gauge interactions with heavy fermions, having both left- and right-handed couplings.

It is now easy to see which of our models satisfy either of these two criteria. For instance, neither is satisfied by a Type I or Type II 2HDM, since the only chiral symmetry breaking couplings in these models are the small Yukawa couplings themselves, and the only flavour-changing couplings to the only significantly massive fermion – the top quark – are the purely left-handed charged-current interactions. Loop corrections therefore cannot significantly modify the tree-level predictions these models make relating Yukawa couplings to fermion masses. Of course, this is particularly clear in models for which the Type I or Type II couplings are enforced by a discrete symmetry of some sort.

Supersymmetric models, on the other hand, are of Type II form because of supersym-

metry. However, in practice supersymmetry is broken and loops involving heavy superpartners of light particles might be expected to generate couplings of the ‘wrong’ Higgs doublet to fermions. These new terms have certain nondecoupling properties, i.e. they do not vanish if the masses of quarks and gauginos, trilinear soft-breaking terms, and μ parameter are simultaneously made heavy. Furthermore, as was discussed earlier, the supersymmetric models can satisfy criterion 2, depending on whether the same chiral symmetry is preserved by the supersymmetry-breaking couplings between superpartners of left- and right-handed squarks. Of course, the SUSY-breaking couplings can themselves be set up to preserve the chiral symmetry in the small-fermion-mass limit, and this is often the choice made within some of the MSSM’s found in the literature. In this case, it can also happen that the MSSM predictions can approach those of the 2HDM (and so, for some parameter values, also those of the SM) in the limit that all superpartners are taken to be arbitrarily heavy.

Clearly LR models satisfy criterion 1, and so top-quark loops may be expected to significantly modify the b -quark yukawa coupling. In order of magnitude one expects $\delta y_b \sim (\alpha_w/4\pi)\epsilon y_t$ where ϵ is the relative strength of the right- and left-handed couplings of the light W boson, which is constrained by experiment to be $\epsilon \lesssim 10^{-3}$. Since LR models are neither Type I nor Type II in the couplings of the bidoublet scalar to fermions, the resulting correction is more difficult to test experimentally.

6.2.3) Loop Contributions to c_γ and c_g :

Another class of loop corrections which can be important are the contributions to the effective couplings c_γ and c_g (and their CP-violating counterparts). Comparing the measured size of these couplings with the measured Yukawa and gauge-boson couplings of the new scalar provides independent information about the nature of the underlying physics.

We have seen that measurements of these couplings with sufficient precision can usefully distinguish models. For example, the relative size of c_g compared to c_γ reflects differences in the kinds of coloured and electrically-charged heavy states in the model. Similarly, comparing $\tilde{c}_{g,\gamma}$ with $c_{g,\gamma}$ gives information about the P and T breaking scalar

interactions, *etc..*

Unfortunately, the utility of this comparison is limited until these couplings are known with relatively good precision. This is because the $c_{g,\gamma}$'s are comparatively difficult to disentangle from the $\tilde{c}_{g,\gamma}$'s experimentally, and because new-physics contributions to c_g and c_γ must be extracted from relatively large, competing SM effects.

6.3) Outlook

In conclusion, we have shown how the properties of a new scalar particle may be encapsulated into a low-energy effective lagrangian, so long as other new particles are not also light enough to be close to discovery. (We should be so lucky!) These effective scalar couplings can be related to observables once-and-for-all (we give explicit formulae), and provide a complete summary of the information which experiments can provide about the scalar's properties. Finally, we have compared how these couplings depend on more microscopic parameters within a reasonably wide selection of models.

We conclude that the first round of experiments are likely to distinguish only amongst broad classes of models, as summarized in Table (2). Later, more precise, experiments can sharpen this process and in the event that no other new particles are discovered, much can be learned in principle about the underlying model if all effective couplings become measured to levels of a few percent.

Acknowledgments

We thank G. Azuelos and F. Corriveau for helpful conversations. This research was partially funded by N.S.E.R.C. of Canada, les Fonds F.C.A.R. du Québec, and was supported in part by the Department of Energy under Grant No. DE-FG02-94ER40823. C.B. thanks the University of Barcelona for its generous support, and congenial hospitality, while part of this research was being carried out. J.M acknowledges financial support from a Marie Curie EC grant (TMR-ERBFMBICT 972147) and thanks the Physics Department of McGill University for the kind hospitality and nice atmosphere when completing this work.

7. References

- [1] M. Carena, P. Zerwas and the Higgs Physics Working Group, *Physics at LEP-2*, published in CERN yellow report, CERN-96-01 edited by G. Altarelli, T. Sjostrand and F. Zwirner, (hep-ph/9602250).
- [2] M. Carena, J. Conway, H. Haber and J. Hobbs et al., Report of the Higgs Working Group of the RunII Workshop, Fermilab, 1999, in preparation see <http://fnth37.fnal.gov/higgs.html>.
- [3] J. Gunion, H. Haber, G. Kane and S. Dawson, *The Higgs Hunter's Guide*, Addison-Wesley, 1990.
- [4] T. Appelquist and C. Bernard, *Phys. Rev.* **D22** (1980) 200; A.C. Longhitano, *Phys. Rev.* **D22** (1980) 1166; *Nucl. Phys.* **B188** (1981) 118; M.S. Chanowitz and M.K. Gaillard, *Nucl. Phys.* **B261** (1985) 379; M.S. Chanowitz, M. Golden and H. Georgi, *Phys. Rev.* **D36** (1987) 1490; M.S. Chanowitz, *Ann. Rev. Nucl. Part. Sci.* **38**, (1988) 323; R.D. Peccei and X. Zhang, *Nucl. Phys.* **B337** (1990) 269; B. Holdom and J. Terning, *Phys. Lett.* **247B** (1990) 88; J. Bagger, S. Dawson and G. Valencia, report BNL-45782; M. Golden and L. Randall, *Nucl. Phys.* **B361** (1991) 3; B. Holdom, *Phys. Lett.* **259B** (1991) 329; A. Dobado, M.J. Herrero and D. Espriu, *Phys. Lett.* **255B** (1991) 405; R.D. Peccei and S. Peris, *Phys. Rev.* **D44** (1991) 809; A. Dobado and J.M. Herrero, report CERN-TH-6272/91.
- [5] C.P. Burgess and D. London, *Phys. Rev. Lett.* **69** (1992) 3428; *Phys. Rev.* **D48** (1993) 4337.
- [6] J.M. Cornwall, D.N. Levin and G. Tiktopoulos, *Phys. Rev.* **D10** (1974) 1145; M.S. Chanowitz, M. Golden and H. Georgi, *Phys. Rev.* **D36** (1987) 1490.
- [7] I. Maksymyk, C.P. Burgess and D. London, *Phys. Rev.* **D50** (1994) 529; C.P Burgess, S. Godfrey, H. König, D. London and I. Maksymyk, *Phys. Lett.* **326B** (1994) 276;

Phys. Rev. **D49** (1994) 6115.

- [8] R. Barbieri and A. Strumia, *Phys. Lett.* **462B** (1999) 144.
- [9] J. Ellis, M.K. Gaillard and D.V. Nanopoulos, *Nucl. Phys.* **B106** (1976) 292
- [10] T. Inami, T. Kubota and Y. Okada, *Zeit. Phys.* **C18** (1983) 69; A. Djouadi, M. Spira and P.M. Zerwas, *Phys. Lett.* **264B** (1991) 440
- [11] M. Spira, A. Djouadi, D. Graudenz and P.M. Zerwas, *Nucl. Phys.* **B453** (1995) 17
- [12] M. Spira, *Fortsch. Phys.* **46** (1998) 203
- [13] M. Pospelov, hep-ph/9511368 (unpublished).
- [14] A.I. Vainshtein, M.B. Voloshin, V.I. Sakharov and M. Shifman, *Sov. J. Nucl. Phys.* **30** (1979) 711.
- [15] T.G. Rizzo, *Phys. Rev.* **D22** (1980) 389; W.-Y. Keung and W.J. Marciano, *Phys. Rev.* **D30** (1984) 248.
- [16] G. Sterman and S. Weinberg, *Phys. Rev. Lett.* **39** (1977) 1436
- [17] A. Barroso, J. Pulido and J.C. Romão, *Nucl. Phys.* **B267** (1993) 1.
- [18] A. Abbasabadi, D. Bowser-Chao, D.A. Dicus and W.W. Repko, *Phys. Rev.* **D52** (1995) 3919.
- [19] H. Georgi, S. Glashow, M. Machacek and D. Nanopoulos, *Phys. Rev. Lett.* **40** (1978) 692.
- [20] A. Stange, W. Marciano and S. Willenbrock, *Phys. Rev.* **D50** (1994) 4491; Future Electroweak Physics at the Fermilab Tevatron, D. Amidei and R. Brock, in ref. [1]; M. Spira, in ref.[2] (hep-ph/9810289).

- [21] M. Carena, S. Mrenna and C.E.M. Wagner, *Phys. Rev.* **D60** (1999) 075010 (hep-ph/9808312).
- [22] D. Graudenz, M. Spira and P.M. Zerwas, *Phys. Rev. Lett.* **70** (1993) 1372.
- [23] G. Altarelli and G. Parisi, *Nucl. Phys.* **B126** (1977) 298.
- [24] T. Han, G. Valencia and S. Willenbrock, *Phys. Rev. Lett.* **69** (1992) 3274.
- [25] G. Abbiendi et al. (OPAL Collaboration) preprint CERN-EP-99-097, Jul 1999, hep-ex/9908008.
- [26] C. Adloff *et.al.* (H1 Collaboration), *Eur. Phys. J.* **C11** (1999) 447–471, hep-ex/9907002.
- [27] B.B. Levchenko, preprint SINP-TNP-96-71 (unpublished) (hep-ph/9608295); M.Krawczyk, in *Future physics at HERA*, the proceedings of the Workshop on Future Physics at HERA, Hamburg, pp 244-255, (hep-ph/9609477).
- [28] M.E. Peskin and T. Takeuchi, *Phys. Rev. Lett.* **65** (1990) 964; *Phys. Rev.* **D46** (1992) 381; W.J. Marciano and J.L. Rosner, *Phys. Rev. Lett.* **65** (1990) 2963; D.C. Kennedy and P. Langacker, *Phys. Rev. Lett.* **65** (1990) 2967; G. Altarelli and R. Barbieri, *Phys. Lett.* **253B** (1991) 161.
- [29] M. Golden and L. Randall, *Nucl. Phys.* **B361** (1991) 3; B.Holdom and J. Terning, *Phys. Lett.* **259B** (1991) 329.
- [30] I. Maksymyk, C.P. Burgess and D. London, *Phys. Rev.* **D50** (1994) 529.
- [31] Particle Data Group: *Review of Particle Properties*, *Eur. J. Phys.* **C3** (1998) 280.
- [32] I.B. Khriplovich and S.K. Lamoreaux, *"CP Violation Without Strangeness"*, Springer, 1997.
- [33] K.F. Smith *et al.*, *Phys. Lett.* **234B** (1990) 191; I.S. Altarev *et al.*, *Phys. Lett.* **276B**

(1992) 242.

- [34] E.D. Commins *et al.*, *Phys. Rev.* **A50** (1994) 2960.
- [35] J.P. Jacobs *et al.*, *Phys. Rev. Lett.* **71** (1993) 3782.
- [36] V.M. Khatsimovsky, I.B. Khriplovich and A.S. Yelkhovsky, *Ann. Phys. (NY)* **186** (1988) 1; V.M. Khatsimovsky and I.B. Khriplovich, *Phys. Lett.* **296B** (1994) 219; C. Hamzaoui, M. Pospelov, *Phys. Rev.* **D60** (1999) 036003.
- [37] T. Falk, K. Olive, M. Pospelov and R. Roiban, hep-ph/9904393, to appear in *Nucl. Phys.B*.
- [38] S. Weinberg, *Phys. Rev. Lett.* **63** (1989) 2333.
- [39] V. Barger, K. Cheung, K. Hagiwara and D. Zeppenfeld, *Phys. Rev.* **D57** (1998) 391.
- [40] E. Farhi, L. Susskind, *Phys. Rep.* **74** (1981) 277–321;
T. Appelquist, in *Beijing 1993, Particle physics at the Fermi scale*, proceedings of the CCAST Symposium on Particle Physics at the Fermi Scale, Beijing, China, 27 May - 4 Jun 1993.
- [41] S.W. Weinberg, *Phys. Rev. Lett.* **29** (1972) 1698; L. Susskind, *Phys. Rev.* **D20** (1979) 2619
- [42] For a recent review see, for example, C. Burgess, *Physics Reports* to appear, (hep-th/9808176).
- [43] R. Casalbuoni, A. Deandrea, S. de Curtis, D. Dominici, F. Feruglio, R. Gatto, M. Grazzini, *Phys. Lett.* **349B** (1995) 533; R. Casalbuoni, A. Deandrea, S. de Curtis, D. Dominici, R. Gatto, M. Grazzini, *Phys. Rev.* **D53** (1996) 5201; R. Casalbuoni, S. de Curtis, D. Dominici, M. Grazzini *Phys. Rev.* **D56** (1997) 2812; R. Casalbuoni, A. Deandrea, S. de Curtis, D. Dominici, R. Gatto, J.F. Gunion, hep-ph/9904268.

[44] V. Barger, W.Y. Keung, *Phys. Lett.* **185B** (1987) 431; V. Barger, R. Phillips, *Collider Physics*, ed. by Addison-Wesley 1987.

[45] G.B. Gelmini and M. Roncadelli, *Phys. Lett.* **99B** (1981) 411.

[46] For a recent review of triplet models, with references, see: H. E. Logan, Ph.D. thesis, UC Santa Cruz (hep-ph/9906332).

[47] Y. Chikashige, R.N. Mohapatra and R.D. Peccei, *Phys. Rev. Lett.* **45** (1980) 1926; *Phys. Lett.* **98B** (1981) 265.

[48] A.K. Grant, *Phys. Rev.* **D51** (1995) 207.

[49] J.C. Pati and A. Salam, *Phys. Rev.* **D10** (1974) 275; R.N. Mohapatra and J.C. Pati, *Phys. Rev.* **D11** (1975) 566; G. Senjanovic and R.N. Mohapatra, *Phys. Rev.* **D12** (1975) 1502; F. Feruglio, L. Maiani and A. Masiero, *Phys. Lett.* **233B** (1989) 512; A. Deandrea, F. Feruglio and G.L. Fogli, *Nucl. Phys.* **B402** (1993) 3; A. Pilaftsis, *Phys. Rev.* **D52** (1995) 459 and references therein.

[50] A. Donini, F. Feruglio, J. Matias and F. Zwirner, *Nucl. Phys.* **B507** (1997) 51.

[51] G. Beall, M. Bander and A. Soni, *Phys. Rev. Lett.* **48** (1982) 848; G. Ecker and W. Grimus, *Nucl. Phys.* **B258** (1985) 328; G. Barenboim, J. Bernabeu and M. Raidal, *Nucl. Phys.* **B478** (1996) 527; P. Ball, J.M. Frere and J. Matias, preprint CERN-TH-99-297 (hep-ph/9910211).

[52] J.F. Gunion, J. Grifols, A. Mendez, B. Kayser and F. Olness, *Phys. Rev.* **D44** (1989) 1546.

[53] F.G. Gilman and M.H. Reno, *Phys. Lett.* **127B** (1983) 426; M. Pospelov, *Phys. Rev.* **D56** (1997) 259.

[54] R. Martinez, M.A. Perez and J.J. Toscano *Phys. Rev.* **D40** (1989) 1722

[55] S. Dimopoulos and L. Hall, *Phys. Lett.* **207B** (1988) 210; V. Barger, G.F. Giudice and T. Han, *Phys. Rev.* **D40** (1989) 2987.

[56] H.E. Haber and R. Hempfling, *Phys. Rev. Lett.* **66** (1991) 1815; J.R. Espinosa and M. Quiros, *Phys. Lett.* **302B** (1993) 51-58, (hep-ph/9212305); J.A. Casas, J.R. Espinosa, M. Quiros and A. Riotto, *Nucl. Phys.* **B436** (1995) 3-29, erratum *Nucl. Phys.* **B439** (1995) 466-468, (hep-ph/9407389).

[57] R. Hempfling, *Phys. Rev.* **D49** (1994) 6168

[58] K.S. Babu and C. Kolda, *Phys. Lett.* **451B** (1999) 77 (hep-ph/98113080).

[59] F. Borzumati, G.R. Farrar, N. Polonsky and S. Thomas, *Nucl. Phys.* **B555** (1999) 53–115 (hep-ph/9902443).

[60] A. Djouadi, V. Driesen, W. Hollik and J.I. Illana, *Eur. Phys. J.* **C1** (1998) 149–162 (hep-ph/9612362).